ENERGY LABORATORY

MASSACHUSETTS INSTITUTE
OF TECHNOLOGY

ADSORPTION OF INORGANIC CONTAMINANTS IN PONDED EFFLUENTS FROM COAL-FIRED POWER PLANTS

by
David A. Dzombak and François M.M. Morel

Energy Laboratory Report No. MIT-EL 85-005

June 1985

ADSORPTION OF INORGANIC CONTAMINANTS IN PONDED EFFLUENTS FROM COAL-FIRED POWER PLANTS

by

David A. Dzombak

François M.M. Morel

Ralph M. Parsons Laboratory
Department of Civil Engineering

Massachusetts Institute of Technology
Cambridge, Massachusetts 02139

Sponsored by:

Duke Power Company
American Electric Power Service Corporation

under the

MIT Energy Laboratory Electric Utility Program

MIT Energy Laboratory Report No. MIT-EL 85-005

June 1985

ABSTRACT

The objectives of this study were [1] to conduct some experimental tests of the surface precipitation adsorption model, and [2] to work on the development of a simple yet widely applicable approach to modelling adsorption of inorganic ions on oxide surfaces. The latter represents the first portion of our continuing effort to develop a data base for adsorption of inorganic contaminants in oxide suspensions.

An investigation of the kinetics of cadmium adsorption on hydrous ferric oxide at different initial adsorbate/adsorbent ratios was conducted as a partial test of the surface precipitation model. Kinetics of cadmium adsorption were observed to slow considerably as the adsorbate/adsorbent ratio was increased. The results confirm our hypothesis that adsorption kinetics should decrease as the adsorbate/adsorbent ratio is increased because of the shift from surface complexation to surface precipitation as the dominant adsorption mechanism.

A number of constant pH equilibrium adsorption experiments with cadmium and hydrous ferric oxide were conducted in order to verify the isotherm predicted by the surface precipitation model. A recently published, extensive isotherm for zinc adsorption on hydrous ferric oxide was also examined. This investigation revealed that cation adsorption isotherms exhibit adsorptive saturation at high adsorbate concentrations and that the smooth transition from adsorption to precipitation predicted by the surface precipitation model occurs above this saturation. To model these data, a two site-type model with surface precipitation on weak binding sites is needed.

As the first step in our effort to develop a data base for adsorption of inorganics, we reviewed available adsorption data and surface complexation models and identified a modelling approach capable of describing all existing data. The model that we propose is a two site surface complexation model with surface precipitation on weak binding sites, combined with the diffuse layer model for electrostatic corrections. For proton and anion binding, two site-types and surface precipitation will usually not be necessary - these refinements are included for accurate description of cation binding. The basic diffuse layer surface complexation model is thus the nucleus of the proposed universal model.

TABLE OF CONTENTS

TABLE OF CONTENTS

CHAPTER I. INTRODUCTION

Background

Sluicing systems are commonly used at coal-fired electric power plants to remove combustion residues, i.e. fly ash and bottom ash, from the plant. In most cases these sluicing streams are directed into ponds in which settling of the ash particles takes place. The sluicing water, minus most of the solids, is usually then discharged into a stream or lake, though in some plants a portion or all of the sluicing water is recycled (1).

A variety of soluble chemical species are present in ash sluice streams from leaching of the fly ash and bottom ash and also possibly from addition of plant liquid wastes to the sluice water. Disposal of liquid wastes in sluice water is a practice that varies from plant to plant. Liquid wastes produced in the operation of a coal-fired power plant include boiler and cooling tower blowdown, wastes from boiler cleaning and other cleaning procedures, coal pile runoff, etc.

The chemical contaminants of most concern in sluice waters are inorganic, in particular metals. These are derived from input of liquid wastes and from leaching of ash particles, which consist primarily of oxides of iron, aluminum, and silicon but also contain a number of other metals at lower levels (2,3). Fly ashes generally contain little organic matter (4,5), and less than one percent of the organic carbon present is extractable in benzene (5).

Upon contact with water, ash particles tend to form coatings of hydrous aluminum and iron oxides, with the latter dominant (3,6,7). Because these surface coatings happen to have large adsorptive affinities and capacities for metal ions, ash settling ponds also serve as treatment

systems for removal of trace metals (8,9). In addition to adsorption/desorption reactions, other chemical processes governing the fate of dissolved metals in ash ponds are precipitation/dissolution and possibly redox reactions in the bottom layers of some ponds.

In previous work performed at MIT, Farley et al. (10) developed a physical-chemical model capable of predicting fluid and particle transport as well as chemical equilibrium in ash ponds. The novel and most critical features of this ponding model are the submodels for sedimentation and adsorption. The sedimentation submodel (10,11) emphasizes the importance of coagulation in the sedimentation of suspended particles and is a departure from the common engineering approach to sedimentation in which discrete particle settling is assumed. A simple power law description of sedimentation kinetics was developed by approximating the theoretical coagulation equations and was verified by laboratory experiments. To describe the adsorption of metals in oxide suspensions, a new thermodynamic adsorption model -- the surface precipitation model (10,12) -- was developed because existing adsorption models were found to be inadequate at the relatively high metal concentrations typical of ash ponds. The surface precipitation model extends the surface complexation approach (13,14) and allows for a continuum between surface reactions and precipitation. This continuum is evident in adsorption data but cannot be described with existing surface complexation models.

Farley et al. (10) used the ponding model to predict the performance of several ash ponds with respect to solids and metal removal. Mass removals of solids predicted by the model agreed with field observations, but prediction of the chemical composition of pond effluent was somewhat less successful. The discrepancies between predicted and observed

effluent chemical composition were due in part to the use of inappropriate analytical techniques to characterize effluent chemistry (neutron activation analysis, which detects metals fixed in the solid matrix of ash particles in addition to the soluble and leachable metals of interest) and in part to lack of adsorption constants for some chemical species in the sluice water. Despite these problems, the model was successful in predicting trends in effluent chemistry under changing operational conditions.

Objectives and Scope

In order to make the ponding model a predictive tool for chemical removal, our long rang objectives are [1] to obtain experimental verification of the surface precipitation model, [2] to develop a complete data base for the surface precipitation model, and [3] to demonstrate the predictive ability of the surface precipitation model (using the enlarged data base) when applied to complex systems. To use the surface precipitation model (or any chemical adsorption model) in a predictive way, development of a data base specific to the chosen model is needed. Existing data for the adsorption of inorganic ions on metal oxides have been interpreted by individual investigators with a great variety of adsorption models which are not consistent with each other and do not yield similar values for equivalent parameters (15).

Our work in 1984 encompassed important parts of the first two of the objectives above. We conducted adsorption kinetics and equilibrium experiments to test several aspects of the surface precipitation model, and we worked on development of a simple yet widely applicable approach to modelling adsorption of inorganic ions on oxide surfaces. The latter represents the first portion of our larger effort to develop a complete

set of mass law adsorption constants for the surface precipitation model. The experimental work related to surface precipitation is presented in Chapter II and the theoretical investigation related to adsorption modelling is described in Chapter III. Three appendices are also included. Appendices A and B contain listings of the raw experimental data while Appendix C is a brief critique of the quality of equilibrium adsorption data for inorganics reported in the literature. The third appendix is intended to serve as an aid in choosing experimental data for extraction of adsorption constants and is thus an extension of the "Guidelines" section of Chapter III. In addition, Appendix C will serve as our reference for assessment of data quality in our future work aimed at development of an adsorption data base.

REFERENCES

1. Litherland, S.T., Nassos, P.A., Owen, M.L., and Winton, S.L., "Pilot-Scale Investigation of Closed Loop Ash Sluicing," DCN-83-211-004-35, Radian Corp., Austin, TX, 1983.

2. Suloway, J.J., Skelly, T.M., Roy, W.R., Dickerson, D.R., Schuller, R.M., and Griffin, R.A., "Chemical and Toxicological Properties of Coal Fly Ash," Environmenatal Geology Notes (Illinois State Geological Survey), No. 105, 1983.

3. Theis, T.L. and Wirth, J.L., "Sorptive Behavior of Trace Metals on Fly Ash in Aqueous Systems," Environmental Science and Technology, Vol. 11, No. 12, 1977, pp. 1096-1100.

4. Theis, T.L. and Richter, R.O., "Chemical Speciation of Heavy Metals in Power Plant Ash Pond Leachate," Environmental Science and Technology, Vol. 13, No. 2, 1979, pp. 219-224.

5. Roy, W.R., Griffin, R.A., Dickerson, D.R., and Schuller, R.M., "Illinois Basin Coal Fly Ashes. 1.Chemical Characterization and Solubility," Environmental Science and Technology, Vol. 18, No. 10, 1984, pp. 734-739.

6. Hulett, L.D., Weinberger, A.J., Ferguson, N.M., Northcutt, K.J., and Lyon, W.S., "Trace Element and Phase Relations in Fly Ash," EPRI EA-1822, Electric Power Research Institute, Palo Alto, CA, 1981, pp. 55-58.

7. Roy, W.R. and Griffin, R.A., "Illinois Basin Coal Fly Ashes. 2. Equilibria Relationships and Qualitative Modeling of Ash-Water Reactions," Environmental Science and Technology, Vol. 18, No. 10, 1984, pp. 739-742.

8. Leckie, J.O., Benjamin, M.M., Hayes, K.F., Kaufman, G., and Altmann, S., "Adsorption/Coprecipitation of Trace Elements from Water with Iron Oxyhydroxide," EPRI RP-910-1, Electric Power Research Institute, Palo Alto, CA, 1980.

9. Leckie, J.O., Appleton, A.R., Ball, N.B., Hayes, K.F., and Honeyman, B.D., "Adsorptive Removal of Trace Elements from Fly-Ash Pond Effluents onto Iron Oxyhydroxide," EPRI RP-910-1, Electric Power Research Institute, Palo Alto, CA, 1984.

10. Farley, K.J., Harleman, D.R.F, and Morel, F.M.M., "Ponding of Effluents from Fossil Fuel Steam Electric Power Plants," MIT-EL 84-007, MIT Energy Laboratory, Cambridge, MA, 1984.

11. Farley, K.J. and Morel, F.M.M., "The Role of Coagulation in the Kinetics of Sedimentation," Environmental Science and Technology, submitted, 1985.

12. Farley, K.J., Dzombak, D.A., and Morel, F.M.M., "A Surface Precipitation Model for the Sorption of Cations on Metal Oxides," Journal of Colloid and Interface Science, in press, 1985.

13. Schindler, P.W., "Surface Complexes at Oxide-Water Interfaces," Adsorption of Inorganics at Solid-Liquid Interfaces, M.A. Anderson and A.J. Rubin, eds., Ann Arbor Science, Ann Arbor, MI, 1981, pp. 1-49.

14. Morel, F.M.M., Principles of Aquatic Chemistry, John Wiley and Sons, Inc., New York, NY, 1983.

15. Morel, F.M.M., Yeasted, J.G., and Westall, J.C., "Adsorption Models: A Mathematical Analysis in the Framework of General Equilibrium Calculations," Adsorption of Inorganics at Solid-Liquid Interfaces, M.A. Anderson and A.J. Rubin, eds., Ann Arbor Science, Ann Arbor, MI, 1981, pp. 263-294.

CHAPTER II. SURFACE PRECIPITATION: AN EXPERIMENTAL INQUIRY

II.A KINETICS OF CADMIUM ADSORPTION ON HYDROUS FERRIC OXIDE

Introduction

Many experimental studies of cation adsorption on hydrous metal oxides have been conducted over the past two decades, the primary objective being to obtain equilibrium adsorption data under a variety of solution conditions. Given the common objective in these studies and the similarity in experimental designs, the relatively wide range of equilibration times reported in the literature (minutes-weeks) is at first glance a bit surprising. Moreover, it is often difficult to evaluate the validity of equilibration times because they are established in "preliminary experiments" which are not reported in detail. Though adsorption of cations by hydrous metal oxides is frequently reported to be very rapid (e.g. for adsorption of cations on MnO_2 - Refs. 1,2,3), other investigators may employ much longer equilibration times in adsorption experiments with the same oxide (4,5).

Equilibration time discrepancies in the literature are traceable to the two step character of the kinetics of cation adsorption on hydrous oxides at constant pH. The two step process comprises a rapid initial uptake followed by a slower step in which the equilibrium adsorption density is approached asymptotically. In many adsorption studies it is assumed that the contribution of the slow adsorption step is small and short equilibration times are selected. However, it has been demonstrated that under certain conditions the

slow adsorption step can represent a significant portion of total adsorption (5,6,7). There has not been much investigation of factors that determine cation adsorption kinetics, but some factors that appear to slow adsorption kinetics and increase the importance of the second adsorption step are increased ionic strength (1,8) and increased adsorbate/adsorbent ratio (8,9). Adsorption kinetics are also likely to be influenced by pH, but effects of pH have been studied over narrow ranges only (8,10).

In this study we examined the effect of the initial adsorbate/adsorbent ratio on the kinetics of cadmium adsorption on hydrous ferric oxide (HFO). The study was undertaken as a partial test of the hypothesis that adsorption of metal cations on hydrous oxides at high adsorbate/adsorbent ratios involves a different mechanism than at low ratios, i.e. surface precipitation rather than surface complexation (11). An additional objective was to investigate the importance of the adsorbate/adsorbent ratio in the design of equilibrium adsorption experiments.

Experimental

Experiments were conducted in a closed system consisting of a 200 mL Teflon beaker inside a 250 mL jacketed glass beaker (see Figure A.1) and a nitrogen atmosphere was maintained in the system. Nitrogen gas was passed through an Ascarite-filled drying tube to remove CO_2 and then through Millipore Q-water to saturate it before it entered the reaction vessel. The reaction vessel was maintained at 25.0 ± 0.1°C using a circulating water bath.

A check for CO_2 contamination in the reaction vessel was performed by measuring $CO_2(aq)$ and $O_2(aq)$ in a 100 mL solution of

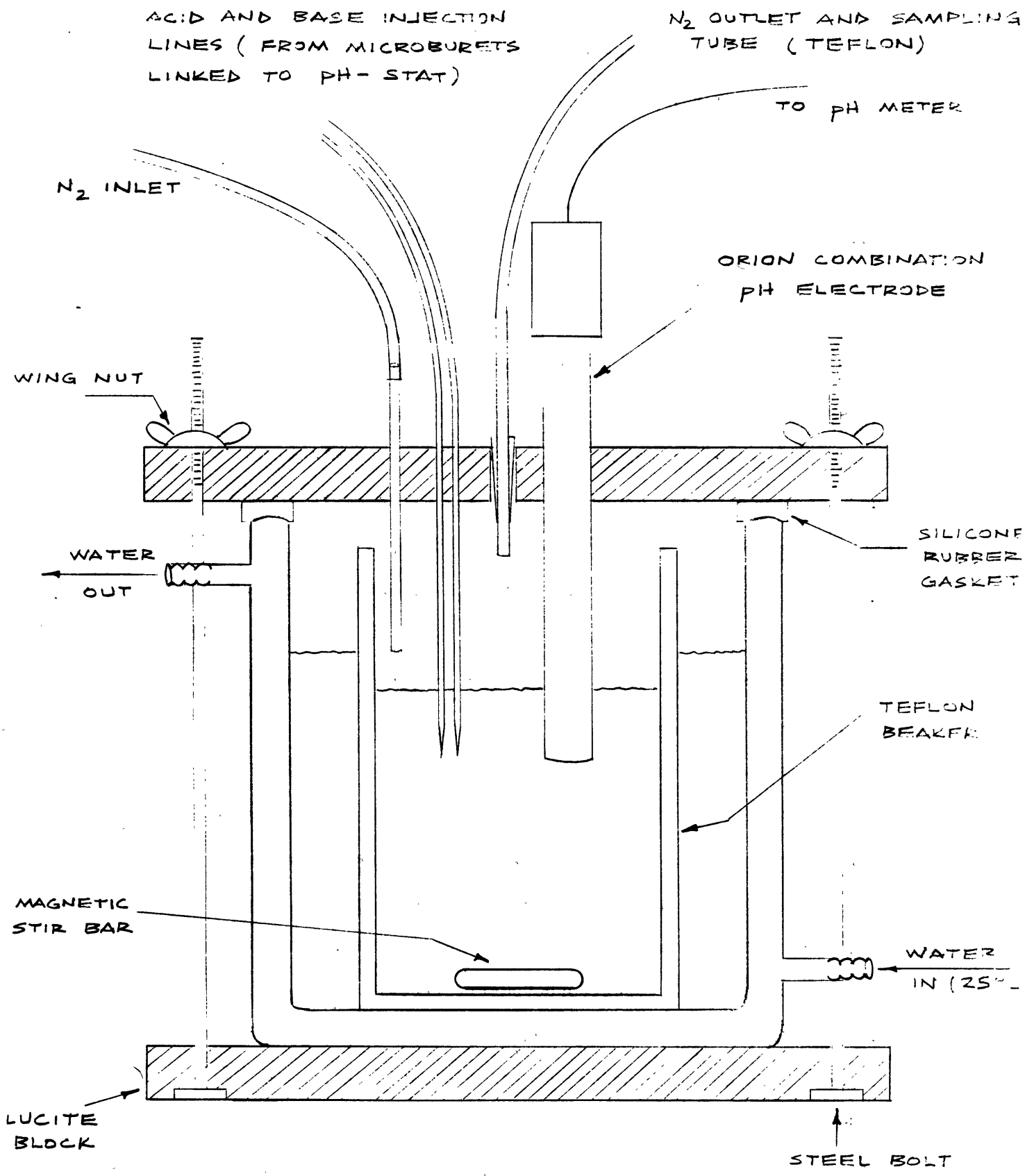

Figure A.1 Reaction chamber used in the adsorption experiments.

0.1N $NaNO_3$ using gas chromatography. After confinement in the reaction vessel for 4 hours, 80 mL of the solution were withdrawn with a gas tight syringe and samples were prepared for GC analysis using a head space equilibration technique (12). Gas samples from these equilibrations were injected into a gas chromatograph with a thermal conductivity detector; a Carbosieve-B column was employed for $CO_2(g)$ analyses while a molecular sieve 5A column was used for $O_2(g)$. The concentration of $CO_2(aq)$ so determined was below the detection limit (less than 5 μM) and the concentration of $O_2(aq)$ was negligible, the latter confirming no atmospheric contamination.

The pH was monitored continuously in all experiments (Orion combination pH electrode 91-05; Orion Model 801 digital pH meter) and maintained at 7.50 ± 0.05 by addition of CO_3-free NaOH as needed. These tasks were automated using a pH-stat; that is, the pH meter was linked to a microcomputer which in turn was used to control base delivery from a Gilmont microburet.

All Teflonware in contact with the solution was soaked in 3N HNO_3 at least 24 hours prior to use. Chemicals used to prepare metal stock solutions were reagent grade, dilutions were made with Millipore Q-water, and all stocks were acidified to pH < 2 with distilled HNO_3. Concentrations of stock solutions were checked by means of atomic absorption spectrophotometry (Perkin Elmer Model 372 with HGA 400 graphite furnace). A check for cadmium contamination in 10^{-3}M and 10^{-4}M $Fe(NO_3)_3$ solutions by AAS indicated less than 10^{-8}M total cadmium contamination.

Hydrous ferric oxide (HFO) was precipitated <u>in situ</u> by dropwise addition of CO_3-free NaOH to a 100 mL ferric nitrate solution; the ionic strength was fixed at 0.1N with $NaNO_3$ in all experiments. The

resulting suspension was aged 4 hours at pH = 7.50 ±0.05 with constant stirring. Physical-chemical characteristics of the amorphous colloids formed upon precipitation of ferric nitrate have been examined in detail in a number of recent studies (13, 14, 15, 16).

At the end of the aging period cadmium nitrate was added which contained radioactive Cd-109 (New England Nuclear) as a tracer. Samples (ca. 500 to 1000 µL) were withdrawn at various times using Teflon tubing connected to a Plastipak 5 mL syringe. The samples were expressed through 0.025 µM Millipore membrane filters (cat. no. VSWP 01300) which were held in Millipore 13 mm polypropylene filter holders. Cadmium was measured in the acidified filtrate by liquid scintillation counting of the Cd-109 tracer. Sample volumes were small in order to avoid significant drawdown in the reaction vessel since adsorption of HFO to the walls of the Teflon beaker was significant. [This sticking of adsorbent to the vessel walls in unknown quantities eliminated the possibility of determining adsorption by counting the Cd-109 on the solids retained by the filter.] To compute the percent adsorbed, it was assumed that all HFO in the vessel was reactive. At least two experiments were conducted for each combination of total Cd concentration (TOTCd) and total iron concentration (TOTFe). In a carbonate-free system at pH = 7.50, Cd^{2+} is by far the dominant dissolved cadmium species [(Cd^{2+})/TOTCd = 0.9975; $(CdOH^{+})$/TOTCd = 0.0025; based on stability constants from Morel (17)].

Adsorptive losses of Cd to the reaction vessel walls and on the filtration apparatus were investigated and quantified. An experiment with TOTCd = 5×10^{-5} M and no solid present indicated that maximum

adsorption to reaction vessel walls was 3±2 percent after 27 hours. No correction was applied to the adsorption data for this effect because of the large uncertainty and the likelihood that HFO coatings on the vessel walls would outcompete any exposed Teflon surface. To examine adsorptive losses in the course of filtration, experiments were conducted with TOTCd ranging from 6.5×10^{-7} to 10^{-2} M and no solid present. Samples were withdrawn and filtered after a 2 hour incubation period. In all experiments with TOTCd < 10^{-3} M , 10 ± 3 percent of TOTCd was adsorbed on the filtration apparatus, perhaps because of the pre-soaking in HNO_3 (18). Since less than millimolar TOTCd was employed in the experiments reported here, measured solution concentrations were corrected for a 10 percent adsorptive loss in filtration, i.e. true (Cd^{2+}) = 1.125 x measured (Cd^{2+}).

Results and Discussion

The initial adsorbate/adsorbent ratio was shown to influence adsorption kinetics in two complementary sets of experiments. In one, the concentration of HFO was held constant and TOTCd was varied (Figure A.2) while in the other TOTCd was fixed and the adsorbent concentration was varied (Figure A.3). Adsorption kinetics slowed with increasing adsorbate/adsorbent ratio in both sets of experiments. The raw experimental data are listed in Appendix A.

The mechanism of adsorption, at least for low adsorbate/adsorbent ratios, likely involves the formation of surface complexes between the adsorbate cation and functional groups on the oxide surface (19, 20, 21). At higher adsorbate/adsorbent ratios, however, adsorption may proceed via another mechanism (11, 21). In terms of the surface precipitation model (11), the slowing of

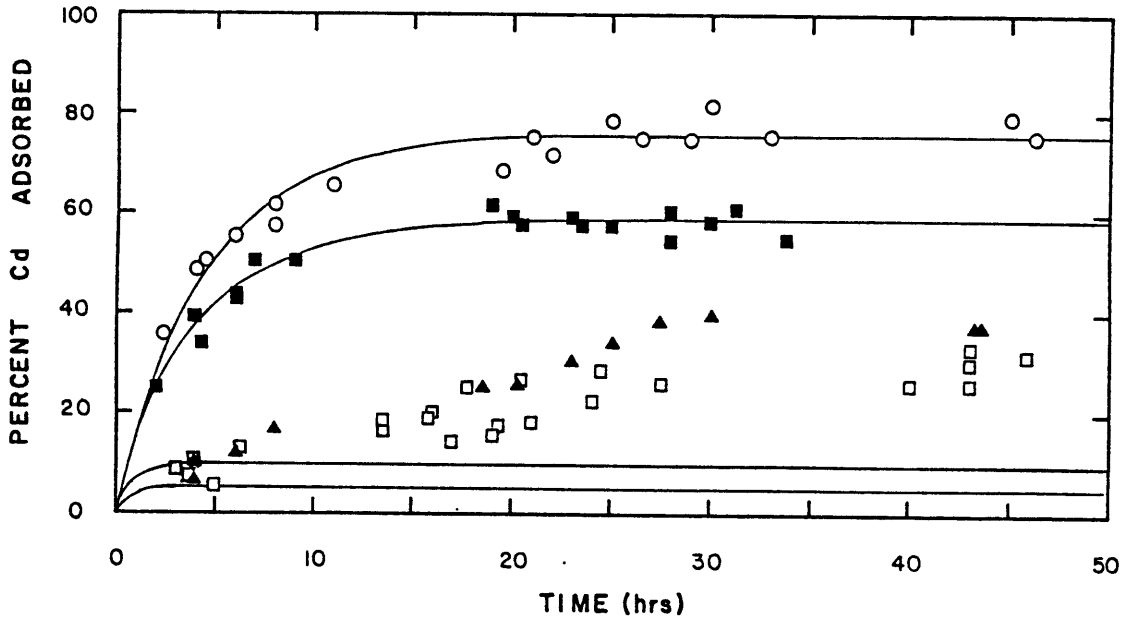

Figure A.2 Kinetics of Cd^{2+} adsorption on hydrous ferric oxide. pH = 7.50, I = 0.1 M $NaNO_3$, T = 25.0°C. Solid concentration fixed (TOTFe = 10^{-3} M), adsorbate/adsorbent ratio varied by changing total cadmium concentration: TOTCd = 6.5×10^{-7} M (○), 5×10^{-6} M (■), 5×10^{-5} M (▲), 1×10^{-4} M (□).

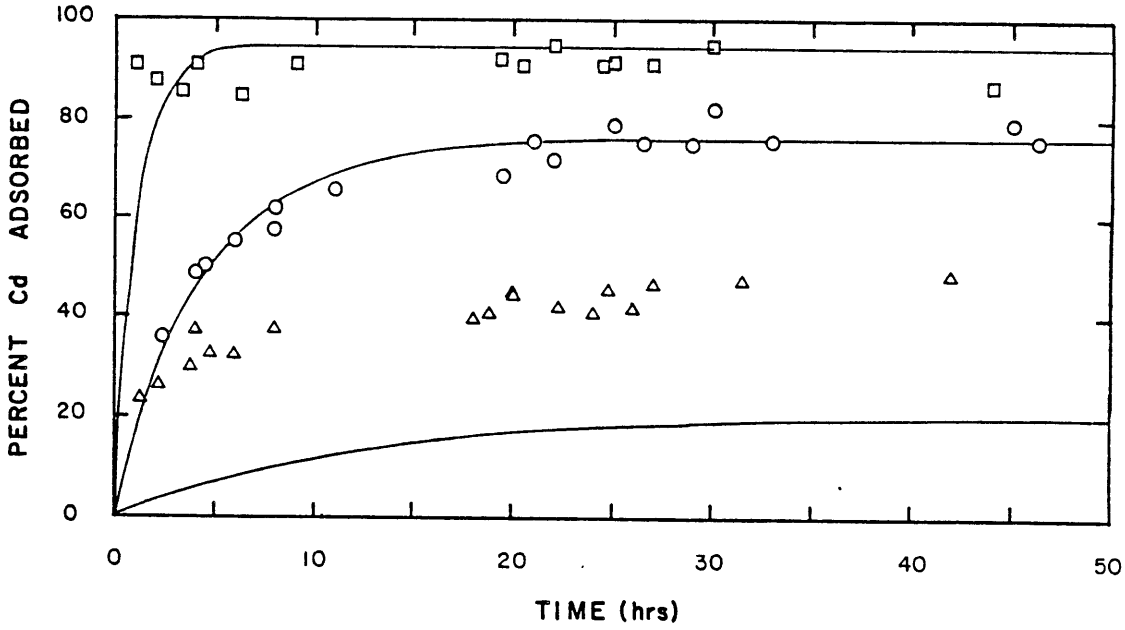

Figure A.3 Kinetics of Cd^{2+} adsorption on hydrous ferric oxide. pH = 7.50, I = 0.1 M $NaNO_3$, T = 25.0°C. Total adsorbate concentration fixed (TOTCd = 6.5 x 10^{-7} M), adsorbate/adsorbent ratio varied by changing solid concentration: TOTFe = 5 x 10^{-3} M (□), 10^{-3} M (○), 10^{-4} M (△).

adsorption kinetics with increasing adsorbate/adsorbent ratio is due to the shift to solid solution formation as the dominant adsorption mechanism. Indeed, Harvey and Linton (21) recently detected the formation of increasing amounts of $Zn(OH)_{2(s)}$ surface precipitate on HFO with increasing equilibration time.

The possibility of a shift in the mechanism of adsorption at higher adsorbate/adsorbent ratios is supported by the fact that only the adsorption kinetics data for lower TOTCd/TOTFe ratios can be fit with a rate expression corresponding to a surface complexation reaction, e.g.

$$\equiv FeOH_2^+ + Cd^{2+} = \equiv FeO\text{-}Cd^+ + 2H^+ \quad ;K \qquad [A.1]$$

where $\equiv FeOH_2^+$ represents a positively charged site on the surface of HFO and $\equiv FeO\text{-}Cd^+$ is the surface complex resulting from adsorption of Cd^{2+}. At equilibrium,

$$K = \frac{\{\equiv FeO\text{-}Cd^+\}\ \{H^+\}^2}{\{\equiv FeOH_2^+\}\ \{Cd^{2+}\}} = \frac{f}{b} \qquad [A.2]$$

where {} represent activities and f and b are forward and reverse reaction rate constants, respectively. For constant pH and electrolyte concentration, it is convenient to work with a conditional constant that incorporates pH effects as well as activity corrections, including electrostatic effects due to the charged surface.

$$K^{app} = \frac{(\equiv FeO\text{-}Cd^+)}{(\equiv FeOH_2^+)\ (Cd^{2+})} = \frac{\gamma_{s1}\gamma_{Cd}\ K}{\gamma_{s2}\{H^+\}^2} = \frac{f'}{b'} \qquad [A.3]$$

The parentheses in Eq.[A.3] represent concentrations, γ_{Cd} is the activity coefficient for Cd^{2+}, and γ_{s1} and γ_{s2} are the activity coefficients for the two surface species. To simplify notation, let

$$X = \equiv FeOH_2^+$$

$$C = Cd^{2+}$$

$$XC = \equiv FeO\text{-}Cd^+$$

In this notation, the rate expression for the surface complexation reaction in Eq. [A.3] is written

$$d(XC)/dt = f'(X)(C) - b'(XC) \qquad [A.4]$$

Equation [A.4] can be expressed in terms of (XC) by substituting for (X) and (C) from the applicable conservation equations:

$$X_T = \text{total X} = (X) + (XC) \qquad [A.5]$$

$$C_T = \text{total C} = (C) + (XC) \qquad [A.6]$$

After substituting for (X) and (C) and some algebraic manipulation, Eq. [A.4] can be rewritten as

$$d(XC)/dt = f'(XC)^2 - (XC)[f'X_T + f'C_T + b'] + f'X_TC_T \qquad [A.7]$$

which is a first order, nonlinear differential equation with constant coefficients that can be solved numerically for (XC) as a function of time. It is possible to obtain estimates of K^{app} and X_T by

considering simultaneous mass law equations for two equilibrium conditions.

$$(XC)_1 = [K^{app} X_T - K^{app} (XC)_1] (C)_1 \qquad [A.8]$$

$$(XC)_2 = [K^{app} X_T - K^{app} (XC)_2] (C)_2 \qquad [A.9]$$

By substituting equilibrium (XC) and (C) values for the cases TOTFe = 10^{-3} M, TOTCd = 6.5×10^{-7} M and TOTFe = 10^{-3} M, TOTCd = 5.0×10^{-6} M into Eqs.[A.8] and [A.9], the following estimates were obtained:

$$K^{app} = 7.04 \times 10^{5}$$

$$X_T = 5.0 \times 10^{-6} \text{ M}$$

Using a fourth order Runge-Kutta formula to solve Eq. [A.7], values of f' and b' that enabled fits of the top two data sets in Figure A.2 were determined subject to the constraint that $K^{app} = f'/b'$. The parameter values selected were

$$f' = 3.52 \times 10^{4} \text{ hr}^{-1} \text{ M}^{-1}$$

$$b' = 0.05 \text{ hr}^{-1}$$

which provide excellent fits of the two data sets corresponding to the lower adsorbate/adsorbent ratios. As indicated in Figure A.2, the two data sets corresponding to higher ratios could not be fit with the same parameter values. Adsorption was significantly underpredicted for the lower two data sets for all times. The reason for this underprediction is apparent by noting that the values of TOTCd in both cases exceed X_T by at least an order of magnitude.

Hence, in both cases only a small fraction of TOTCd could be associated with the surface if the adsorption process was only one of surface complexation.

The same rate constants were employed to obtain the curves shown in Figure A.3. X_T was adjusted for the different values of TOTFe [M] using the relationship

$$X_T = 5 \times 10^{-3} \times \text{TOTFe} \qquad [A.10]$$

i.e., it was assumed that X_T is linearly related to TOTFe. As seen in Figure A.3, good fits are obtained for data sets with TOTCd < X_T. For the case TOTCd = 6.5×10^{-7} M, TOTFe = 10^{-4} M, however, adsorption is underpredicted for all times. Though TOTCd is greater than the X_T (= 5×10^{-7} M) in this case if Eq. [A.10] is valid, TOTCd does not exceed X_T to a sufficient extent to entirely explain the poor fit obtained. A better fit would result if either K_{app} or X_T were increased, but such changes would mean that either binding intensity or site density decreases with solid concentration. These possibilities are discussed in the next section of this report. For the present we simply conclude that adsorption rates slow with increasing adsorbate/adsorbent ratio and that a rate expression based on a surface complexation reaction only works for systems with low adsorbate/adsorbent ratios.

These experiments demonstrate that the commonly employed 1-4 hour equilibration times are adequate only for systems with low adsorbate/adsorbent ratios, i.e. systems with surface sites in great excess. At higher ratios, equilibration times of 30-48 hours or greater may be necessary. Considering the kinetics data for Cd

adsorption reported here, the data for Ag and Hg reported by Avotins (6) and Davis (7), and the data for Zn reported by Kinniburgh (22), 48 hour equilibration times would seem to be appropriate for adsorption experiments with HFO at higher TOTM/TOTFe ratios.

Summary

A systematic investigation of the kinetics of cadmium adsorption on hydrous ferric oxide at different initial adsorbate/adsorbent ratios was conducted. The kinetics of Cd^{2+} adsorption were observed to slow considerably as the adsorbate/adsorbent ratio was increased. At the lower ratios examined, reaction times of 0-15 hours were required for equilibrium while at the higher ratios equilibration times were on the order of 30-48 hours. The kinetics data obtained for systems with low ratios of adsorbate/adsorbent could be fit with a rate expression derived with the assumption of surface complex formation. Data obtained at higher adsorbate/adsorbent ratios could not be fit with the same rate expression. At the higher ratios the dominant adsorption mechanism may involve solid solution formation which would explain the continued adsorption after site saturation and the slower reaction kinetics. In any case, these results show that the adsorbate/adsorbent ratio must be taken into account in the design of equilibrium adsorption experiments with hydrous oxides and in the assessment of reported adsorption data for use in equilibrium models.

ACKNOWLEDGEMENT

The authors thank Thomas Army for the GC analyses.

REFERENCES

1. Morgan, J.J. and Stumm, W., "Colloid-Chemical Properties of Manganese Dioxide," Journal of Colloid Science, Vol. 19, 1964, pp. 347-359.

2. Murray, J.W., "The Interaction of Cobalt with Hydrous Manganese Dioxide," Geochimica et Cosmochimica Acta, Vol. 39, 1975, pp. 635-647.

3. Zasoski, R.J. and Burau, R.G., "A Technique for Studying the Kinetics of Adsorption in Suspensions," Soil Science Society of America Journal, Vol. 42, 1978, pp. 372-374.

4. Loganathan, P. and Burau, R.G., "Sorption of Heavy Metal Ions by a Hydrous Manganese Oxide," Geochimica et Cosmochimica Acta, Vol. 37, 1973, pp. 1277-1293.

5. McKenzie, R.M., "The Reaction of Cobalt with Manganese Dioxide Minerals," Australian Journal of Soil Research, Vol. 8, 1970, pp. 97-106.

6. Avotins, P.V. "Adsorption and Coprecipitation Studies of Mercury on Hydrous Iron Oxides," Ph.D. Thesis, Stanford University, 1975.

7. Davis, J.A. "Adsorption of Trace Metals and Complexing Ligands at the Oxide/Water Interface," Ph.D. Thesis, Stanford University, 1977.

8. Kurbatov, M.H. and Wood, G.B., "Rate of Adsorption of Cobalt Ions on Hydrous Ferric Oxide," Journal of Physical Chemistry, Vol. 56, 1952, pp. 698-701.

9. Kurbatov, M.H., Wood, G.B. and Kurbatov, J.D., "Isothermal Adsorption of Cobalt from Dilute Solutions," Journal of Physical Chemistry, Vol. 55, 1951, pp. 1170-1182.

10. Simon, V.J., Schulze, W. and Votz, M., "Eine kinetische Untersuchung der Cd^{2+}-Sorption an gelartigem Aluminiumhydroxid," Z. Anorg. Allg. Chem., Vol. 394, 1972, pp. 233-242.

11. Farley, K.J., Dzombak, D.A. and Morel, F.M.M., "A Surface Precipitation Model for the Sorption of Cations on Metal Oxides," Journal of Colloid and Interface Science, in press, 1985.

12. McAuliffe, C., "G.C. Determination of Solutes by Multiple Phase Equilibration," Chemical Technology, Vol. 1, 1971, pp. 46-51.

13. Crosby, S.A. et al., "Surface Areas and Porosities of Fe(III)- and Fe(II)-Derived Oxyhydroxides," Environmental Science and Technology, Vol. 17, 1983, pp. 709-713.

14. Davis, J.A. and Leckie, J.O., "Surface Ionization and Complexation at the Oxide/Water Interface. II," Journal of Colloid and Interface Science, Vol. 67, No. 1, 1978, pp. 90-107.

15. Murphy, P.J., Posner, A.M. and Quirk, J.P., "Characterization of Partially Neutralized Ferric Nitrate Solutions," Journal of Colloid and Interface Science, Vol. 56, No. 2, 1976, pp. 270-283.

16. van der Woude, J.H.A. and DeBruyn, P.L., "Formation of Colloidal Dispersions from Supersaturated Iron(III) Nitrate Solutions. I. Precipitation of Amorphous Iron Hydroxide," Colloids and Surfaces, Vol. 8, 1983, pp. 55-78.

17. Morel, F.M.M. Principles of Aquatic Chemistry, John Wiley and Sons, Inc., New York, NY, 1983.

18. Nyffeler, U.P., Li, Y.H. and Santschi, P.H., "A Kinetic Approach to Describe Trace-Element Distribution Between Particles and Solution in Natural Aquatic Systems," Geochimica et Cosmochimica Acta, Vol. 48, 1984, pp. 1513-1522.

19. Schindler, P.W., "Surface Complexes at Oxide-Water Interfaces," Adsorption of Inorganics at Solid-Liquid Interfaces, M.A. Anderson and A.J. Rubin, eds., Ann Arbor Science, Ann Arbor, MI, 1981, pp. 1-49.

20. Rudin, M. and Motschi, H., "A Molecular Model for the Structure of Copper Complexes on Hydrous Oxide Surfaces: An ENDOR Study of Ternary Cu(II) Complexes on δ-Alumina," Journal of Colloid and Interface Science, Vol. 98, No. 2, 1984, pp. 385-393.

21. Harvey, D.T. and Linton, R.W., "X-ray Photoelectron Spectroscopy (XPS) of Adsorbed Zinc on Amorphous Hydrous Ferric Oxide," Colloids and Surfaces, Vol. 11, 1984, pp. 81-96.

22. Kinniburgh, D.G., "The H^+/M^{2+} Exchange Stoichiometry of Calcium and Zinc Adsorption by Ferrihydrite," Journal of Soil Science, Vol. 34, 1983, pp. 759-768.

II.B EQUILIBRIUM ADSORPTION OF CADMIUM AND ZINC ON HYDROUS FERRIC OXIDE

Introduction

In the surface precipitation model for equilibrium metal ion adsorption on hydrous oxides (1,2), a transition from surface complexation to surface precipitation (solid solution formation) is considered to occur as reactive surface sites become completely occupied. This mechanism, which is depicted schematically in Figure B.1 for the adsorption of a metal cation to hydrous ferric oxide, is somewhat analogous to the mechanism proposed by Brunauer et al. (3) for adsorption of gases onto solids. The BET theory for multilayer adsorption at the gas/solid interface involves a transition from adsorption at reactive sites to condensation of gas molecules adsorbing subsequently at the occupied sites.

At constant pH, the mathematical formulation of the surface precipitation model reduces to an isotherm equation which is similar to the BET isotherm equation. This similarity is evident by comparing the classic BET isotherm plot with isotherm plots computed with the surface precipitation model, e.g Figure B.2 for the adsorption of a metal cation on hydrous ferric oxide. At low metal concentrations, surface complexation is the dominant adsorption mechanism and adsorption follows a Langmuir isotherm. As metal concentration is increased and saturation of reactive sites is approached, surface precipitation becomes increasingly important. In this range adsorption follows a Freundlich isotherm. With further increases in metal concentration surface precipitation dominates the adsorption process and the model predicts a smooth transition between surface reactions and bulk solution precipitation of the adsorbate metal.

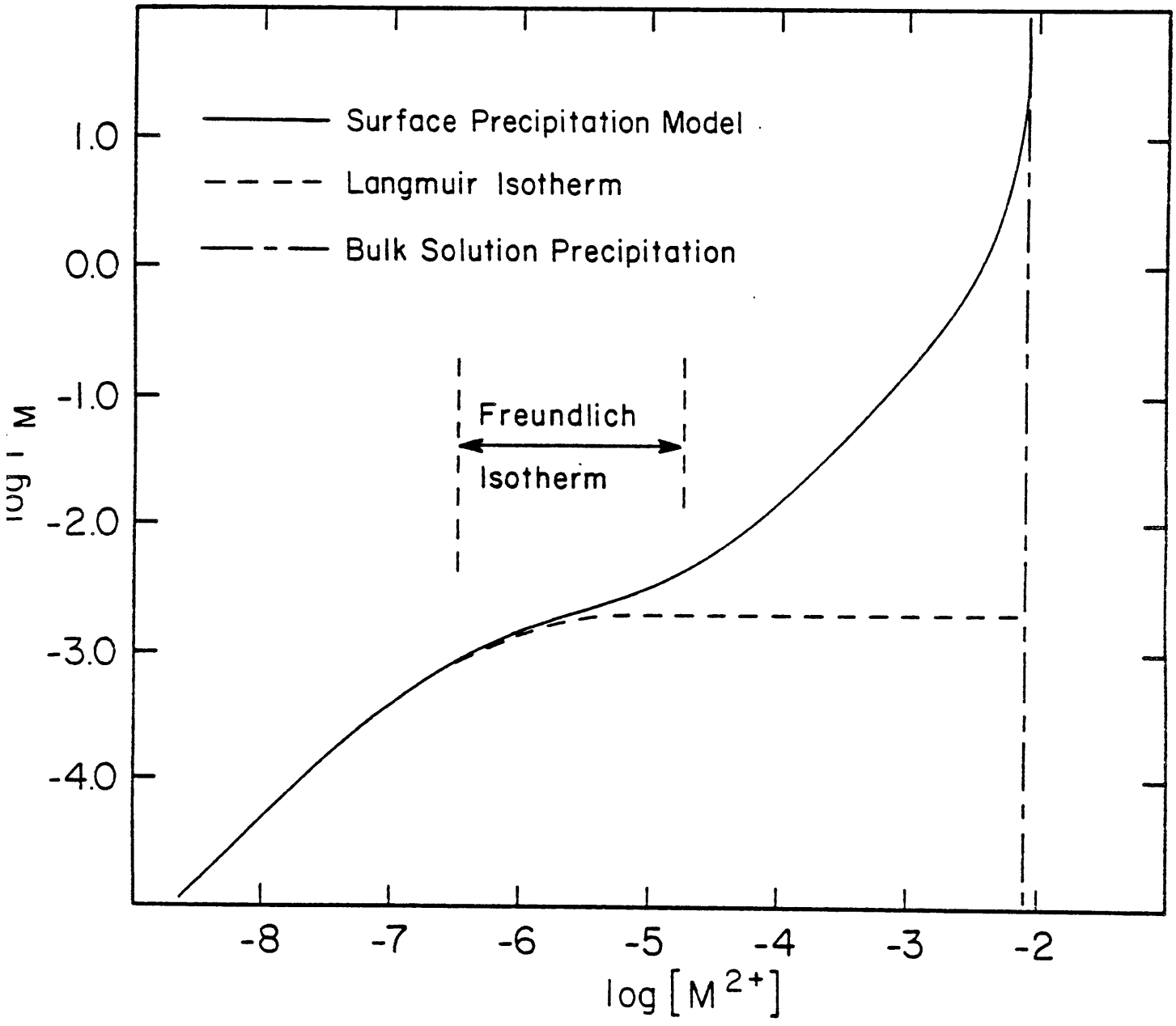

Figure B.1 Adsorption isotherms predicted by the basic surface complexation model and the surface precipitation model.

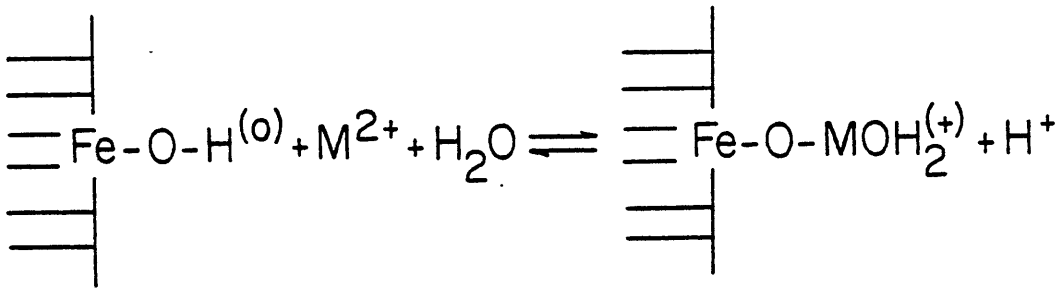

Schematic of surface complexation model

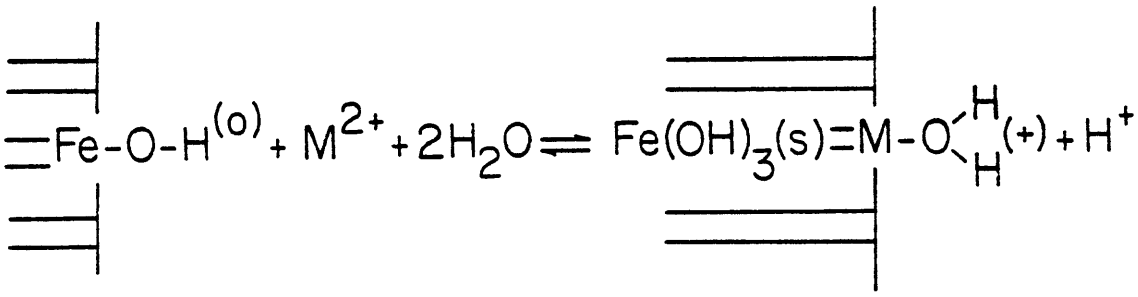

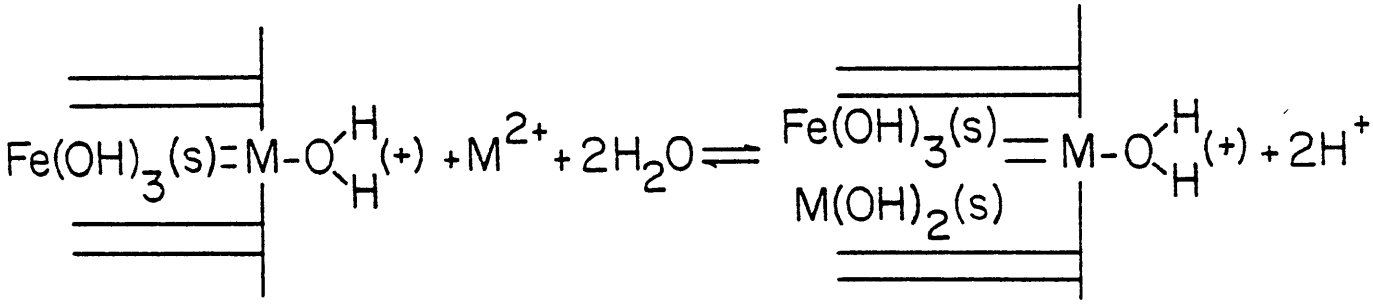

Schematic of surface precipitation model

Figure B.2 Conceptual models for cation adsorption on hydrous ferric oxide.

Though the linear (surface complexation) and nonlinear (transition) regions of the isotherm shown in Figure B.2 have been observed experimentally, past experimental studies of metal adsorption have not been carried out at sufficiently high adsorbate concentrations to verify the shape of the isotherm in the region where surface precipitation is expected to dominate. At metal concentrations that approach bulk solution precipitation, the surface precipitation model predicts a rapid increase in adsorption density. To test this prediction, we conducted equilibrium adsorption experiments with cadmium and hydrous ferric oxide (HFO) for a wide range of adsorbate concentrations in order to develop a complete adsorption isotherm. In this section we present the results of these experiments and interpret them in terms of the surface precipitation model. We also compare our results with some recent data for zinc adsorption on HFO that span a wide range of Zn concentrations.

Experimental

Experimental materials and methods were the same as described in Section II.A with the following exceptions. The equilibration time for all experiments was 48 hours. Samples were withdrawn and analyzed two or three times after 24 hours to insure the attainment of equilibrium at 48 hours. For TOTCd greater than 10^{-3} M, no correction for adsorption onto the filter apparatus was necessary. In some of the systems with very high TOTCd and TOTFe inputs, lesser amounts (or no) $NaNO_3$ was necessary to achieve an ionic strength of 0.1 M. For the highest TOTCd and TOTFe systems, ionic strength was greater than 0.1 M but in no case exceeded 0.5 M (see raw data in Appendix B).

Results and Discussion

Results from the equilibrium adsorption experiments with cadmium and hydrous ferric oxide at pH=7.50 and 0.1 M ionic strength are presented in Figure B.3. Data obtained by Benjamin (1978) under the same conditions of pH and ionic strength but with somewhat different experimental methods are also given for comparison.

The Cd-HFO isotherm appears to exhibit a linear relationship between p(Cd) and $p\Gamma_{Cd}$ at low metal concentrations (less than 10^{-6} M), especially if the data obtained in systems with lower (10^{-4}, $2x10^{-4}$ M TOTFe) and higher (10^{-3}, $5x10^{-3}$ M TOTFe) solid concentrations are considered separately. The approximate 0.3 log unit difference in adsorption density between the two sets of data indicates that adsorption at the lower solid concentrations exceeds that at the higher concentrations by a factor of two. Honeyman (4) has observed a solid concentration effect of similar magnitude for Cr(VI) adsorption onto Al_2O_3 and HFO. Wheter this solid concentration effect is due to experimental artifacts (5), to a decrease in effective surface area by coagulation, or to some other process is not known. The scatter in the Cd-HFO isotherm is reduced significantly if data for only one solid concentration are considered (Figure B.4).

The line with slope 1.0 drawn on Figure B.3 through the data at low metal concentrations was computed with the assumption of a surface complexation reaction as described in Section II.A (Eq. [A.1]); the stability constant K and the site concentration X_T derived in Section II.A were used for the calculation. Recall that K and X_T were derived by solving simultaneous mass law expressions for two systems with TOTFe = 10^{-3} M (points indicated by check marks in Figure B.3). The noncoincidence of the isotherms for the low and high solid

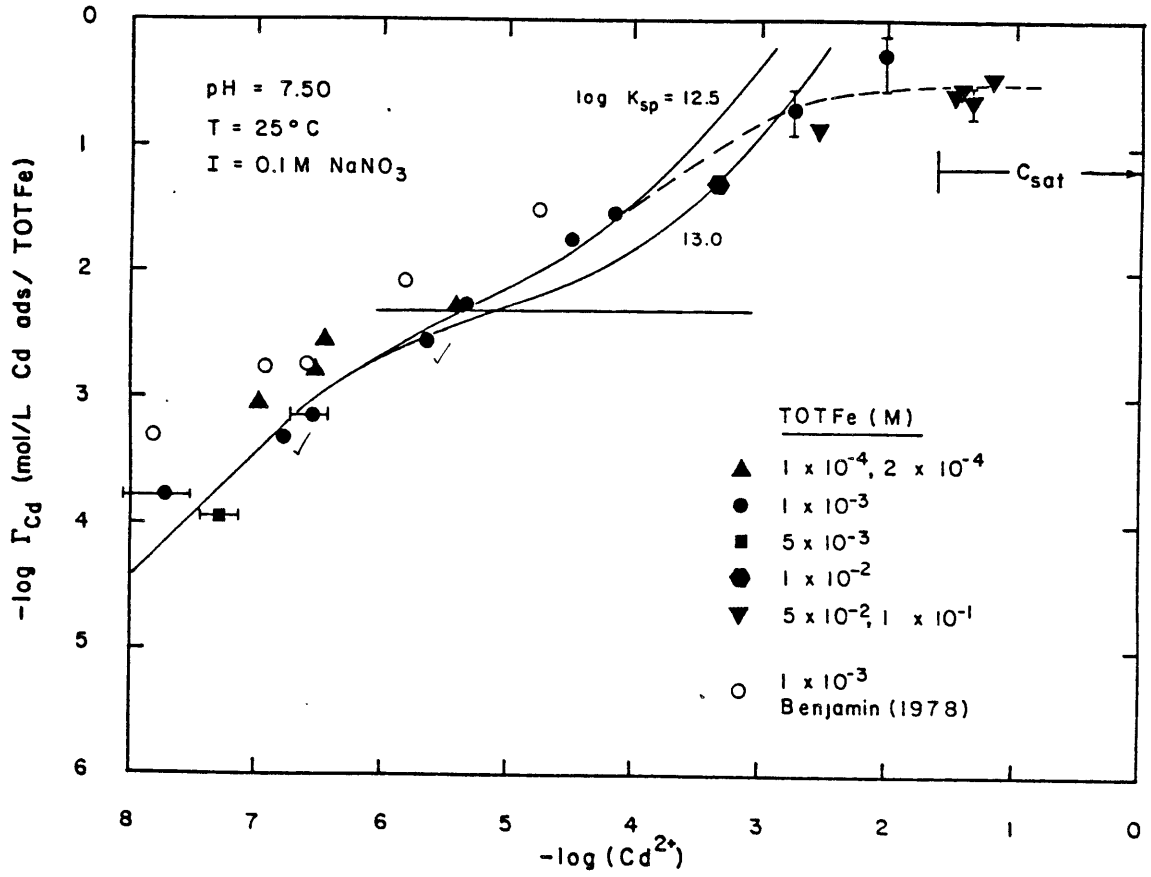

Figure B.3 Adsorption isotherm for adsorption of Cd^{2+} on hydrous ferric oxide at pH = 7.50. The various fitted curves are described in the text. C_{sat} represents Cd^{2+} concentrations at which bulk solution precipitation of $Cd(OH)_{2(s)}$ is expected based on reported solubility products.

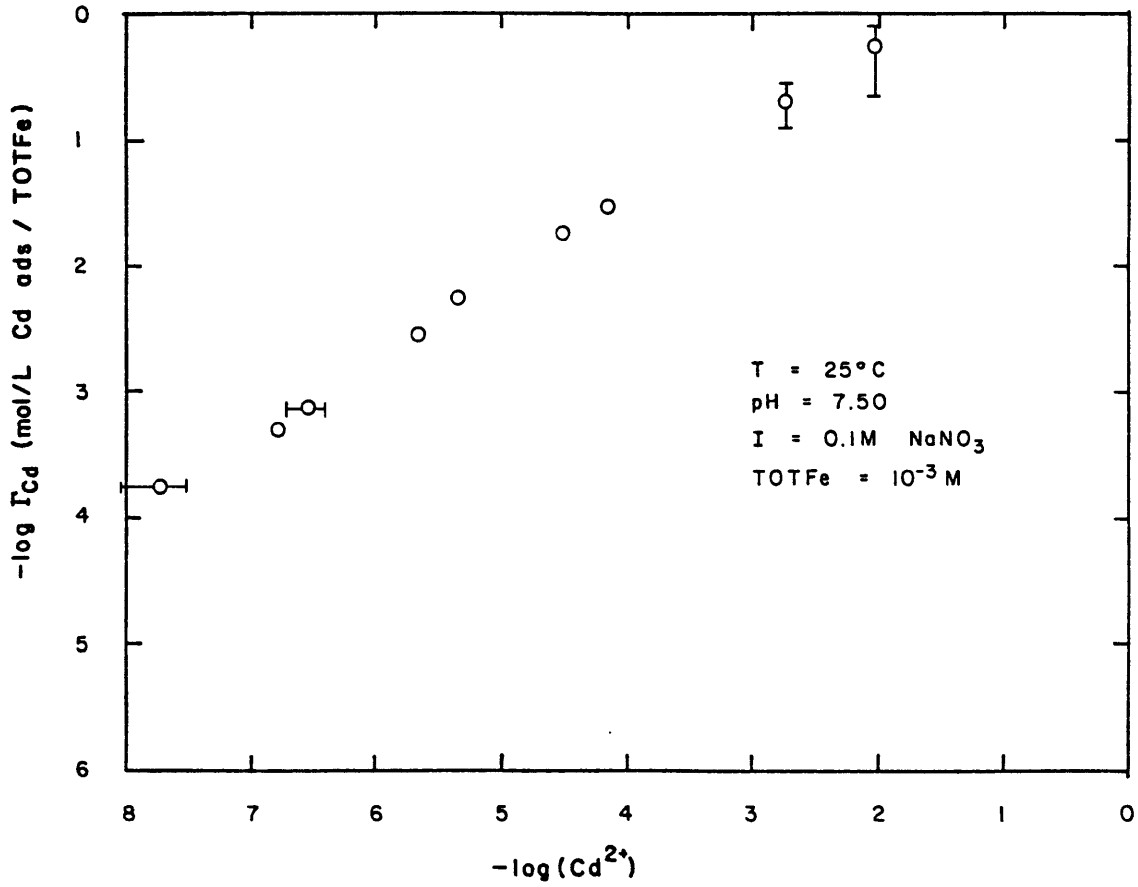

Figure B.4 Adsorption isotherm for adsorption of Cd^{2+} on hydrous ferric oxide at pH = 7.50. These data are extracted from Figure B.3 and correspond to a constant solid concentration of TOTFe = 10^{-3} M.

concentration systems (the solid concentration effect) explains why the kinetics data for TOTFe = 10^{-4} M (Figure A.3; bottom plot) could not be fit with the same rate constants as the kinetics data for TOTFe = 10^{-3}, $5x10^{-3}$ M (Figures A.2, A.3; top two plots). The forward (f) and reverse (b) rate constants were selected such that f/b = K, where the value of the stability constant K was optimal for TOTFe = 10^{-3} M. Note in Figure A.3 that adsorption is underpredicted by approximately a factor of 2 for TOTFe = 10^{-4} M. This is precisely what one would expect from the isotherm data in that adsorption densities for TOTFe = 10^{-4} M systems are about a factor of 2 higher than those for systems with TOTFe = 10^{-3}, $5x10^{-3}$ M.

In terms of the surface precipitation model, the surface complexation reaction of Cd^{2+} with HFO can be expressed as

$$\equiv FeOH_2^+ + Cd^{2+} + 3H_2O = Fe(OH)_{3(s)} + =CdOH_2^+ + 2H^+ \qquad [B.1]$$

where the surface symbols ≡ and = are used to denote bonds of the metal atoms at the surface of the solid and have different meanings for Fe^{3+} and Cd^{2+}: ≡FeOH° represents $[Fe(OH)_3]_n$ and =CdOH° represents $[Cd(OH)_2]_n$. Thus, reaction [B.1] is balanced with respect to H and O. The stability constant for reaction [B.1] is given by

$$K = \frac{\{Fe(OH)_{3(s)}\}\ (=CdOH_2^+)\ \{H^+\}^2}{(\equiv FeOH_2^+)\ (Cd^{2+})} \qquad [B.2]$$

At low Cd^{2+} concentrations the activity of the hydrous ferric oxide is very close to unity; hence Eq. [B.2] is equivalent to Eq. [A.1] and the same stability constant is applicable. The line with slope 1.0 drawn through the isotherm for (Cd^{2+}) less than 10^{-6} M corresponds to

Eq. [B.2], with unit solid activity and pK = 9.15, combined with conservation equations for total sites and total adsorbate (see Eqs. [A.5] and [A.6]). The horizontal line drawn on Figure B.2 indicates saturation of binding sites, i.e. log of TOT(≡FeOH)/TOTFe.

As adsorbate concentrations are increased the surface precipitation model predicts that the dominant adsorption mechanism shifts from surface complexation to solid solution formation (details given in Refs. 1,2). Metals at the solid/liquid interface are treated as surface complexes, while metals buried within the solid phase are treated as solid species. Activities of solution species and surface complexes are assumed to be equal to their concentrations while the activities of the solid species, for a first approximation, are assumed to be equal to their mole fractions (ideal solid solution behavior). For adsorption of Cd^{2+} on HFO, the equations which define the surface precipitation model (for constant pH) include Eq. [B.2] and the following:

$$=CdOH_2^+ + Cd^{2+} + 2H_2O = Cd(OH)_{2(s)} + =CdOH_2^+ + 2H^+ \qquad 1/K_{SP(Cd)} \qquad [B.3]$$

$$\equiv FeOH_2^+ + Fe^{3+} + 3H_2O = Fe(OH)_{3(s)} + \equiv FeOH_2^+ + 3H^+ \qquad 1/K_{SP(Fe)} \qquad [B.4]$$

$$TOTCd = (Cd^{2+}) + (=CdOH_2^+) + (Cd(OH)_{2(s)}) \qquad [B.5]$$

$$TOTFe = (Fe^{3+}) + (\equiv FeOH_2^+) + (Fe(OH)_{3(s)}) \qquad [B.6]$$

$$TOT(\equiv FeOH) = (\equiv FeOH_2^+) + (=CdOH_2^+) \qquad [B.7]$$

$$\{Fe(OH)_{3(s)}\} = (Fe(OH)_{3(s)})/[(Fe(OH)_{3(s)}) + (Cd(OH)_{2(s)})] \qquad [B.8]$$

$$\{Cd(OH)_{2(s)}\} = (Cd(OH)_{2(s)})/[(Fe(OH)_{3(s)}) + (Cd(OH)_{2(s)})] \qquad [B.9]$$

Since this system of 8 equations contains 8 unknowns, ($\equiv Cd(OH)_2^+$) and ($Cd(OH)_{2(s)}$) can be determined explicitly and an analytical isotherm (constant pH) expression can be derived (1,2). If the solubility product for HFO ($K_{SP(Fe)}$) is regarded as fixed, the surface precipitation isotherm equation contains three fitting parameters: K, TOT(≡FeOH), and $K_{SP(Cd)}$. The use of $K_{SP(Cd)}$ as a fitting parameter means that the solid phase activity coefficient for $Cd(OH)_{2(s)}$ is not unity, i.e. deviation from ideal solid solution behavior is allowed.

For the Cd-HFO adsorption data in Figure B.3, the two solid curves that coincide and become linear for p(Cd) > 6 are isotherms predicted with the surface precipitation model for log $K_{SP(Cd)}$ equal to 12.5 and 13.0; values for the surface complexation constant and total binding sites were derived previously (pK = 9.15, TOT(≡FeOH) = $5x10^{-6}$ M). The range of values reported in the literature for $K_{SP(Cd)}$ is 13.4 to 15.4. As evident in Figure B.3, the surface precipitation model provides an adequate fit of the data at low to moderate values of (Cd^{2+}). At high values of free cadmium, however, the predicted rapid increase in adsorption density is not observed. Instead, the data indicate a maximum adsorption density. To our knowledge, this is the first time that surface saturation has been observed for adsorption of a metal cation on a hydrous oxide. Harvey and Linton (6) reported saturation for Zn adsorption on HFO at pH values less than 6.5, but their experiments were conducted with only four hour equilibration times. As demonstrated in Section II.A (and in fact also by Harvey and Linton), longer equilibration times are appropriate at high adsorbate/adsorbent ratios.

The leveling off of the Cd-HFO isotherm indicates adsorptive saturation but at higher concentrations a transition to precipitation must occur in the isotherm. [In this study experiments at higher TOTCd (and TOTFe) concentrations could not be conducted without the ionic strength greatly exceeding 0.1 M. On the basis of prior theoretical work we expected a rapid increase in adsorption density at a lower Cd concentration, and so for consistency with much other data we chose to use I = 0.1 M.] Indeed, there is evidence for a smooth transition between adsorption and precipitation in some recent data for zinc adsorption on HFO. Nevertheless, it is clear that neither the single site-type surface complexation model nor the surface precipitation model with only one type of reactive site is capable of the fitting the data in Figure B.3. A two site surface complexation model [$TOT(\equiv FeOH)_I = 5x10^{-6}$ M, $pK_I = 9.15$; $TOT(\equiv FeOH)_{II} = 3.16x10^{-4}$ M, $pK_{II} = 12.0$] provides a better fit of the data (dashed curve in Figure B.3), but is not consistent with a smooth transition between adsorption and precipitation..

The surface precipitation model (2) is not exclusive of a multiple site model(7), and a merger of the two seems appropriate in view of the Cd-HFO adsorption data obtained in this study and the Zn-HFO data discussed below. For example, surface precipitation can be incorporated in a two site model by considering surface precipitation reactions to occur at type II sites. This combined model would give a smooth transition between adsorption and precipitation but at higher metal concentrations as observed.

Figure B.5 shows the data of Kinniburgh and Jackson (8) for adsorption of Zn on HFO at pH=6.5, with supplemental data from

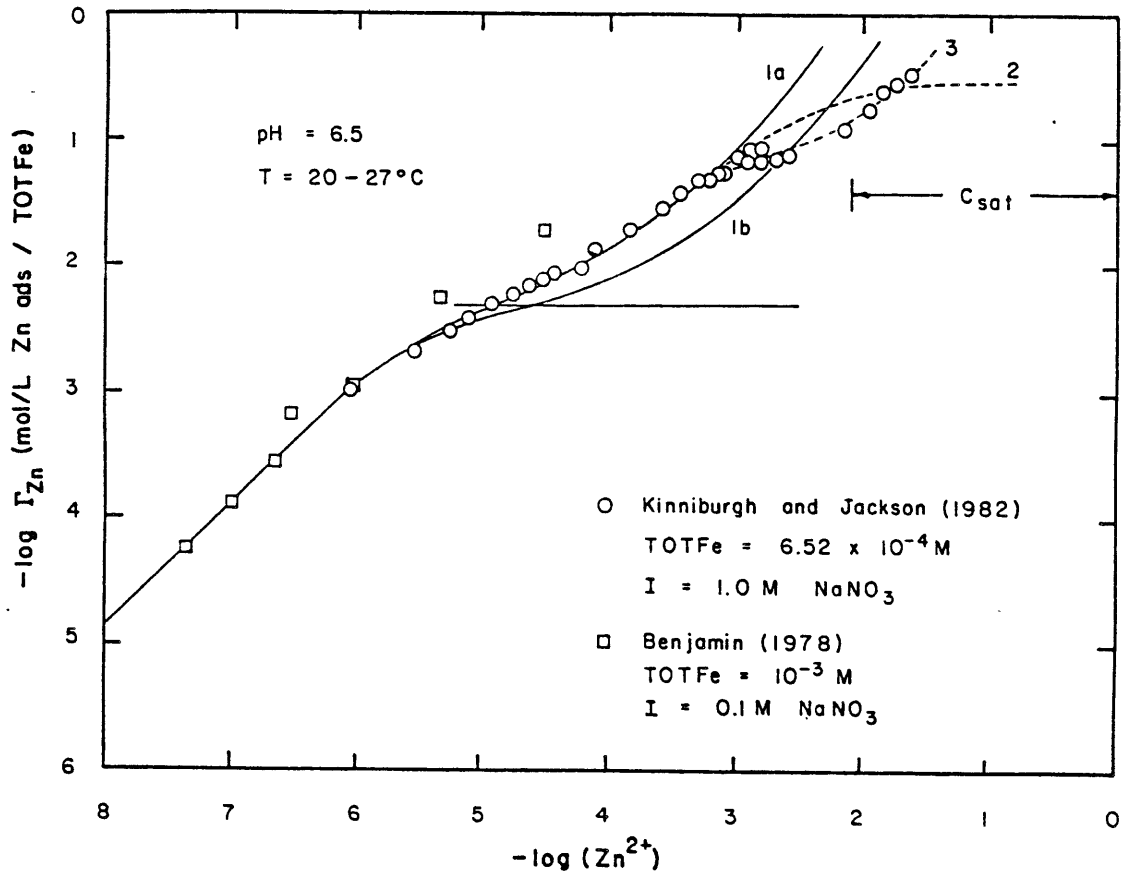

Figure B.5 Adsorption isotherm for adsorption of Zn^{2+} on hydrous ferric oxide at pH = 6.50. The various fitted curves are described in the text. C_{sat} represents Zn^{2+} concentrations at which bulk solution precipitation of $Zn(OH)_{2(s)}$ is expected based on reported solubility products.

Benjamin (9). The curves fitted to the data are

(1a) surface precipitation model, one site type (substitute Zn for Cd in Eqs. [B.3]-[B.9]): $\log K_{SP(Zn)} = 11.1$; pK = 7.6; $TOT(\equiv FeOH) = 3.26 \times 10^{-6}$ M

(1b) same as (1a), but with $\log K_{SP(Zn)} = 11.5$;

(2) two site model: $TOT(\equiv FeOH)_I = 3.26 \times 10^{-6}$ M, $pK_I = 7.6$; $TOT(\equiv FeOH)_{II} = 2.06 \times 10^{-4}$ M, $pK_{II} = 10.5$

(3) two site model with surface precipitation on type II sites: $TOT(\equiv FeOH)_I = 3.26 \times 10^{-6}$ M, $pK_I = 7.6$; $TOT(\equiv FeOH)_{II} = 5.18 \times 10^{-5}$ M, $pK_{II} = 7.2$; $\log K_{SP(Zn)} = 12.1$

Reported values for the log of the solubility product for $Zn(OH)_{2(s)}$ range from 10.9 to 12.5. As seen in Figure B.4, the combined two site surface precipitation model provides an excellent fit of the data at high concentrations of (Zn^{2+}), while either model alone tends to overestimate adsorption in this region of the isotherm. [Note that the number of Type II sites could be lowered for case (2), say to the level used in case (3), and adsorption would be underestimated for $(Zn^{2+}) = 10^{-3} - 10^{-1.5}$ M]. Kinniburgh and Jackson (8) note that for (Zn^{2+}) greater than $10^{-1.5}$ M adsorption density continued to increase rapidly but they do not present the data.

In a study of the mechanism of Zn adsorption on HFO using X-ray photoelectron spectroscopy, Harvey and Linton (6) found evidence for surface precipitation of $Zn(OH)_{2(s)}$ at relatively high TOTZn concentrations under solution conditions not conducive to bulk solution precipitation. In fact, they began to observe surface precipitation at zinc concentrations slightly in excess of our estimated concentration of Type I sites. Thus, there is some

experimental evidence that seems to corroborate our hypothesis of surface precipitation occurring on weaker (Type II) binding sites.

The Cd-HFO isotherm developed in this study (Figure B.3) and the Zn-HFO isotherm developed by Kinniburgh and Jackson (Figure B.5) both span much wider ranges in free metal concentrations than any published metal cation adsorption data. Both isotherms have data in the high metal concentration region near bulk solution precipitation of the hydroxide of the adsorbate metal. On a log-log plot these isotherms essentially consist of two linear segments, one for low concentrations and one for moderate to high concentrations. Ignoring for the moment the region of the isotherm close to precipitation, it seems that for low to moderate metal concentrations the two site model is the simplest way to fit data. [For HFO, the site concentrations can be fixed according to the ratios $TOT(\equiv FeOH)_I/TOTFe \cong 0.005$ and $TOT(\equiv FeOH)_{II}/TOTFe \cong 0.1\text{-}0.3$, and the surface complexation constants can be determined by fitting existing data.] In the range of metal concentrations of interest in aquatic systems, the refinement offered by the surface precipitation model will probably not be necessary. Nevertheless, it provides a reliable means for modelling the transition between adsorption and precipitation at high metal concentrations which may be encountered in some treatment processes. On the basis of the Zn-HFO adsorption data examined in this study, it appears that the bulk solution solubility product of the adsorbate metal can be used reliably as a first approximation in the surface precipitation model. Thus, the surface precipitation model can be incorporated in a two site surface complexation model without increasing the number of fitting parameters.

Summary

Equilibrium adsorption experiments with cadmium and hydrous ferric oxide were conducted for a wide range of adsorbate concentrations in order to develop a complete isotherm. Past experimental studies have not been carried out at sufficiently high adsorbate concentrations to verify the shape of the isotherm in the region where surface precipitation is expected to dominate.

The Cd-HFO adsorption data obtained in this study follow a Langmuir isotherm at low free metal concentrations (less than 10^{-6}M) and a Freundlich isotherm at low to moderate concentrations (10^{-6}M - 10^{-4}M). Similar isotherm characteristics have been observed in previous metal adsorption studies. At the highest free metal concentrations examined here, a plateau in adsorption density was observed. To our knowledge,this is the first time that surface saturation has been observed for adsorption of a metal cation on a hydrous oxide. Another interesting feature of the isotherm is that, for the same soluble Cd concentration, the adsorption density of Cd on HFO is a function of solid concentration; i.e., the partition coefficient decreases with increasing solid concentration. Whether this solid concentration effect is due to experimental artifacts, to a decrease in effective surface area by coagulation, or to some other process is not known.

The Cd-HFO isotherm was best modelled with a two site surface complexation model since at the highest Cd concentrations examined a maximum adsorption density was observed. Though the rapid increase in adsorption density predicted by the surface precipitation model was not observed for the range of Cd concentrations studied, it has been observed in isotherm data for Zn adsorption on HFO (8). To fit the Zn

data, a two site surface complexation model with surface precipitation of Type II sites is necessary. The idea of surface precipitation at high adsorption densities (and hence on weaker binding sites) seems to be corroborated by some recent XPS measurements (6).

A two site surface complexation model coupled with surface precipitation on Type II sites is capable of fitting all available metal adsorption data. Such a model involves a minimum of four and possibly five adjustable parameters: total Type I and Type II binding sites, surface complexation constants for each site type, and, possibly, the solubility product for the adsorbate metal. On the basis of the Zn-HFO adsorption data, it appears that the surface precipitation model can be incorporated in a two site surface complexation model without increasing the number of fitting parameters. In the range of metal concentrations of interest in most aquatic systems, a two site model will be sufficient for adsorption modelling. However, inclusion of surface precipitation will be necessary at high metal concentrations which may be encountered in some treatment processes.

REFERENCES

1. Farley, K.J., Harleman, D.R.F., and Morel, F.M.M., "Ponding of Effluents from Fossil Fuel Steam Electric Power Plants," MIT-EL 84-007, MIT Energy Laboratory, Cambridge, MA, 1984.

2. Farley, K.J., Dzombak, D.A., and Morel, F.M.M., "A Surface Precipitation Model for the Sorption of Cations on Metal Oxides," Journal of Colloid and Interface Science, in press, 1985.

3. Brunauer, S., Emmett, P.H., and Teller, E., "Adsorption of Gases in Multimolecular Layers," Journal of American Chemical Society, Vol. 60, 1938, pp. 309-319.

4. Honeyman, B., "Cation and Anion Adsorption at the Oxide/Solution Interface in Systems Containing Binary Mixtures of Adsorbents: An Investigation of the Concept of Adsorptive Additivity," Ph.D. Thesis, Stanford University, 1984.

5. Gschwend, P.M. and Wu, S.C., "On the Constancy of Sediment-Water Partition Coefficients of Hydrophobic Organic Pollutants," Environmental Science and Technology, Vol. 19, No. 1, 1985, pp. 90-96.

6. Harvey, D.T. and Linton, R.W., "X-ray Photoelectron Spectroscopy (XPS) of Adsorbed Zinc on Amorphous Hydrous Ferric Oxide," Colloids and Surfaces, Vol. 11, 1984, pp. 81-96.

7. Benjamin, M.M. and Leckie, J.O., "Multiple-Site Adsorption of Cd, Cu, Zn, and Pb on Amorphous Iron Oxyhydroxide," Journal of Colloid and Interface Science, Vol. 79, No. 1, 1981, pp. 209-221.

8. Kinniburgh, D.G. and Jackson, M.L., "Concentration and pH Dependence of Calcium and Zinc Adsorption by Iron Hydrous Oxide Gel," Soil Science Society of America Journal, Vol. 46, 1982, pp. 56-61.

9. Benjamin, M.M., "Effects of Competing Metals and Complexing Ligands on Trace Metal Adsorption at the Oxide/Solution Interface," Ph.D. Thesis, Stanford University, 1978.

CHAPTER III

MODELS FOR ADSORPTION OF INORGANIC CONTAMINANTS IN AQUATIC SYSTEMS

INTRODUCTION

The fate of trace pollutants in natural waters and water treatment processes is often controlled by adsorption reactions with mobile or fixed adsorbents. In addition to affecting the physical transport of dissolved species, adsorption can lead to changes in chemical reactivity and/or biological availability.

In a recent review article, Karickhoff (1) expounded the dominant scientific concepts now used to explain and model the adsorption of trace organic pollutants in aquatic systems. Here we wish to discuss the concepts and the models used to describe and quantify the adsorption of trace inorganic compounds. These two related fields, trace organic and trace inorganic adsorption, can be contrasted both in their underlying principles and in their intents.

Trace organic (ad)sorption is conceived as a solvent partitioning process, a view which provides great generality of application but little insight into the details of molecular association between solids and solutes. The major interest here is order of magnitude prediction for the partitioning of many compounds under many conditions. Indeed, sorption of hydrophobic trace organic compounds can be roughly predicted with a remarkably small number of parameters describing the solid and the solute (e.g., organic content and octanol/water partition coefficient).

In contrast, adsorption of trace inorganic solutes, mostly ions, is conceived as a surface coordination process implying a detailed molecular picture. A major goal of this approach is to provide a physical-chemical explanation for the interrelation between electrostatic charge development on solid surfaces, and ion adsorption.

While the electrostatic interaction between the solid and the solute is amenable to a general treatment, the dominant chemical interaction is specific for each solid-solute pair and its description requires extensive empirical information. The resulting thermodynamic models are (or at least appear) complicated, data intensive, and not as general as one would wish. The specificity of the physical-chemical interactions demands this level of detail, however. Similar site-specific models will likely be needed to describe adsorption of polar organic compounds since available empirical formulations for "nonhydrophobic" contributions are unsatisfactory (1).

Unlike hydrophobic sorption which depends chiefly on the organic content of the solid, surface coordination of ions depends strongly on the nature of the adsorbing phase. One must thus decide in a review like this which particular solid phases to consider as important adsorbents. Potential adsorbents in aquatic systems comprise biotic (e.g. algae, bacteria, zooplankton) and abiotic particles, both inorganic and organic. The most common inorganic adsorbents are hydrous metal oxides (as homogeneous phases or coatings), clays, and sands, while the most common organic adsorbents consist of plant and animal remains and humic coatings on mineral surfaces.

Among the inorganic adsorbents, metal oxides have the highest affinity for ions because of their charged, reactive hydroxyl surface sites combined with their high surface area. Hydrous oxides also are prevalent as coatings on all types of particles, including clays (whose edges have an oxide structure), other mineral phases, particulate organic matter (2,3), fly ash in settling ponds (4,5), and even the surfaces of algal cells (6). Because of their ubiquitous presence and their strong affinity for inorganic ions, we focus here on adsorption on

hydrous metal oxides -- chiefly, oxides of iron, manganese, aluminum and silicon which are the dominant inorganic adsorbents in natural waters (2,3,7) and in many water treatment processes as well (5,8,9,10,11).

Adsorption of ions by organic coatings on mineral surfaces is suspected to be significant in aquatic systems with an abundance of dissolved humic material. Many studies of ion binding by dissolved humic material have been performed, but investigations of ion binding by mineral surfaces coated with humic material have only recently commenced. Factors that govern the accumulation of humic material on mineral surfaces and the effects of the accumulated material on metal binding are not well understood and are given only scant treatment in this review.

The historical development of the scientific concepts used to describe surface phenomena in oxide suspensions has oscillated between physical and chemical paradigms (12). Our understanding of the processes at electrified interfaces in solution is now based on the classical double layer theory (Gouy-Chapman) and its extensions (Stern-Grahame). The charge development mechanism for oxides is different from that of reversible electrodes such as AgI, however. Early theoretical studies, which focused on the application of electrode theory to oxides, served to elucidate the differences (see Ref. 13). Out of this work a common modelling approach has emerged based on the surface ionization concept first introduced in studies of ion binding by proteins (14).

In the surface ionization (or complexation) approach, surface charge is considered to develop on oxides via ionization reactions at specific surface sites. Adsorption of ions on oxide surfaces is viewed as analogous to the formation of soluble complexes: i.e. ions

(including H^+ and OH^-) bind to functional groups at the surface and these reactions can be described by mass law equations. With knowledge of the number of functional groups and their binding constants, surface charge can be computed for different conditions in solution. Models combining the classical Gouy-Chapman-Stern-Grahame approach and the surface ionization concept have performed reasonably well in describing surface acid-base chemistry and ion binding to oxide surfaces.

Various empirical approaches have also been used to model ion binding by oxide surfaces, including partition coefficients, isotherm equations, and Kurbatov plots (15,16). Empirical descriptions are necessarily limited to particular conditions and are not easily extrapolated to other conditions of pH and ionic strength. On the other hand, models based on chemical theory, even if containing some empirical components, enable prediction of equilibrium adsorption beyond the range of available data.

Due to their apparent complexity and to their multiplicity, current inorganic adsorption models have only been used by those directly involved in the field and their practical application lags far behind that of partitioning models for hydrophobic organics. The intent of this article is to remedy that situation by providing a simple and compact review of the dominant paradigms of inorganic adsorption, by defining the field of applicability as well as the limitations of the resulting models, and by demonstrating their usefulness in practical situations.

Hydroxyl Surface Sites

When a metallic oxide is exposed to water or its vapor, surface hydroxyls are formed as illustrated in Figure 1. Metal ions in the surface layer of a dry oxide are not fully coordinated (Figure 1a), and water molecules when present occupy these vacant coordination sites via chemisorption (Figure 1b). The surface becomes hydroxylated by proton transfer from the bound water molecules to the neighboring oxide ions (Figure 1c). Proton transfer is energetically favored because better charge neutralization in the lattice is achieved; i.e. the univalent hydroxide ions can fit nearer to the centers of positive charge than the divalent oxide ions (17).

Infrared spectroscopic studies have indicated the existence of different types of hydroxyl sites on hydrous oxide surfaces. Typically, several chemically distinct site types are inferred from infrared spectra obtained for different degrees of surface dehydration (e.g. see Ref. 18). In the idealized structural model of Figure 1c two types of OH groups can be distinguished: those bound to one metal ion and those bound to two metal ions. Boehm (17) observed that the doubly-coordinated OH groups should be strongly polarized by the cations, thus loosening the bond to hydrogen and resulting in acidic character. For the singly-coordinated OH groups the polarization should be much weaker; these groups should be basic in character and possibly exchangeable for other anions. Acidic and basic surface OH groups have been detected by means of infrared hydroxyl stretching frequencies (19) and approximately quantified via reaction with site-specific reagents (17).

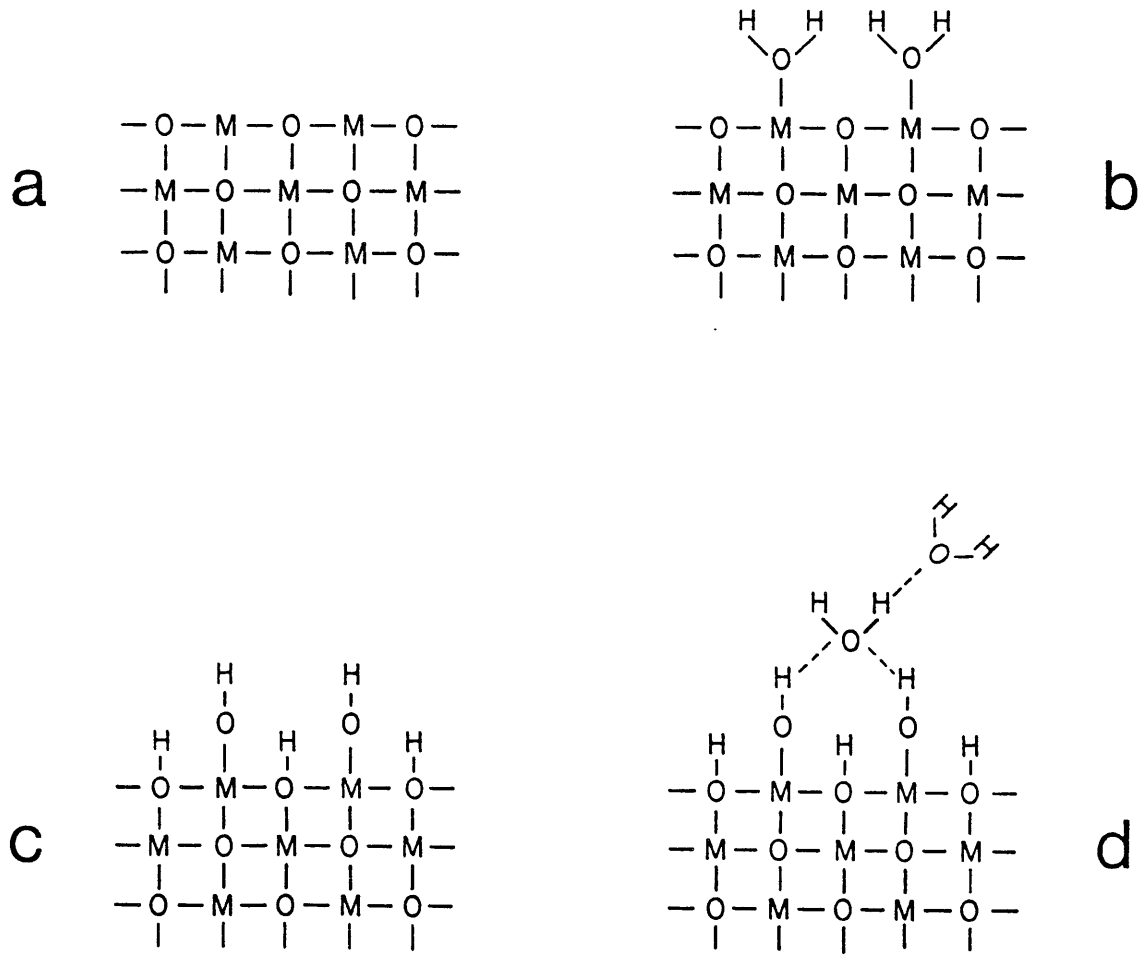

FIG. 1.-Cross-section of the surface layer of a metal oxide.
Adapted from Refs. 21 and 55.
(a) Surface ions are coordinatively unsaturated.
(b) Surface metal ions coordinate H_2O molecules in the presence of water.
(c) Dissociative chemisorption leads to a hydroxylated surface.
(d) Physisorption of water on the hydroxylated surface.

Water binds to surface OH groups and is thus structured at the oxide/water interface. Heat of immersion studies (20,21) and surface spectroscopy (22) suggest water adsorption to the surface, possibly as illustrated in Figure 1d. The first layer of water is formed by hydrogen bonding of a single water molecule to two surface hydroxyls, and an ice-like structure (restricted rotation, stronger hydrogen bonding than liquid water) is developed in the next few layers. This structuring of interfacial water may tend to give uniform effective properties to surface hydroxyl groups.

Amphoteric Behavior

The common metallic oxides all exhibit amphoteric behavior in water. Hydroxylated oxide surfaces can acquire both positive and negative charge, and the sign and magnitude of this charge is dependent on pH. For a system consisting purely of water and an immersed oxide, surface charge is established by adsorption and desorption of H^+ and OH^- ions (23) as depicted schematically in Figure 2.

It has generally been assumed that oxide surfaces are truly amphoteric. That is, all surface hydroxyls have been considered exchangeable and capable of losing protons; they are thus modelled as diprotic acid groups (Figure 2). This approach, which has enabled successful description of the pH-dependent charge of various oxides (13,24,25,26), is the one we follow in this discussion. Nonetheless, it is important to remember that the amphoteric property of individual surface hydroxyls is assumed. The overall amphoteric behavior of the surface could also be described by considering independent acidic and basic surface groups (27).

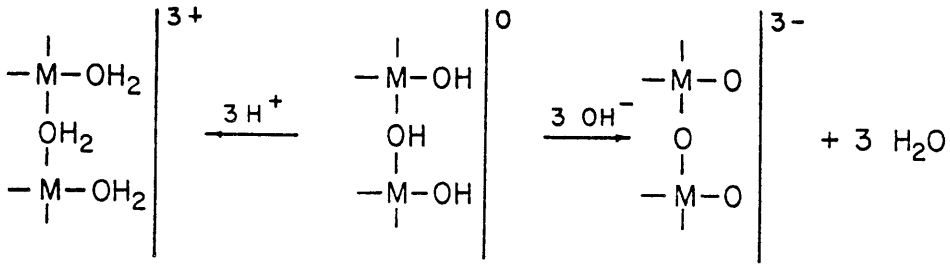

DIPROTIC ACID

$$\equiv SOH_2^+ \rightleftharpoons \equiv SOH^0 + H^+$$

$$\equiv SOH^0 \rightleftharpoons \equiv SO^- + H^+$$

ACIDIC AND BASIC SITES

$$\equiv SOH^0 + H^+ \rightleftharpoons \equiv SOH_2^+$$

$$\equiv SOH^0 + OH^- \rightleftharpoons \equiv SO^- + H_2O$$

FIG. 2.-Schematic representation of charge development on oxide surfaces.

Surface Charge

Oxide particles may be considered as having fixed surface charges determined primarily by acid-base surface reactions. In the absence of other specifically adsorbed cations and anions, the surface charge $\sigma_o(C/m^2)$ is computed as

$$\sigma_o = F/AS\ [(\equiv SOH_2^+) - (\equiv SO^-)] = F[\ \Gamma_H - \Gamma_{OH}\ ] \qquad [1]$$

where F is the Faraday constant (96500 C/mol), A is the specific surface surface area (m^2/g; obtained for example from measurements of $N_2(g)$ adsorption), S is the solid concentration (g/L), and Γ_H, Γ_{OH} are the adsorption densities (mol/m^2) of H^+ and OH^- ions. The pH at which the proton excess at the surface is zero ($\Gamma_H - \Gamma_{OH} = 0$) is known as the zero proton condition, or ZPC; in the absence of other adsorbates, the zero proton condition corresponds to the zero point of charge (28). The surface is then negatively charged when pH exceeds the ZPC and positively charged when pH is less than the ZPC.

The surface charge is determined experimentally by comparing the titration curve of an oxide suspension with that of the medium alone. The net consumption of H^+ or OH^- by the solid phase can be determined by difference and a net adsorption curve (surface proton excess) can be plotted (see Ref. 26 for a detailed example computation). The surface charge can then be calculated as a function of pH. As discussed below, the surface charge of oxides increases with ionic strength as the electrical double layer is compressed and proton exchange reactions are facilitated.

Electrical Double Layer; Surface Potential

When a charged particle is introduced into an aqueous system, a localized disturbance of electroneutrality occurs and is counteracted by the development of an excess density of oppositely charged electrolyte ions near the particle surface. The separation of charges in this "electrical double layer" (EDL) results in a potential difference across the interface. Although the potential difference across an oxide/water interface is typically not large (e.g. 0.01 - 0.1 V), the thickness of the interphase region is very small (e.g. 1 nm) and thus the electric field strength is very large -- on the order of 10^5 to 10^6 V/cm. This strong electric field dictates the distribution of nearby ions in solution and affects the transport of ions coming to or leaving the surface.

Classical EDL theory , developed from investigations of completely polarizable (mercury) and completely reversible (silver iodide) electrodes, provides an accurate description of the spatial distribution of counterions in the vicinity of these model surfaces (Figure 3). Stern (see Refs. 29,30) and Grahame (29) refined the original Gouy-Chapman model (see Refs. 29,30) by taking into account the finite size of ions and proposing that counterions can approach a charged surface only to within a certain distance. These modifications eliminate the problem of predicting physically impossible ion densities very close to the surface (29,30).

Classical EDL theory is readily applicable to the diffuse part of the double layer at the oxide/water interface. Difficulties and differences among adsorption models occur in the geometric description of specific adsorption, i.e. in the treatment of the compact layer at the oxide/water interface. Both the Stern and the Grahame descriptions

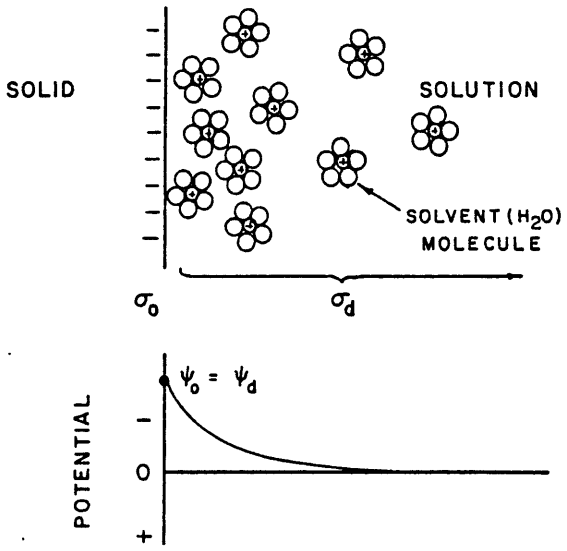

GOUY – CHAPMAN

$$\sigma_0 + \sigma_d = 0$$

$$\sigma_d = -0.1174\sqrt{I}\,\sinh\left(\frac{zF\psi_d}{2RT}\right) \quad [C/m^2]$$

FIG. 3a.-Schematic representation of electrical double layer structure according to Gouy and Chapman.

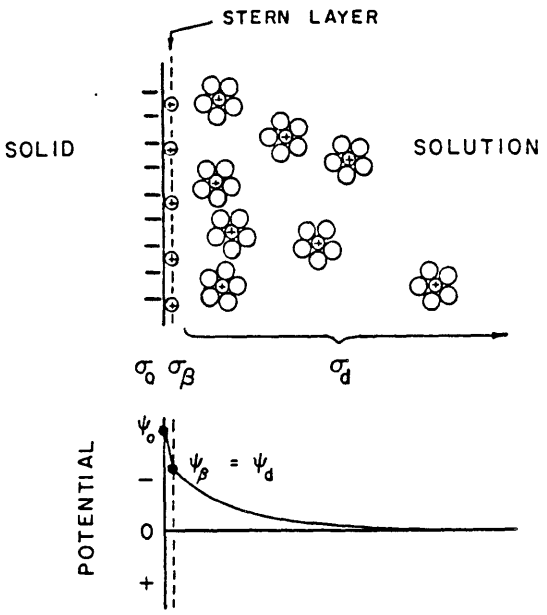

STERN

$$\sigma_0 + \sigma_\beta + \sigma_d = 0$$

$$\sigma_d = -0.1174 \sqrt{I} \sinh\left(\frac{zF\psi_d}{2RT}\right) \quad [C/m^2]$$

$$\psi_0 - \psi_d = \frac{\sigma_0}{C_1} = \frac{-\sigma_d}{C_1}$$

FIG. 3b.-Schematic representation of electrical double layer structure according to Stern.

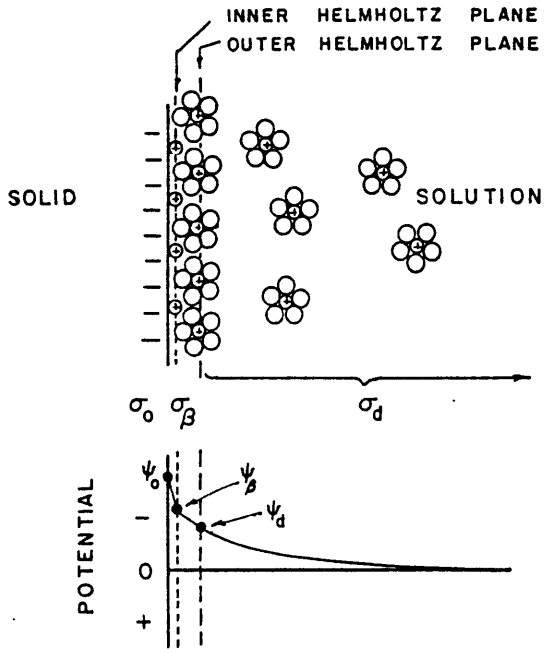

GRAHAME

$$\sigma_o + \sigma_\beta + \sigma_d = 0$$

$$\sigma_d = -0.1174 \sqrt{I} \sinh\left(\frac{zF\psi_d}{2RT}\right) \quad [C/m^2]$$

$$\psi_o - \psi_\beta = \frac{\sigma_o}{C_1}$$

$$\psi_\beta - \psi_d = \frac{\sigma_o + \sigma_\beta}{C_2} = \frac{-\sigma_d}{C_2}$$

FIG. 3c.-Schematic representation of electrical double layer structure according to Grahame.

have been applied along with several other modifications which are described below. Investigations of the oxide/water interface have not yielded a consensus model for specific adsorption because, unlike the mercury and silver iodide electrodes, neither the structural characteristics nor the binding mechanisms associated with oxide surfaces are well understood. The structuring of water on oxide surfaces complicates matters further.

Zeta Potential

Potential differences across solid/water interfaces can be measured by means of electrokinetic methods, primarily electrophoresis. In this technique the movement of charged particles in an applied electric field is observed and the average particle velocity is used to estimate the charge per particle. Surface potential is then calculated from the average charge using Poisson's equation. This so-called zeta(ζ) potential is often considered to be the potential at the edge of the diffuse layer, Ψ_d (Figure 3).

The zeta potential corresponds to the effective shear or slipping plane between the moving and stationary phases and this shear plane does not necessarily coincide with the outer edge of the layer of adsorbed ions. Since water near a charged surface has high viscosity and moves with the solid (31), it is likely that in aqueous systems the shear plane occurs beyond the edge of the 'Stern' layer so that $\zeta < \Psi_d$. In general the location of the shear plane is not certain because the amount of bound water is unknown. Studies with silver iodide (31,32) have shown that equivalence of ζ(observed) and Ψ_d(calculated from Gouy-Chapman theory) holds only for low potentials and low ionic strengths. With higher potentials and higher ionic strengths, and hence

stronger interfacial electric fields, the shear plane apparently moves further from the surface and the difference between ζ and Ψ_d increases greatly (31).

Calculation of zeta potentials from electrophoretic mobility measurements requires that the mobility-zeta potential relationship be known for the colloid of interest. Such relationships have been derived and tested for particles with simple geometries (33,34). For irregularly shaped particles such as oxides, however, mobility-zeta potential relationships are generally unknown. Oxide particles are usually approximated as uniformly charged spheres in order to calculate zeta potentials (35). Hence, for most oxides, zeta potentials calculated from electrophoresis data are not accurate and arguably they are of little use in understanding the EDL properties of colloidal oxide systems.

ADSORPTION OF IONS ONTO OXIDE SURFACES

Proton Adsorption

The amphoteric ionization reactions of surface sites which cause charge development on oxide surfaces can be expressed by

$$\equiv SOH_2^+ = \equiv SOH^o + H_s^+ \qquad K_{a1}^{int} \qquad [2]$$

$$\equiv SOH^o = \equiv SO^- + H_s^+ \qquad K_{a2}^{int} \qquad [3]$$

where H_s^+ denotes protons in the surface plane. For equilibrium

conditions, corresponding mass law equations can be written:

$$K_{a1}^{int} = \frac{\{\equiv SOH^{o}\}\ \{H_s^{+}\}}{\{\equiv SOH_2^{+}\}} \qquad [4]$$

$$K_{a2}^{int} = \frac{\{\equiv SO^{-}\}\ \{H_s^{+}\}}{\{\equiv SOH^{o}\}} \qquad [5]$$

where {} represent activities. Protons at the surface are distinguished from protons in bulk solution because the electrical potential difference(Ψ_o) between these regions results in a different chemical potential of the proton. Electrostatic energy is required to move ions through the interfacial potential gradient. The proton activity at the surface is related to the bulk solution activity according to the Boltzmann distribution:

$$\{H_s^{+}\} = \{H^{+}\} \exp(-F\Psi_o/RT) \qquad [6]$$

where Ψ_o represents the surface potential (compared to a reference potential of zero in the bulk solution) and R, T, F are the gas constant, absolute temperature, and Faraday constant, respectively. This separation of chemical and electrical effects is arbitrary, however, since the chemical and electrical parts of an electrochemical potential are not thermodynamically distinguishable (36,37). Substituting Eq.[6] into Eqs. [4] and [5] yields

$$K_{a1}^{int} = \frac{(\equiv SOH^{o})\ \{H^{+}\}}{(\equiv SOH_2^{+})} \exp(-F\Psi_o/RT) = K_{a1}^{app} \exp(-y_o) \qquad [7]$$

$$K_{a2}^{int} = \frac{(\equiv SO^{-})\ \{H^{+}\}}{(\equiv SOH^{o})} \exp(-F\Psi_o/RT) = K_{a2}^{app} \exp(-y_o) \qquad [8]$$

which implies that the apparent acidity constants are functions of the extent of ionization. Each coordination or dissociation of a proton at the surface changes the surface charge and thus affects the acidity, an effect which has been observed experimentally. Concentrations of surface species can be employed as in Eqs. [7] and [8] by either assuming that the ratio of the activity coefficients for the surface species is near unity (38) or that the surface activity coefficients are included in the coulombic term, itself an explicit activity coefficient (39,40).

The variation of the acidity constants for an oxide is illustrated in Figure 4 where the acid-base behavior of a hypothetical oxide is presented for two ionic strengths. With increasingly positive surface charge it becomes more difficult to bind protons; vice versa, with increasingly negative charge it becomes more difficult to dissociate protons.

Cation Adsorption

Metal cations which form strong complexes with OH^- ions in solution also bind strongly to hydrous oxides in certain pH ranges. Metal adsorption to oxides is analogous to metal hydrolysis in solution in that both adsorption and hydrolysis increase as the pH is increased and both are accompanied by the release of protons (41,42,43).

Adsorption of metal cations onto oxide surfaces is highly pH dependent. For all adsorbing metals the fraction bound increases from zero to one over a narrow pH range, typically one pH unit. Such "pH adsorption edges" are presented graphically in Figure 5a where the percentage of metal bound is plotted against pH.

FIG. 4.-Surface speciation for a hypothetical oxide computed with the diffuse layer model. pK_{a1}^{int} = 7.66, pK_{a2}^{int} = 8.98, N_s = 1.05 mM, A = 129 m^2/g, solid conc. = 8.174 g/L, and (a) I = 0.1 M, (b) I = 0.001 M. (c) Variation of pK_{a1}^{app} and pK_{a2}^{app} with pH and ionic strength. Apparent acidity constants were computed from the corresponding equilibrium concentrations in (a) and (b).

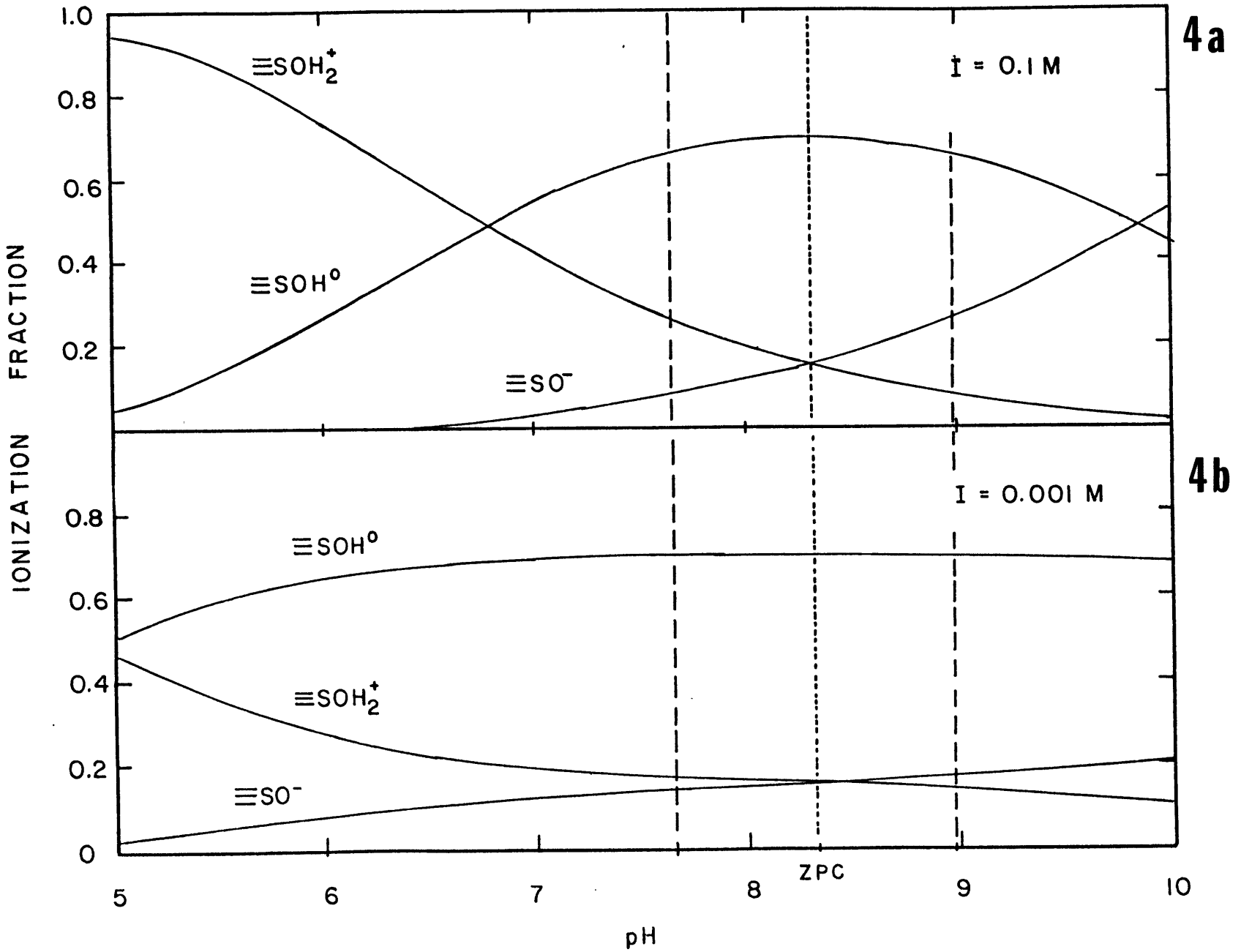
4a
I = 0.1 M
≡SOH$_2^+$
≡SOH^o
≡SO$^-$
4b
I = 0.001 M
≡SOH^o
≡SOH$_2^+$
≡SO$^-$
IONIZATION FRACTION
1.0
0.8
0.6
0.4
0.2
0
5
6
7
8
9
10
ZPC
pH

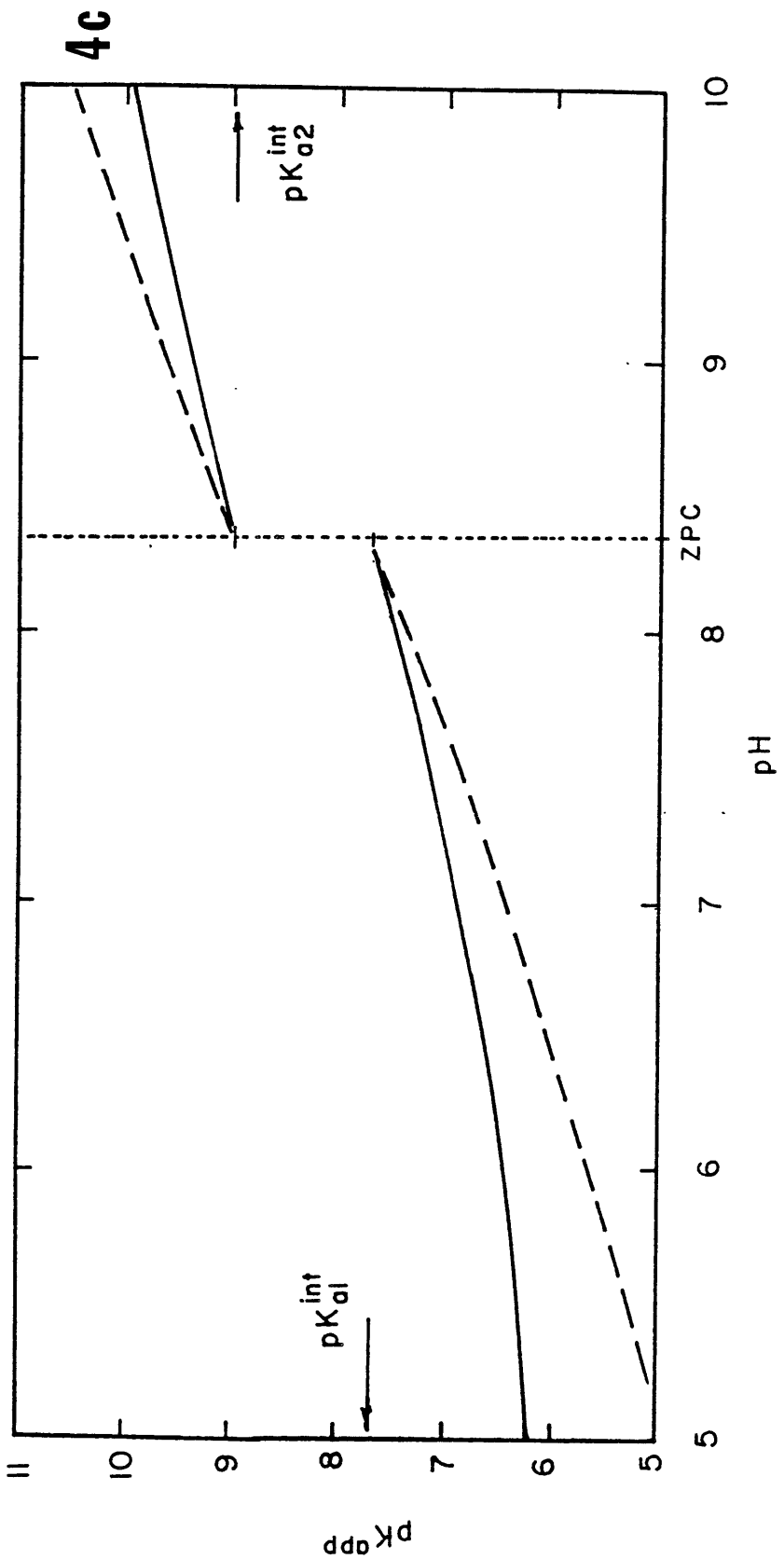
4c
pK$_{a2}^{int}$
pK$_{a1}^{int}$
ZPC
pH
pK$_{app}$
5
6
7
8
9
10
11

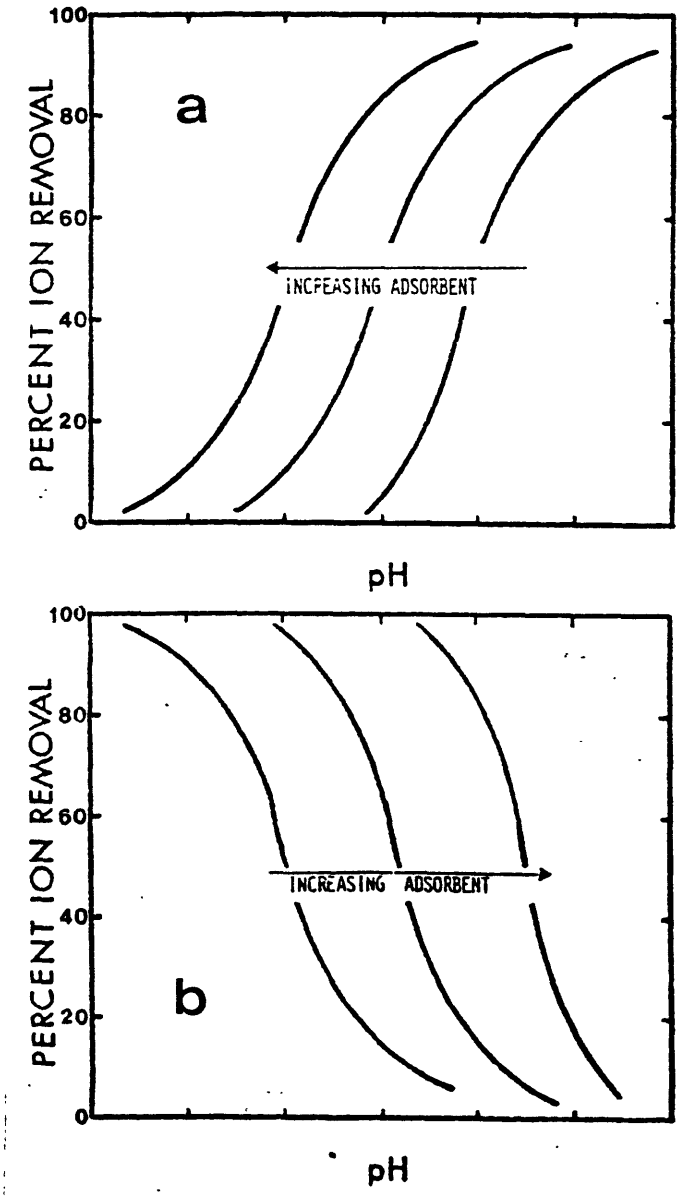

FIG. 5.-(a) Typical pH edges for cation adsorption.
(b) Typical pH edges for anion adsorption.

Proton release associated with cation adsorption can be measured by back titrating to constant pH an oxide suspension to which a cation has been added (44,45) or by measuring the displacement of acid-base titration curves. In the presence of adsorbing metal cations, titration curves for hydrous oxides are shifted to higher pH values (Figure 6) and the pH of zero proton condition (ZPC) is lowered.

In most cation adsorption experiments, one observes that the pH edge shifts to the right as the adsorbate/adsorbent ratio is increased (15,46). As total cation concentration is increased or the amount of oxide in the system is decreased, the fractional adsorption at a given pH value is reduced (Figure 5a). However, there appears to be a threshold adsorbate/adsorbent ratio below which no shift in the pH edge is observed.

The decrease in adsorption density with increasing adsorbate/adsorbent ratio is also evident in constant pH isotherms. As shown in Figure 7, isotherms for adsorption of metal cations on oxides are non-Langmuirian across a very wide range of concentrations. Freundlich isotherms (linear with slope less than 1.0 on a log-log plot) such as shown in Figure 7 for the adsorption of zinc on hydrous ferric oxide have been observed for a variety of cations and oxides (16,46). Only at very low cation concentrations ($< 10^{-7}$M) have adsorption isotherms with slopes of 1.0 been reported (46). In order for the pH edge to remain fixed with increasing adsorbate/adsorbent ratio, the isotherm must have a slope of 1.0 on a log-log plot; i.e. the increase in adsorption density must be proportional to the increase in ion concentration. As discussed later, several explanations for the Freundlich isotherms (and pH edge shifts) have been proposed.

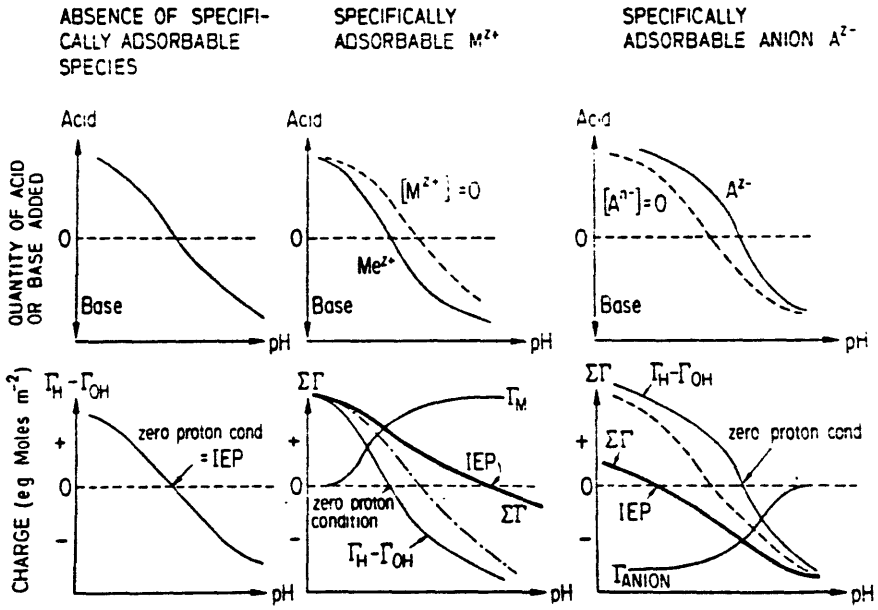

FIG. 6.-The net charge at the hydrous oxide surface is established by proton transfer reactions at the interface and by specific adsorption of cations and anions. This charge can be determined from an acid-base titration curve and measurement of the adsorption of cations and anions. Specifically adsorbed cations (anions) increase (decrease) the pH of the IEP but lower (raise) the pH of the ZPC. From Hohl et al.(49).

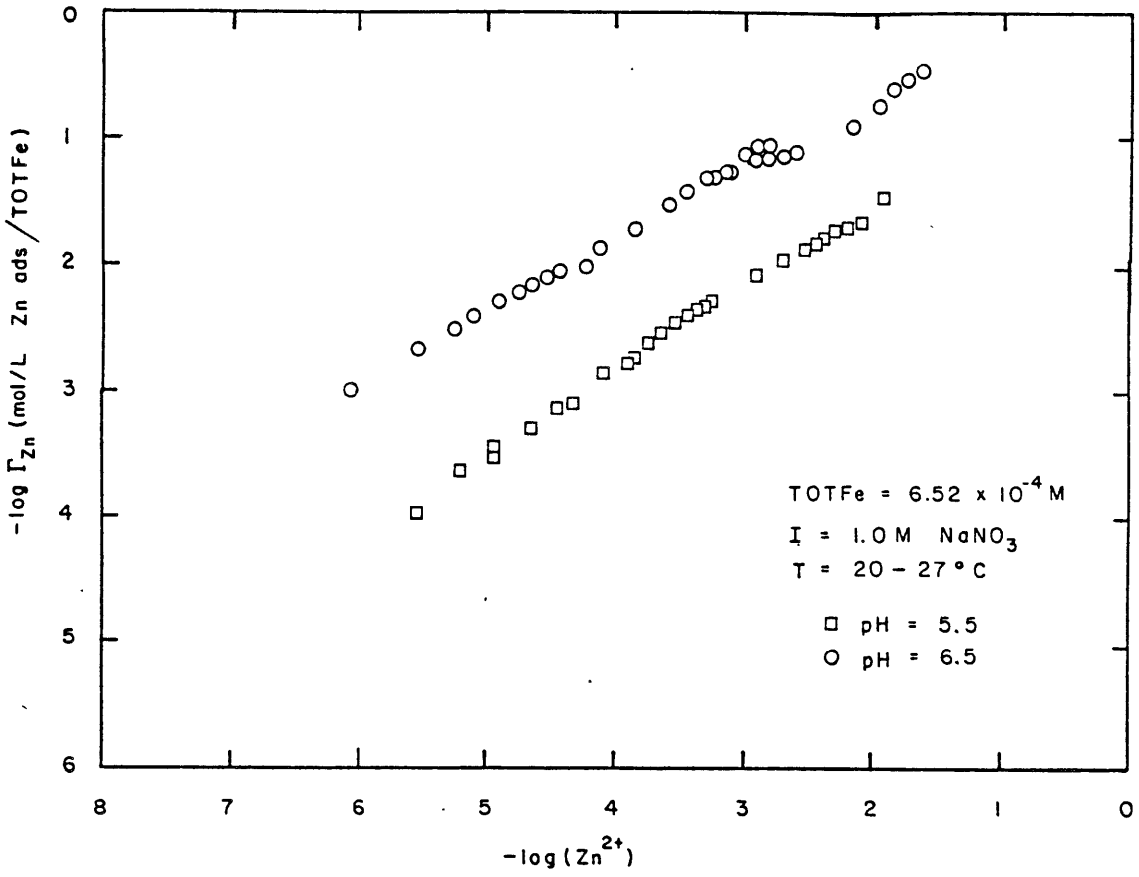

FIG. 7.-Constant pH isotherms for zinc adsorption on hydrous ferric oxide. Data from Kinniburgh and Jackson (16).

Metal cation binding can be characterized quantitatively by considering the formation of surface complexes; for example

$$\equiv SOH^{o} + M^{2+} = \equiv SOM^{+} + H^{+} \qquad K_M \qquad [9]$$

The choice of surface species (or possibly multiple surface species) for a particular situation is dictated by the available experimental data. Proton release associated with sorption of a cation is potentially a constraint on the type of surface species postulated (45,47), but such data are scarce relative to bulk partitioning data.

Cations adsorb onto oxide surfaces in response to both chemical and electrostatic forces. Effects of electrostatic interactions can be taken into account by inclusion of a coulombic term in the adsorption equilibrium constant K_M:

$$K_M = K_M^{int} \exp(-\Delta Z F\Psi/RT) \qquad [10]$$

where ΔZ is the net change in the charge number of the surface species and Ψ is the potential at the plane of adsorption. Electrostatic interactions seem to have a weak influence on cation adsorption, however, since cations can adsorb against electrostatic repulsion (42) and ionic strength appears to have little effect on the extent of cation adsorption (48).

Adsorption of specifically adsorbed cations can be determined directly by measuring concentration changes in solution or on the solid. An indirect determination of adsorption can be made by measuring the shift in the alkalimetric-acidimetric titration curve which occurs in the presence of a coordinating ion (49). The same methods are also used to measure anion adsorption.

Anion Adsorption

Specific adsorption of anions is believed to involve ligand exchange reactions in which hydroxyl surface groups of the oxide are replaced by adsorbate molecules which bind directly to the central metal ions on the surface (50,51). Stumm et al.(50) have shown that several anions have comparable tendencies to form metal complexes in solution and at the oxide/water interface.

Anion adsorption is often referred to as the mirror image of cation adsorption because anion binding decreases as pH increases and the process involves proton uptake or release of hydroxyl ions (51). As is the case with cations, the adsorption of anions onto oxide surfaces is highly pH dependent. For anions, however, adsorption is greatest at low pH and decreases gradually as pH increases, from 100 to zero percent of ligand bound over a range of 3 to 4 pH units (see Figure 5b). The proton uptake (or OH^- release) which accompanies anion adsorption is evidenced by a displacement toward lower pH's of acid-base titration curves for oxides; correspondingly, in the presence of specifically adsorbing anions the ZPC is raised (Figure 6).

Increasing the adsorbate/adsorbent ratio in adsorption experiments with anions above some threshold level causes the pH edge to shift to the left (52). That is, as the total concentration of anion is increased or the amount of oxide is decreased the fractional adsorption at a given pH is decreased (Figure 5b).

In contrast to cation adsorption, anion adsorption typically exhibits clear Langmuir isotherm characteristics at constant pH (see Figure 17): slopes of 1.0 and zero with increasing concentration on a log-log plot. The difference between cation and anion isotherms is probably

explained by the diversity of (hydroxyl) binding sites for cation coordination versus the uniformity of (metal) sites for anion surface coordination.

Ligand exchange reactions of anions at reactive sites on oxide surfaces can be described by surface complexation reactions. For example,

$$\equiv SOH^{o} + A^{2-} = \equiv SA^{-} + OH^{-} \qquad K_A \qquad [11]$$

or for protonated anions

$$\equiv SOH^{o} + HA^{2-} = \equiv SHA^{-} + OH^{-} = \equiv SA^{2-} + H_2O \qquad [12]$$

The types of surface species required for a particular situation depend on the experimental data.

The influence of the interfacial electrostatic field can once again be taken explicitly into account by inclusion of a coulombic term in the adsorption equilibrium constant:

$$K_A = K_A^{int} \exp(-\Delta Z\ F\Psi/RT) \qquad [13]$$

As is the case with cations, adsorption of anions can also take place against electrostatic repulsion and ionic strength has only a weak effect on the extent of adsorption (53).

Cation/Anion Adsorption and Surface Charge

With specific adsorption of cations and anions on oxide surfaces, the measured proton balance [$\sigma_o = F(\Gamma_H - \Gamma_{OH})$] no longer represents the actual surface charge. Consider, for example, the adsorption of Mg^{2+} on alumina (49) in which the surface species $\equiv AlOMg^{+}$ and $(\equiv AlO)_2Mg^{o}$ are

formed. In this case the proton balance is given by

$$\sigma_o = F/AS\ [(\equiv AlOH_2^+) - (\equiv AlO^-) - (\equiv AlOMg^+) - 2((\equiv AlO)_2Mg^o)] \quad [14]$$

Clearly, an uncharged species will not contribute to the charge on the surface and $\equiv AlOMg^+$ will not serve to negate the positive charge associated with $\equiv AlOH_2^+$. The net surface charge

$$\sigma = F/AS\ [(\equiv AlOH_2^+) + (\equiv AlOMg^+) - (\equiv AlO^-)] \quad [15]$$

can be related to the proton balance by

$$\sigma = \sigma_o + F/AS\ [2(\equiv AlOMg^+) + 2((\equiv AlO)_2Mg^o)] \quad [16]$$

In general, the net surface charge is given by

$$\sigma = F\ [\ \Gamma_H - \Gamma_{OH} + \Sigma z\ \Gamma_{M^{z+}} + \Sigma z\ \Gamma_{A^{z-}}\ ] \quad [17]$$

To compute σ for a given pH, the adsorption densities of cations and anions must be known in addition to the proton balance.

In the presence of specifically adsorbed cations and anions the pH at which the surface has zero net charge is called the isoelectric point(IEP). While the zero proton condition (which corresponds to an uncharged surface only in the absence of specifically adsorbed ions other than H^+ or OH^-) is shifted to a lower pH by adsorbed cations, the isoelectric point is shifted to a higher pH. As illustrated in Figure 6, the opposite occurs in the presence of adsorbing anions.

Effects of Competing Adsorbates

In systems containing several specifically adsorbable ions, various solutes may compete with each other for surface sites (52,54). The adsorption of some ions in such systems may thus be limited by site

availability. Factors that determine the effects of competing adsorbates are the relative energies of interaction with the surface, the relative concentrations of the ions, and the pH. As shown in Figures 8 and 9 for both cations and anions, competition effects are not observed until one adsorbing solute is in large excess. This is generally what is expected since, according to the mass law formulation, competition among two species for coordination to a third one should occur only when the third one is nearly saturated. However, calculations of equilibrium partitioning in multiple adsorbate systems on the basis of binding constants obtained from single adsorbate experiments typically overpredict competitive effects. Undoubtedly this is linked to the issue of defining the total concentration of surface sites (which need to be saturated for competitive effects to become important), perhaps the most thorny problem in the modelling of equilibrium ion adsorption.

Effects of Complexation in Solution

Specifically adsorbable cations and anions may form complexes in solution which adsorb more strongly, more weakly, or the same as the free cations or anions (52,55,56,57,58). As shown in Figure 10, the presence of chloride or sulfate inhibits the adsorption of cadmium onto hydrous ferric oxide indicating that the strong solution complexes formed between cadmium and the two anions adsorb less strongly than free cadmium. In these cases the ligands adsorb weakly or not at all under the conditions studied and decrease the adsorption of cadmium by outcompeting the surface for cadmium. However, in some instances the

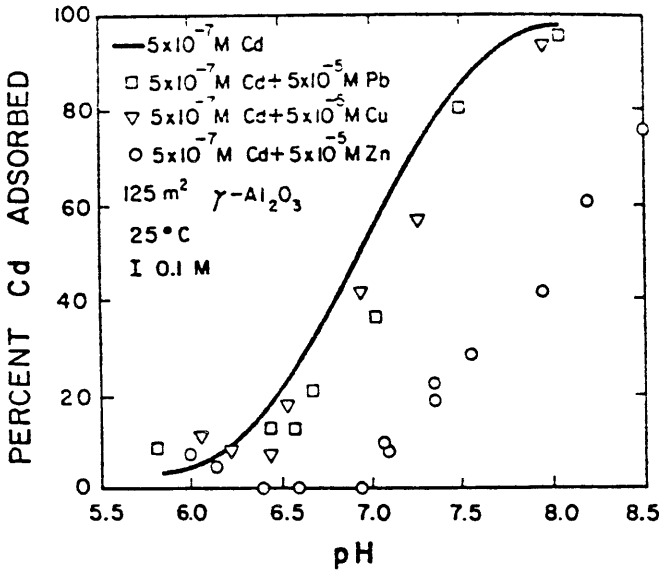

FIG. 8.-The effect of Pb, Cu, and Zn on the adsorption of Cd onto α-Al_2O_3. Competition for adsorption sites decreases the fractional adsorption of Cd. From Benjamin et al.(5).

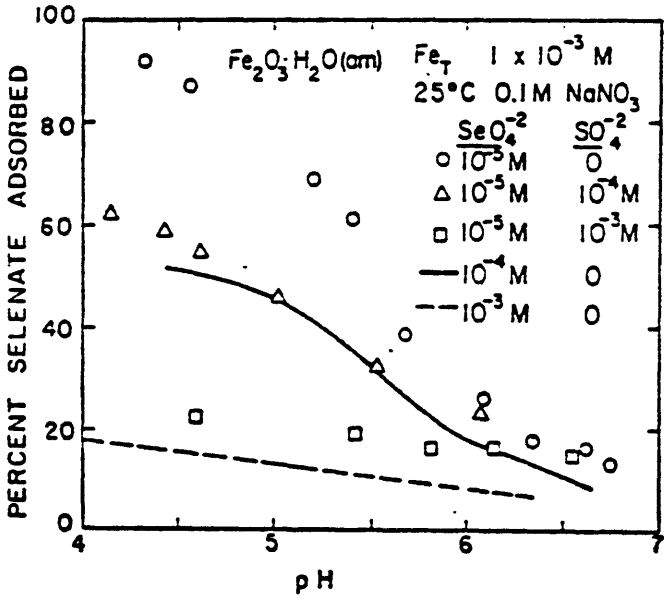

FIG. 9.-The effect of SO_4 on the adsorption of SeO_4 onto hydrous ferric oxide. Competition for adsorption sites decreases the fractional adsorption of SeO_4. From Benjamin et al.(5).

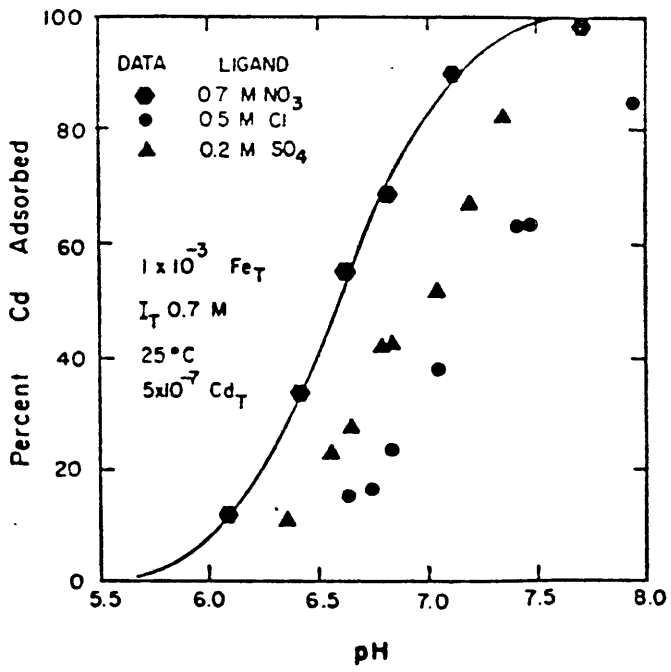

FIG. 10.-The effect of complexation by Cl or SO_4 on Cd adsorption onto hydrous ferric oxide. From Benjamin et al.(5).

metal cation may serve as a bridge between the surface and a ligand as indicated in Eq. [18].

$$\equiv SOH^{\bullet} + M^{2+} + L^{-} = \equiv SOML^{\bullet} + H^{+} \qquad [18]$$

Formation of so-called Type I ternary surface complexes (55) will tend to increase the adsorption of L^{-} at higher pH values; concomitantly, the adsorption of M^{2+} will decrease if ML complexes form in solution. Consequently, the individual pH adsorption edges for M^{2+} and L^{-} will become less steep, or smeared. At lower pH values where ligands adsorb strongly and metal cations do not, a ligand may act as a bridge between the surface and the metal (ternary complex - Type II) to form what is effectively a dinuclear complex.

$$\equiv SOH^{\bullet} + L^{-} + M^{2+} = \equiv SLM^{2+} + OH^{-} \qquad [19]$$

Unless ML solution complexes form at low pH, the pH edge for L^{-} will not be much affected by the formation of a Type II surface complex. Formation of such a complex will tend to increase adsorption of M^{2+} at lower pH values and thus the pH edge for M^{2+} will be smeared.

In principle, the formation of ternary complexes can be taken into account by obtaining mass law constants for reactions such as those given in Eqs. [18] and [19] (59). At present, however, adsorption data for solution complexes are limited and factors responsible for cation-like or anion-like adsorption of solution complexes are poorly understood. Although Davis and Leckie (56) have suggested some criteria for determining how particular complexes will behave, accurate predictions are not possible.

Effects of Organic Coatings

It is likely that in many natural systems adsorbed organic matter, chiefly humic compounds, affect the adsorption of metal ions to oxide surfaces. Humates are important natural metal-complexing ligands (60,61,62) and they bind to inorganic particles (63,64,65,66). Carboxyl (pK_a's 2.5 to 7) and phenolic (pK_a's 8 to 11) groups are the primary functional moieties associated with natural organic matter, and the adsorption behavior is similar to that of inorganic anions. pH edges for the binding of natural organic matter on oxides indicate that adsorption is greatest at low pH and decreases with pH and increasing concentration of organic matter (65). As with other anions, protons are also consumed by reactions of humic materials with oxide surfaces (65). One notable difference between typical anion adsorption and adsorption of natural organic matter is that there is an upper limit on the percent removal for organic matter; that is, natural organic matter apparently comprises an adsorbable and a nonadsorbable fraction (67).

Although the adsorption of simple organic acids has been modelled successfully with surface complexation models (56,68), data for binding of humic material to oxide surfaces are not readily amenable to surface complexation modelling. The major reason for this is that the concentrations of the humic functional groups cannot be readily determined (65) and adsorption reactions such as [11] and [12] cannot be quantified.

In order to model metal cation binding in systems containing adsorbable humic material, Davis (69) described the fraction of surface-bound ligand and of soluble ligand as a function of pH by an empirical relationship based on experimental data. Cation binding could then be modelled using complexation constants for cation binding to the

surface and to solution ligands if surface sites were in excess and no competition occurred. This approach does enable quantitative description of a particular data set but is obviously not general.

Studies of the effects of organic coatings on metal binding by oxides have begun only recently, but indications are that natural organic matter has a strong influence on surface properties and adsorptive equilibria in many aquatic systems (65,70). For example an increase of metal cation adsorption at low pH due to the formation of Type II ternary surface complexes and a decrease at high pH due to competition between the oxide surface and the desorbed ligands have been observed. However, the data base is small and there are many questions yet to be answered. It is not known, for example, if anions can compete with humic material for surface sites or if inorganic ions can penetrate organic coatings in some circumstances (71). Such questions are starting to be investigated and much information should be forthcoming over the next decade. In this review we limit our discussion to adsorption on "clean" oxides only because this has been the focus of past experimental and theoretical work. Nevertheless, it is important to remember that organic matter can significantly affect ion binding in aquatic systems.

SURFACE COMPLEXATION MODELS

The fundamental concept upon which all surface complexation models are based is that adsorption takes place at defined coordination sites (present in finite numbers) and that adsorption reactions can be described quantitatively via mass law equations. Different assumptions concerning appropriate electrostatic interaction terms (viz, activity coefficients) distinguish the various models, often described diagramatically by the geometric location of adsorbed ions at the oxide surface. In the end, though, all of the models reduce to a similar set of simultaneous equations which can be solved numerically. These equations include:

- mass law equations for all possible surface reactions
- a mole balance equation for total surface sites; for different types of surface sites, a mole balance equation for each type
- an equation for computation of surface charge
- a set of equations representing the constraints imposed by the model chosen for EDL structure

It is possible to incorporate any of the surface complexation models in chemical equilibrium computer programs such as MINEQL (72) by including components for surface sites and surface charge and making other modifications to enable coulombic corrections of stability constants (39,73,74,75). Because each of the models is based on a different physical-chemical scenario involving certain kinds of surface reactions taking place in certain locations, the number and nature of parameters involved differs from model to model.

Basic (two layer) Surface Complexation Models

Description - In the basic two layer model of ion adsorption on oxide solids, adsorbates are all considered to be part of the solid surface (one layer) whose resulting electrostatic charge is balanced by an adjacent diffuse layer in the solution (the other layer). The charge on the surface is determined by acid-base reactions as well as surface coordination reactions with other cations and anions. A classical Gouy-Chapman diffuse layer distribution of ionic solutes or a close approximation is typically assumed for the solution side of the interface. In this model all surface coordinating anions and cations are assigned to the same layer as H^+ and OH^- and non-specifically adsorbed counterions are assigned to the diffuse layer. This view of charge distribution at an oxide interface is illustrated in Figure 11.

In the so-called "diffuse layer model" (24,26,76) the relationship between surface charge and potential is fixed by EDL theory. According to the Gouy-Chapman theory (for a symmetrical electrolyte with valence z at 25°C) the surface potential Ψ_o (in volts) is related to the net surface charge σ by

$$\sigma = 0.1174\ I^{\frac{1}{2}} \sinh(zF\Psi_o/2RT) \qquad [C/m^2] \qquad [20]$$

where I is the molar electrolyte concentration. Note that the finite number of surface sites limits the value of the surface charge to reasonable values regardless of the ionic strength.

The "constant capacitance model" (25,42,43) is a special form of the diffuse layer model theoretically applicable only to high ionic strength and/or low potential (< 25 mV) systems. At high ionic

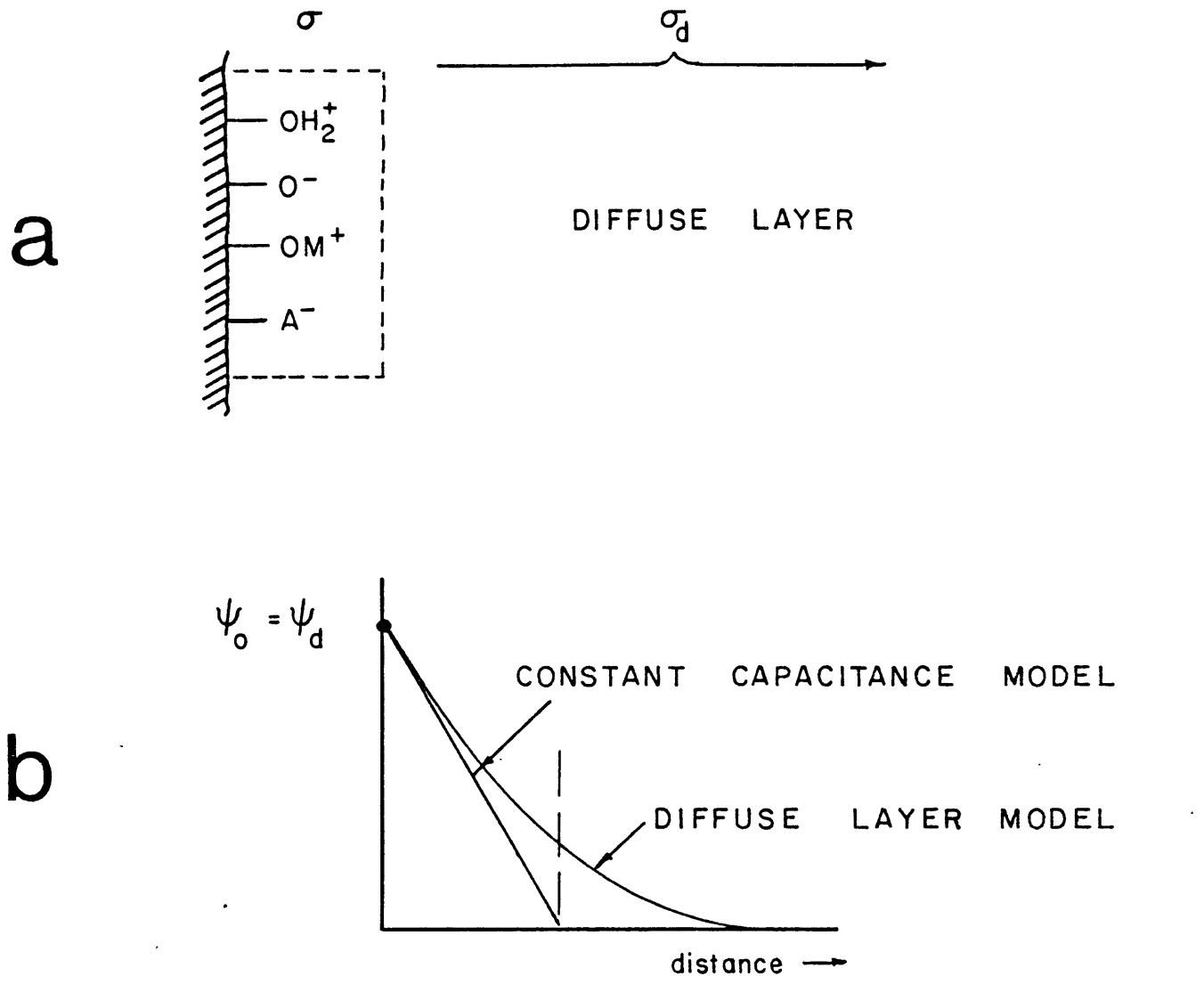

$$\sigma = \frac{F}{AS}\left[(\equiv SOH_2^+) + (\equiv SOM^+) - (\equiv SO^-) - (\equiv SA^-)\right]$$

$$\sigma + \sigma_d = 0$$

FIG. 11.-(a) Schematic representation of ion binding on an oxide surface. This conceptualization is used in the basic (two layer) surface complexation models. (b) Potential variation away from the surface in the diffuse layer.

strengths and low potentials, Eq. [20] can be approximated by

$$\sigma = C \Psi_o \qquad [21]$$

where C is a constant with dimensions of a capacitance (see, for example, Ref. 33). Under these conditions the electrical double layer, consisting of the surface charge and diffuse layer counterion charge, thus acts as a parallel plate capacitor (Figure 11). The capacitance C is dependent on the temperature, ionic strength, and nature of the electrolyte. Though the capacitance can be estimated from the Gouy-Chapman theory, it is often taken as an adjustable parameter and the model is applied to systems of all ionic strengths. Such a model is then intrinsically different from one based on the Gouy-Chapman theory. While there may be good reasons why the theoretical value of the double layer capacitance may be inaccurate (e.g., different permitivitty near the surface, inapplicability of point charge or continuum assumptions, etc.), part of the necessity to adjust the capacitance (usually to higher values) ensues from improper parameter extraction procedures, as described below.

As shown in Table 1, the complete two layer adsorption model consists of mass law equations for all surface reactions, a mole balance equation for surface sites, and Eqs. [17] and [20] or [21] for computation of surface charge and potential, respectively. The model parameters that must be determined from experimental data are (i) the total number of surface sites (N_s) and the intrinsic acidity constants K_{a1}^{int} and K_{a2}^{int} (usually determined from acid-base titrations), (ii) the total number of specific adsorption sites (N_A, N_C), and (iii) one or several intrinsic adsorption constants for each specifically adsorbed

TABLE 1.-The Basic Surface Complexation Model

Mass Law Equations

Surface Acidity

$$\equiv SOH_2^+ = \equiv SOH^\circ + H_s^+ \qquad K_{a1}^{int}$$

$$\equiv SOH^\circ = \equiv SO^- + H_s^+ \qquad K_{a2}^{int}$$

Cation Adsorption

$$\equiv SOH^\circ + M^{2+} = \equiv SOM^+ + H_s^+ \qquad K_M^{int}$$

Anion Adsorption

$$\equiv SOH^\circ + A^{2-} + H_s^+ = \equiv SA^- + H_2O \qquad K_A^{int}$$

Coulombic Correction

$$\{H_s^+\} = \{H^+\} \exp(-F\Psi_o/RT)$$

Mole Balance Equations

$$TOT(\equiv SOH) = N_s = (\equiv SOH^\circ) + (\equiv SOH_2^+) + (\equiv SO^-) + (\equiv SOM^+) + (\equiv SA^-)$$

$$TOTM = \{M^{2+}\} + (\equiv SOM^+)$$

$$TOTA = \{A^{2-}\} + (\equiv SA^-)$$

$$TOTH = \{H^+\} - \{OH^-\} + AS/F\ \sigma_o$$

$$= \{H^+\} - \{OH^-\} + (\equiv SOH_2^+) - (\equiv SO^-) - (\equiv SOM^+) + (\equiv SA^-)$$

Net Surface Charge

$$\sigma = F/AS\ [(\equiv SOH_2^+) + (\equiv SOM^+) - (\equiv SO^-) - (\equiv SA^-)]$$

Charge-Potential Relationship

$$\sigma = 0.1174\ I^{\frac{1}{2}} \sinh(zF\Psi_o/RT) \quad ; \text{ or,}$$

$$\sigma = C\ \Psi_o$$

solute cation or anion. As is the case with all surface complexation models, the surface site concentrations are considered to be adjustable parameters because the accuracy of available techniques for measuring oxide surface areas and site densities is uncertain. For reasons of simplicity, one surface site concentration is typically used for binding of all ions, though in some instances it is necessary to specify high affinity sites for cation binding.

Parameter Estimation - The parameters which describe the acid-base characterisitics of oxide suspensions are usually obtained by simple graphical extrapolation of transformed titration data to zero surface charge. Such procedures have been developed for both the diffuse layer model (26,76) and the constant capacitance model (25,42) and for the more complicated surface complexation models as well. The widely used procedure for the constant capacitance model is described below. Because these graphical procedures incorrectly assume complete dominance of either positive or negative sites on each side of the IEP, they lead to systematic errors in the resulting parameters. Objective determination of surface acidity parameters (pK_a's, C, N_s) from titration data is best accomplished by using numerical optimization techniques (77,78).

Once the surface acidity parameters have been determined from analysis of acid-base titration data, intrinsic constants for cation and anion binding (see Eqs. [10] and [13]) can be determined from adsorption data by trial and error or by using an optimization algorithm. Because the nature of the adsorbed species is unknown and must be assumed, the value of the intrinsic adsorption constant depends on the choice of

surface species. This choice is constrained chiefly by the pH dependency of the adsorption data, and hence specific binding constants are affected by the choice of surface acidity constants. In some instances more than one surface species may be needed to fit experimental data; in this sense the surface species themselves are "fitting parameters."

The critical issue to keep in mind is that the value of each parameter is poorly constrained individually and that all the parameters are strongly interdependent. For example, a fairly wide range of site concentrations (N_s) typically allows accurate fit of acid-base titration data. However, different pK_a's correspond to different values of N_s. In turn, different intrinsic adsorption constants must be used to fit the same adsorption data if different pK_a's are assumed. Consistency among model parameters (and between parameters and model structure) is absolutely necessary for the application of an adsorption model.

A good illustration of parameter interdependency -- in this case between surface acidity constants and surface capacitances -- is given by the common graphical procedure for analyzing acid-base titration data in the context of the constant capacitance model. Consider the logarithmic form of Eq.[7]:

$$\log K_{al}^{int} = \log K_{al}^{app} - \frac{F\Psi_o}{2.3RT} \qquad [22]$$

Substituting for Ψ_o from Eq.[19] and rearranging gives

$$\log K_{al}^{app} = \frac{F}{2.3RT}\frac{1}{C} - \sigma + \log K_{al}^{int} \qquad [23]$$

Equation [23] shows that if $\log K_{al}^{app}$ is plotted against σ, $\log K_{al}^{int}$

can be determined from the intercept and the capacitance C can be obtained from the slope. In order to compute K_{a1}^{app}, however, surface speciation must be known at each step of a titration. Since it is not possible to measure concentrations of surface species, it is commonly assumed that on the positive side of the ZPC the number of sites and the surface charge are given by

$$N_s = (\equiv SOH_2^+) + (\equiv SOH^\circ) \quad ; \quad \sigma = F/AS\ (\equiv SOH_2^+) \qquad [24]$$

and on the negative side of the ZPC

$$N_s = (\equiv SO^-) + (\equiv SOH^\circ) \quad ; \quad \sigma = F/AS\ (\equiv SO^-) \qquad [25]$$

Considering the positive side of the ZPC and assumption [24], K_{a1}^{app} can be expressed

$$K_{a1}^{app} = \frac{(\equiv SOH^\circ)\ \{H^+\}}{(\equiv SOH_2^+)} = \frac{1 - \alpha_+}{\alpha_+}\ \{H^+\} \qquad [26]$$

where $\alpha_+ = (\equiv SOH_2^+)/N_s$. A plot of $\log((1-\alpha_+)/\alpha_+)$-pH vs. α_+ is thus equivalent to the plot described above (note the critical importance of the chosen value of N_s). If assumption [24] is valid, such a plot should yield a straight line whose vertical intercept is $\log K_{a1}^{int}$, and whose slope is inversely proportional to the capacitance. However, assumption [24] is not valid, except at very low pH. As illustrated in Figure 12, the graphical linear extrapolation procedure leads to acidity

FIG. 12.-Linear extrapolation procedure used to determine surface acidity parameters for the constant capacitance model. -- To demonstrate the problems associated with this graphical parameter extraction procedure, a simulated titration of a hypothetical oxide (pK_{a1}^{int} = 6.5; pK_{a2}^{int} = 7.5; N_s = 1.05 mM; A = 129 m^2/g, solid conc. = 8.174 g/L) was performed using MICROQL (74,75). Electrostatic effects were considered to be known perfectly and a linear relationship between surface charge and surface potential was assumed with C = 1.2 F/m^2. The squares represent the results of these calculations. K_{a1}^{app} values were computed using the equilibrium values of ($\equiv SOH_2^+$) and ($\equiv SO^-$), and the difference between these two quantities gave the surface charge. Next, pH and σ_o values corresponding to each of the squares were treated as an experimental data set and Eqs. [24] and [26] were used to recompute K_{a1}^{app}. The results of this second set of calculations are given as the circles. It is clear that the assumption of dominance of positive sites in this case is not valid. The value of pK_{a1}^{int} obtained by extrapolation through the circles to σ_o = 0 is lower than the actual value of pK_{a1}^{int}, and the capacitance (given by the inverse slope of the line) is greater than the actual capacitance. Although the deviations are not huge, remember that the "experimental" data analyzed in this case are as perfect as can be for application of the constant capacitance model. Thus, the graphical parameter extraction procedure is biased toward larger ΔpK values and higher capacitances than may actually exist.

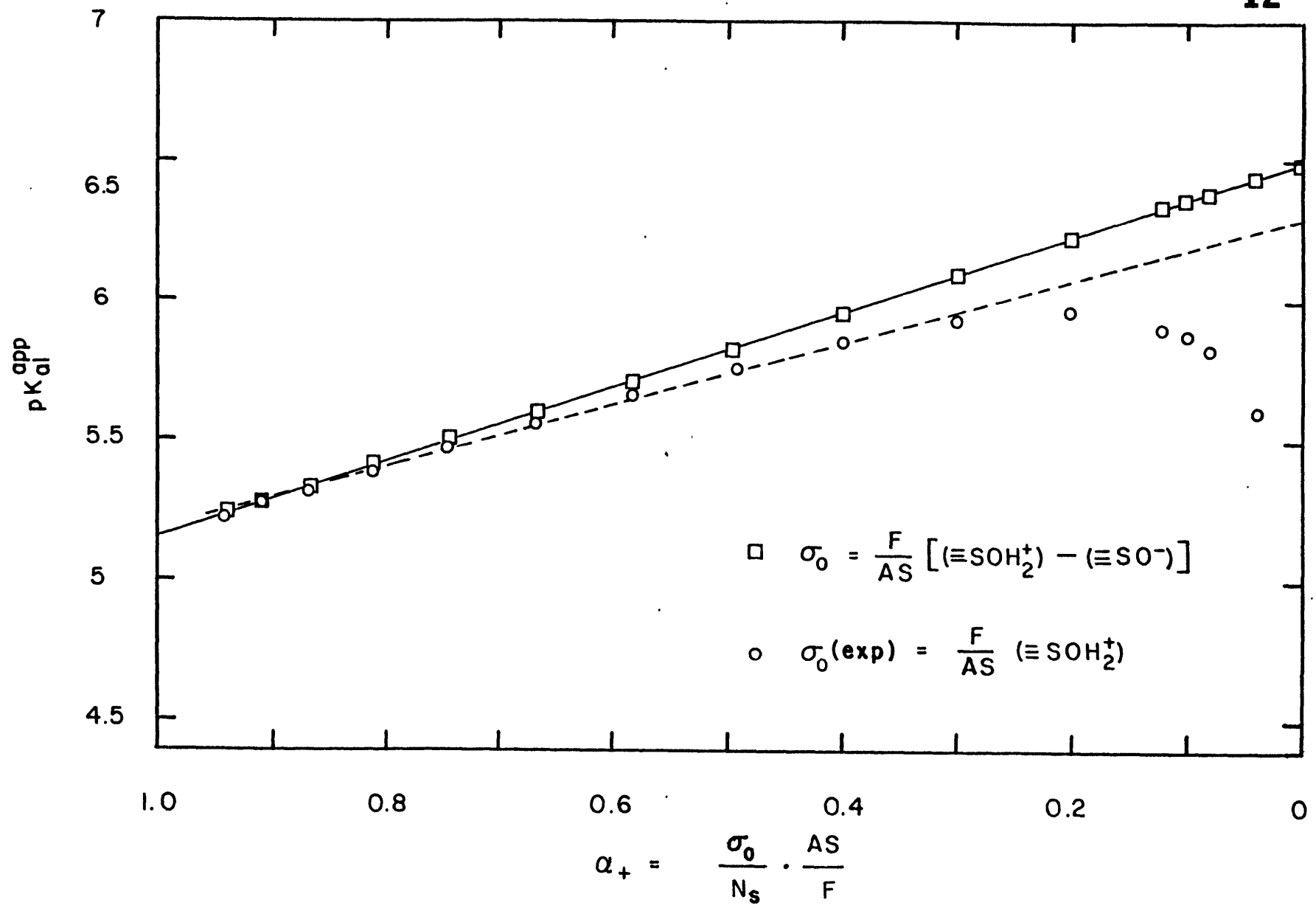
7
6.5
6
5.5
5
4.5
pK_{al}^{app}
1.0
0.8
0.6
0.4
0.2
0
□ $\sigma_0 = \frac{F}{AS}[(\equiv SOH_2^+) - (\equiv SO^-)]$
○ $\sigma_0(exp) = \frac{F}{AS}(\equiv SOH_2^+)$
$\alpha_+ = \frac{\sigma_0}{N_s} \cdot \frac{AS}{F}$

constants that are too far apart and a surface capacitance that is too large. These systematic errors increase with experimental error, limited titration range, and decreasing ionic strength. Good fits of experimental titration data at high ionic strength are still obtained with artificially high ΔpK and C values because they tend to offset each other, as illustrated in Figure 13. Optimization techniques that take into account all surface site types are needed in order to extract from experimental data parameter values that are truly consistent with the chosen model.

Capabilities and Limitations of the Basic Models - The surface complexation approach to modelling adsorption provides a mathematically parsimonious and chemically insightful way to fit a large range of adsorption data. The true test of a model is not in its elegance, however, but in its capacity to predict behavior outside the range of available data since interpolation within the data range can always be achieved with purely empirical formulae (e.g., the Freundlich isotherm equation). In this respect the existing surface complexation models exhibit strengths as well as weaknesses.

Ideally an adsorption model should accurately predict the extent of adsorption at adsorbent concentrations, adsorbate concentrations, pH's and ionic strengths different from those used for parameter extraction. The influence of competing species should also be predictable. Indeed, the basic surface complexation models accurately predict the variation in oxide acid-base properties as a function of ionic strength and the effects of pH and ionic strength on specific adsorption. For example, adsorption (at low adsorbate/adsorbent ratios) at other pH's can usually be predicted using parameter values obtained from one constant pH

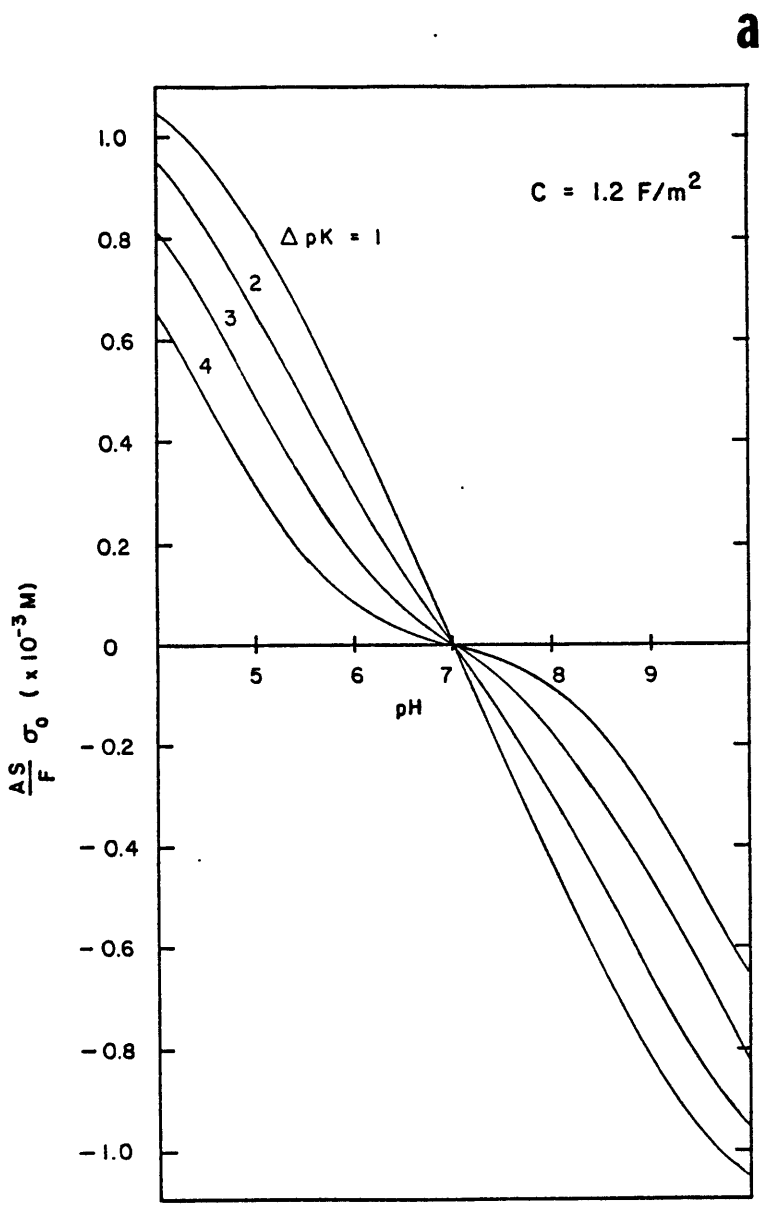

FIG. 13.-Surface charge vs. pH, computed with the constant capacitance model for a hypothetical oxide with ZPC = 7.0, N_s = 1.05 mM, A = 129 m^2/g, solid conc. = 8.174 g/L.

(a) Effect of ΔpK. C = 1.2 F/m^2.

(b) Effect of C. ΔpK = 1.

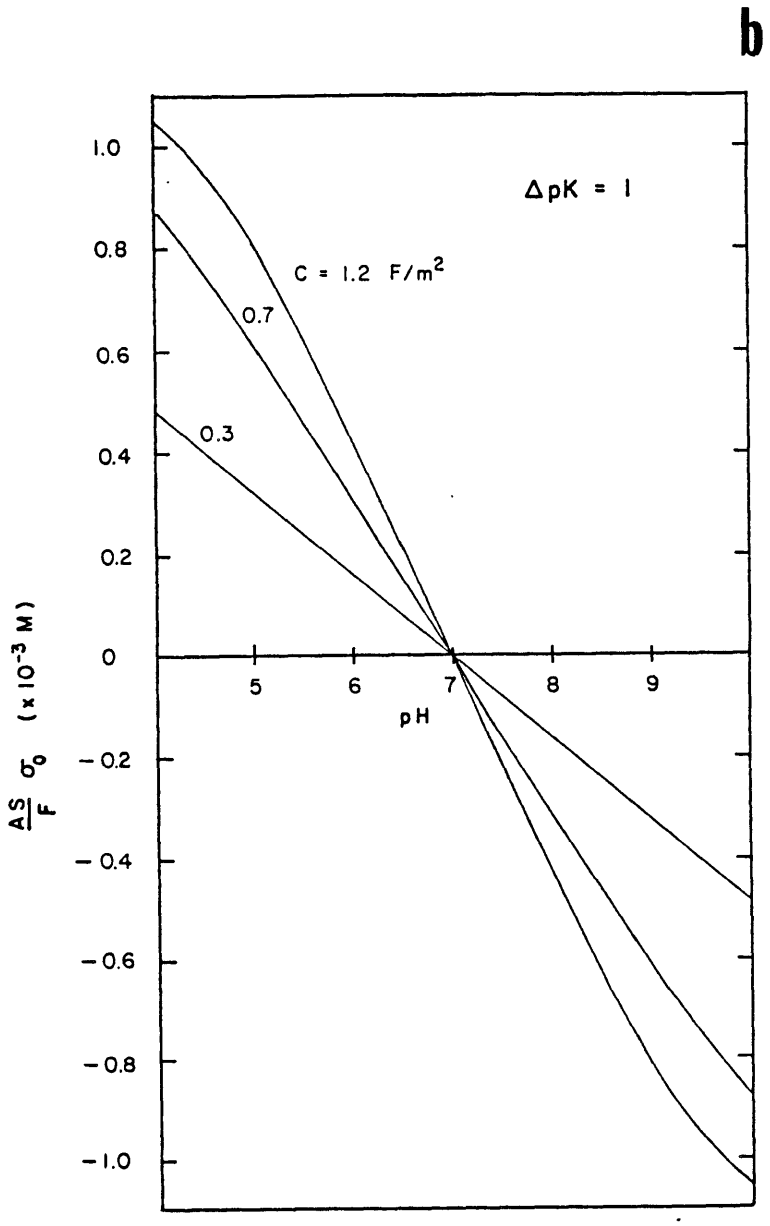

FIG. 13.-Surface charge vs. pH, computed with the constant capacitance model for a hypothetical oxide with ZPC = 7.0, N_s = 1.05 mM, A = 129 m^2/g, solid conc. = 8.174 g/L.

(a) Effect of ΔpK. C = 1.2 F/m^2.

(b) Effect of C. ΔpK = 1.

isotherm, given the acid-base characterization of the oxide. Specific adsorption of cations and anions at other concentrations can be predicted confidently when the available isotherms are Langmuirian. For cations this holds only for low adsorbate/adsorbent ratios since at higher ratios Freundlich isotherms are observed. As a result, predictions of cation adsorption outside the adsorbate/adsorbent range of model calibration is typically inaccurate. Anion adsorption isotherms are Langmuirian (linear with well-defined saturation) for all adsorbate/adsorbent ratios, but prediction of anion adsorption at other pH's usually requires more data than for cations (i.e. two isotherms) owing to the need to characterize the weak acid-base properties exhibited by many anionic surface species.

The Freundlich behavior characteristic of cation adsorption isotherms is also apparent in the parallel pH edge shifts observed for cation adsorption. The surface complexation models do not predict these pH edge shifts but rather predict the same pH edge until total surface sites are exceeded; after the surface is saturated a flattening of the pH edge is predicted. "Flat" pH edges (indicating site saturation) are observed for anion adsorption at higher adsorbate/adsorbent ratios but not for cation adsorption.

Because of the complex shape of cation adsorption isotherms, model calculations of competition among cationic adsorbates at high concentrations (using constants obtained from single ion adsorption data) rarely duplicate experimental observations. Competition among anions, however, is accurately predicted by the basic surface complexation models.

Another weakness of surface complexation models is the uncertainty concerning effects of adsorbing, complexing solution ions on cation and

anion adsorption. This shortcoming, however, is largely attributable to the paucity of data and the situation is likely to improve in the next few years.

Though fairly accurate extrapolation to other adsorbent concentrations is possible with surface complexation models, some recent data indicate that adsorption constants for metal ions decrease with increasing oxide concentration (79,80). A similar phenomenon has been observed for adsorption of hydrophobic organic compounds on soils and sediments (81). Whether this is due to experimental artifacts (82), to a decrease in effective surface area by coagulation, or to some other process is not known.

Finally, for the sake of completeness, the large difference between the surface charge calculated from surface proton excess or deficit and that measured electrokinetically (zeta potentials) must be pointed out. Electrokinetic potential measurements indicate that the diffuse layer charge adjacent to these surfaces is relatively low, seldom exceeding 20 percent of the charge measured by acid-base titration (83). Considering the ambiguity of electrokinetic measurements on oxides, it is not clear that these differences call for a resolution. Nonetheless, such resolution is in fact the major impetus behind the development of some of the more complex extensions of the basic two layer adsorption model.

Model Extensions.I

Two closely related models have been developed to resolve the "issue" of surface charge on oxide surfaces. Both consider separate planes of adsorption for different solutes and include additional surface capacitances as fitting parameters.

The Stern Model - The "variable surface charge - variable surface potential" model proposed by Bowden et al.(84) is essentially equivalent to the Stern model for specific adsorption at an electrified interface. Two discrete planes of charge are assumed at the surface, with H^+ and OH^- ions binding at the innermost plane and other specifically adsorbed ions binding at a second (β) plane separated from the first by a region of dielectric constant ε_1 (see Figure 3b). The solution side of the interface, which is assumed to begin immediately beyond the β-plane of adsorption, is described with a Gouy-Chapman diffuse layer. A linear drop in potential between the planes of surface charge is assumed so that the two adsorption planes act as a parallel plate capacitor with a capacitance C_1.

The Triple Layer Model - The concept of surface structure upon which the triple layer model (85,86) is based is represented schematically in Figure 14. In this model, like the previous one, specific adsorption of ions is assumed to take place in two separate planes (one for H^+ and OH^- ions and one for other specifically adsorbed ions) and a diffuse layer is assumed for the solution side of the interface. In contrast with the previous model, however, the diffuse layer is assumed to begin at the edge of a layer of bound water (dielectric constant ε_2), at some distance from the second adsorption plane. The triple layer model has the same number of fitting parameters as the Stern model if the same kinds of surface reactions are considered and if C_2 is fixed at one value for all oxide systems as was done by Davis et al.(86).

In applying the triple layer model Davis et al.(86) used additional fitting parameters by considering surface reactions with background electrolyte ions. Like the compact layer capacitances, these reactions

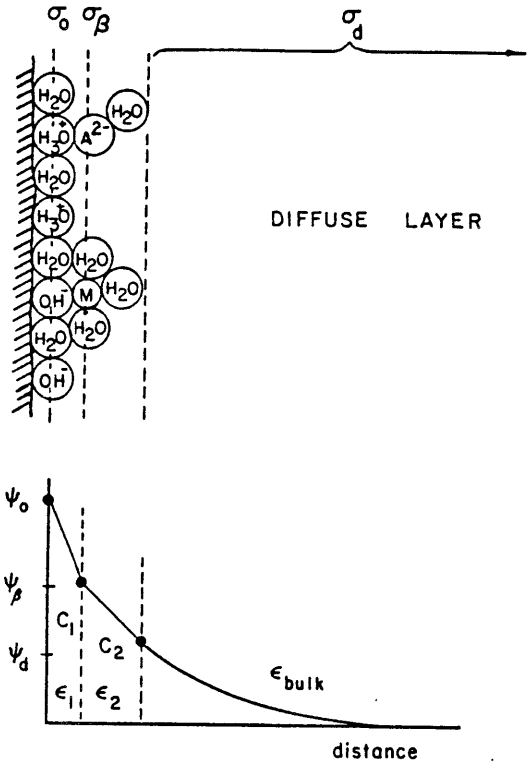

$$\sigma_o = \frac{F}{AS}\left[(\equiv SOH_2^+) + (\equiv SOH_2A^-) - (\equiv SO^-) - (\equiv SOM^+)\right]$$

$$\sigma_\beta = \frac{F}{AS}\left[2\,(\equiv SOM^+) - 2\,(\equiv SOH_2A^-)\right]$$

$$\sigma_o + \sigma_\beta + \sigma_d = \sigma + \sigma_d = 0$$

FIG. 14.-Schematic representation of the charge distribution on an oxide surface and the potential decay away from the surface. This conceptualization is used in the triple layer model. Adapted from Davis et al.(86).

are included for the purpose of obtaining reduced surface charges so that zeta potential data can be modeled. Reduced surface charges are achieved by assuming that a large fraction of the surface charge measured by acid-base titration is balanced by specific adsorption of electrolyte ions. Data related to this assumption are, however, scarce and inconclusive. Consideration of electrolyte binding increases significantly the number of binding constants (and hence the amount of data) needed to model complex systems.

Model Extensions.II

The inability of surface complexation models to predict cation adsorption at high adsorbate concentrations has led to the recent development of two refinements which can be added singly or in tandem to any of the previous models. These refinements are presented below as individual models, but one should keep in mind that they are not exclusive of each other or any of the models discussed earlier.

The Multiple Site-Type Model - The multiple site-type model of Benjamin and Leckie (46) assumes that oxide surfaces consist of several chemically distinct types of sites with varying affinities for adsorbate cations. Although not emphasized by Benjamin and Leckie (46), two site types (small concentration of strong binding sites, large concentration of weak binding sites) are sufficient to model most cation adsorption data. Since multiple site-types are in general not necessary to model acid-base data, different site-types can be assumed to have the same proton transfer characteristics. To model cation adsorption data with a multi-site model a minimum of four adjustable parameters (in addition to surface acidity parameters) is required: total type I and type II metal binding sites, and surface complexation constants for binding to both

site types. The multi-site approach can be implemented in conjunction with any of the surface complexation models discussed previously.

The Surface Precipitation Model - In the surface precipitation model of Farley et al. (87), the mechanism of adsorption is assumed to shift from surface complex formation to surface precipitation at high adsorbate concentrations. Precipitation on the surface is described by the formation of a solid solution whose composition varies continuously between that of the original solid and a pure precipitate of the adsorbing metal ion. The model contains three adjustable parameters (in addition to surface acidity parameters): total cation binding sites, the cation surface complexation constant, and the solubility product for the solid hydroxide of the adsorbing cation (to the extent that it is poorly defined by available data). The values of these parameters are determined by fitting a constant pH isotherm. It is important to note that the surface precipitation model is not exclusive of the multi-site model. For example, surface precipitation could occur at type II sites in a two site model.

Comparison and Validity of Models

Westall and Hohl (77) applied the models described here to acid-base titration data for two oxides and found all of the models to be equally capable of fitting the data. However, to obtain equivalent fits different values were required for analogous parameters in the various models. As shown in Figure 15, the diffuse layer model, the constant capacitance model, and the triple layer model can all fit the TiO_2 titration data of Yates (35). The parameter values required for these fits are listed in Table 2, where it can be seen that the diffuse layer model involved only two fitting parameters (K_{a1}^{int}, K_{a2}^{int}) while the

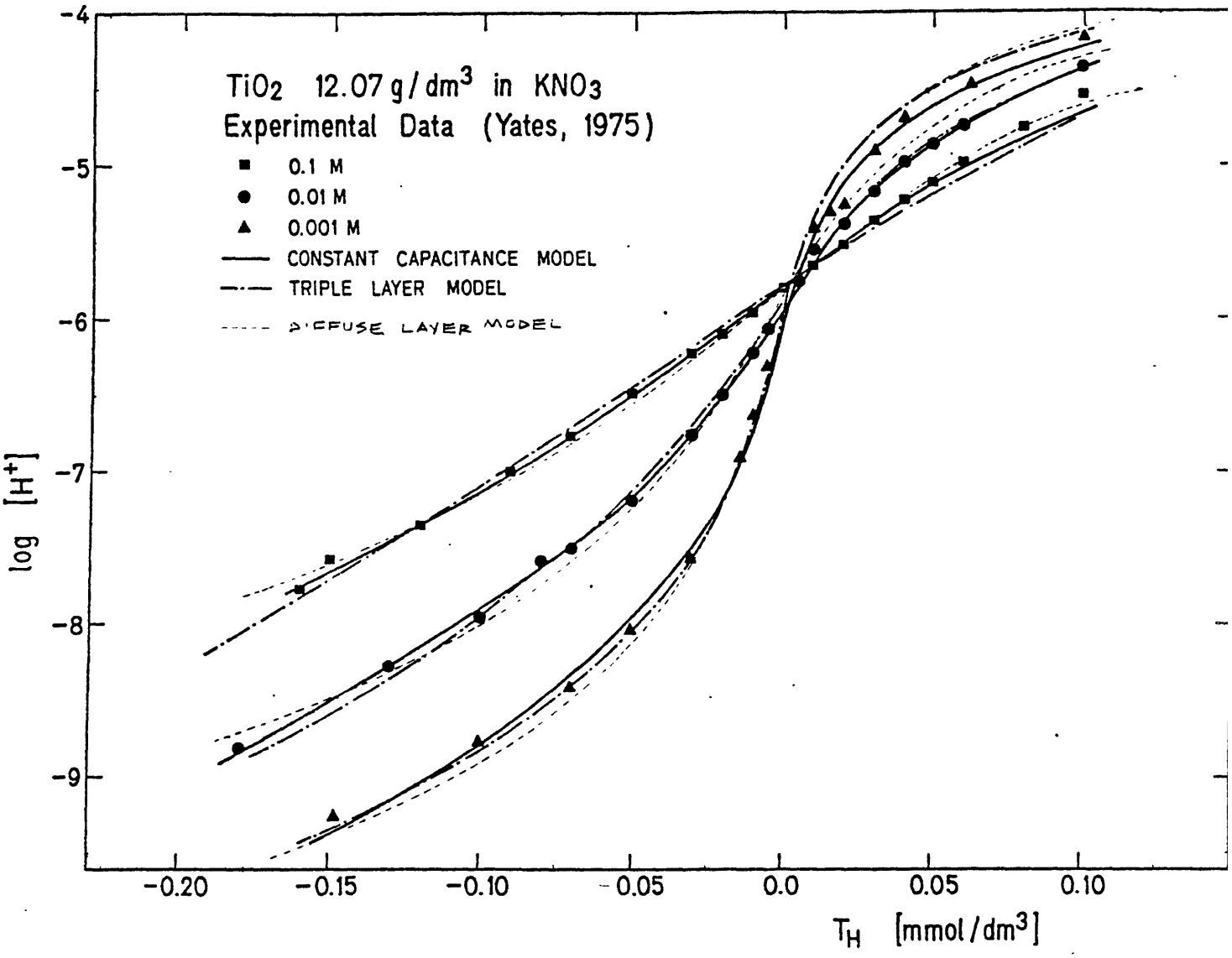

FIG. 15.-Acid-base titration data for TiO_2 in different concentrations of KNO_3. The data are fit equally well with the diffuse layer model, the constant capacitance model, and the triple layer model. Parameter values are given in Table 2.

TABLE 2.-Values of Adjustable Parameters:
Surface Hydrolysis of TiO_2 in KNO_3

Diffuse Layer Model[1]

$$pK_{a1}^{int} = 3.52 \; ; \quad pK_{a2}^{int} = 7.99$$

Constant Capacitance Model[1,2]

I (M)	pK_{a1}^{int}	pK_{a2}^{int}	C [F/m^2]
0.1	3.45	8.05	0.97
0.01	3.11	8.66	0.72
0.001	2.71	9.31	0.53

Triple Layer Model[1,2]

$$pK_{a1}^{int} = 5.15 \; ; \quad pK_{a2}^{int} = 6.61$$

$$C_1 = 0.70 \text{ F/m}^2 \; ; \quad C_2 = 0.40 \text{ F/m}^2$$

$$pK_{(K)}^{int} = 0.0 \; ; \quad pK_{(NO_3)}^{int} = 0.0$$

where

$$K_{(K)}^{int} = \frac{(\equiv SO^- \; K^+)}{(\equiv SO^-) \; \{K^+\}} \exp(F\Psi_\beta/RT)$$

$$K_{(NO_3)}^{int} = \frac{(\equiv SOH_2^+ \; NO_3^-)}{(\equiv SOH_2) \; \{NO_3\}} \exp(-F\Psi_\beta/RT)$$

1. $N_s = 4.83 \times 10^{-3}$ M; surface area = 20 m^2/g; solid conc. = 12.07 g/L

2. from Westall and Hohl (77)

constant capacitance model involved nine (K_{a1}^{int}, K_{a2}^{int}, and C for each ionic strength) and the triple layer model involved five (K_{a1}^{int}, K_{a2}^{int}, K_{C}^{int}, K_{A}^{int}, C_1). Note that the concentration of surface sites was fixed for all models.

From the above fitting exercise and others that we have conducted, we recommend the diffuse layer model for describing adsorption of inorganics on hydrous oxides. The diffuse layer model possesses the attributes of simplicity and applicability to different solution conditions. All specific adsorption is assumed to take place in one surface layer and a Gouy diffuse layer is assumed for the solution side of the interface. This simple view of the interface eliminates multiple planes of adsorption at the surface and the associated fitting parameters. The only capacitance in the model, that of the diffuse layer, is fixed by theory.

Aside from conceptual and mathematical simplicity, a single surface layer can be justified for other reasons. With multiple surface layer models, high inner layer capacitances are consistently required to fit surface charge - pH data for oxides (84,85,86,88,89). These high inner layer capacitances are commonly attributed to the very small separation between the layer of specifically adsorbed ions and the innermost surface plane containing H^+ and OH^- ions. Low outer layer capacitances are required in these models to fit zeta potential data, indicating several layers of structured water between the inner layer and the edge of the diffuse layer. Yates et al. (85) have suggested that this combination of high inner layer capacitance and low outer layer capacitance indicates that the two planes are embedded in a porous, hydrated oxide surface layer. This is consistent with the single surface layer concept incorporated in the diffuse layer model.

The primary criticism of the diffuse layer model in the past has been that the surface potentials predicted by the model for oxides are higher than zeta potential measurements. While the diffuse layer model in general is not successful in describing zeta potential data when the assumption is made that $\zeta = \Psi_d$, an empirical approach is possible in which the location of the shear plane is specified as an empirical function of solution conditions. For example, the distance δ from the surface (edge of the diffuse layer) to the shear plane could be expressed as a function of ionic strength and surface charge. Additional fitting parameters in the form of electrolyte binding constants and the outer layer capacitance C_2 are included in the triple layer model in order to fit zeta potential data (35,90). An empirical expression for the location of the shear plane could accomplish the same objective with fewer fitting parameters.

Ultimately, the validity of a particular model must depend on direct elucidation of the surface structure and of surface coordination. Advanced spectroscopic techniques offer some hope for elucidating the nature of surface complexes at the oxide/water interface, but studies employing such techniques have commenced only recently. Initial results seem to confirm that metal ion adsorption involves the formation of inner sphere complexes (91,92) and there is also some evidence for the formation of surface precipitates at high adsorbate cation concentrations (93,94,95). Rigorous studies of oxide/water interfaces are just beginning, however, and much work remains to be done. The same comment applies to solid/liquid interfaces in general, a new frontier in surface chemistry opened largely by advances in spectroscopic technology.

Finally, it should be emphasized that all the adsorption models we have discussed are applicable to equilibrium conditions only. Adsorption of ions on oxide surfaces is a two step process consisting of a rapid initial uptake (seconds-minutes) followed by a slower step (hours-weeks) in which the equilibrium adsorption density is approached asymptotically. When surface sites are in large excess, i.e. when the ratio of adsorbate/adsorbent is low, the contribution of the slow adsorption step to total adsorption is small and thus equilibrium is achieved rapidly. However, at high adsorbate/adsorbent ratios adsorption kinetics slow considerably and the second step becomes much more important (15,80). For natural waters rapid equilibration is a good assumption for most circumstances, but for treatment processes and other applications with high adsorbate concentrations the validity of assuming equilibrium must be carefully examined.

GUIDELINES FOR USE OF ADSORPTION MODELS

From the preceding discussion it should be evident that surface complexation models have fundamental strengths and several shortcomings. These models can be employed as engineering tools if their limitations are recognized. Use of surface complexation models to date has been limited almost exclusively to those involved in adsorption research. Though the surface complexation approach is still evolving, there is sufficient consensus concerning the use of mass law equations to describe adsorption reactions to justify more widespread application of the models. Surface complexation models can be used to predict at least approximately the influence of adsorption on metal speciation in aquatic systems containing hydrous oxides.

In order to use surface complexation models in a predictive mode they should be applied under the conditions for which they have been successful, i.e. relatively low adsorbate concentrations and little or no dissolved organics. At first these may seem to be severe limitations, but such conditions prevail in a variety of aquatic systems. Examples are groundwater flow through low organic content, iron oxide-coated aquifer material and treatment of low DOC water with aluminum or iron oxide. Despite the relative simplicity of such systems, adsorption can be very difficult to predict without the aid of a surface complexation model under conditions of changing pH, ionic strength, or solid concentration. To model various conditions with an empirical approach it is necessary to find or generate adsorption data that span the particular conditions of interest (e.g. an isotherm equation). With a surface complexation model, however, adsorption behavior can be predicted for a variety of conditions using surface

acidity parameters for the oxide (extracted from titration data) and binding constants for the the adsorbing ions (extracted from adsorption data).

An inevitable result of the multiplicity of the surface complexation models is that values of surface acidity and adsorption parameters extracted from experimental data are entirely model dependent (73,77). Existing titration and adsorption data have been interpreted with different models so that parameter values reported in the literature for similar systems are not consistent. To model adsorption in a particular system it is at present necessary to obtain raw data from the literature and extract the needed constants in terms of the surface complexation model that one has chosen. In view of the large data requirements for obtaining background electrolyte adsorption constants and their limited usefulness for relatively low ionic strength systems, consideration of electrolyte binding should be omitted unless absolutely necessary (i.e. very high ionic strength systems).

In situations involving constant solution conditions such as seawater, it may be convenient to work with conditional constants which include coulombic corrections (55,96,97). That is, the coulombic correction factor and K^{int} in Eqs. [10] and [13] are combined. Conditional constants are extracted from adsorption data obtained under specific solution conditions and can only be applied to systems having the same chemical composition as the original experimental system. Using the surface complexation approach with conditional constants is no more efficient than using an empirical approach. Empirical models do not enable estimates of surface speciation, however, and are not easily incorporated in chemical equilibrium computer programs.

The adsorption of an inorganic ion in systems containing several types of adsorbing surfaces is dependent on the binding intensity (surface complexation constant), binding capacity (site density), and abundance (concentration) of each adsorbent in the mixture. In order to model adsorption of an ion in a system containing a mixture of oxide phases it is thus necessary to know surface complexation constants and total site concentrations for each phase. Relative abundances of oxide phases can be estimated from solution chemistry or by various experimental methods, including extractions (4,98,99,100), if the components of a mixture are unknown. The inherent assumption that each component of an oxide mixture acts independently is supported by experimental observations. It has been demonstrated, for example, that the ZPC for any composition of a mixed oxide system can be calculated by summing the ZPC's of the constituent pure oxides weighted according to mass fraction (101,102). Also, Honeyman (79) recently conducted an extensive study of metal ion binding in binary oxide systems and his results indicate that linear additivity of adsorption to individual components is a valid assumption in most cases.

Chemical equilibrium models (including adsorption subroutines) can be linked to fluid transport models by writing transport equations for the total mass of each component (62,103). Total component concentrations are updated at each time step and the chemical equilibrium problem is solved to obtain concentrations of all species. If adsorption reactions are included in the equilibrium calculations, however, source and sink terms are necessary in the transport equations for components involved in this "non-conservative" chemical process (103). In addition, reaction kinetics are a much more important consideration for adsorption reactions. It may be necessary to

incorporate rate expressions in the set of transport equations. Since suspended particles tend to coagulate and settle, a model of particle-particle interactions (e.g., Ref. 105) and their effects on sedimentation rates and available surface area is needed to describe the transport of adsorbed species in surface waters. In subsurface transport, adsorption is strictly represented as sink/source term because the solid phase is immobile. Nevertheless, surface complexation models can be employed by treating immobile adsorbing sites in the solid matrix as additional complexing ligands (106).

An Example: Removal of Chromate in Water Treatment

To make clear the steps required to implement a surface complexation model and to illustrate how a surface complexation model can be applied in practice, we present here a detailed example involving removal of chromate by hydrous ferric oxide (HFO). Freshly precipitated hydroxides of iron and aluminum are commonly used in water treatment to coagulate and settle suspended particles. In addition to removal of suspended material, soluble inorganic and organic species which adsorb to hydrous oxides are also removed in coagulation treatment. The removal of several metal ions in conventional coagulation treatment was investigated by the U.S. Environmental Protection Agency (EPA) in the 1970's (8,9,10,11), and in this example we show how their results for chromate removal by hydrous ferric oxide can be reasonably predicted with a surface complexation model using parameter values extracted from laboratory adsorption experiments. Our emphasis is not on precise data fitting but on demonstrating how a simple model can be used for practical applications.

The EPA experiments comprised bench scale jar tests and a pilot plant test in which Ohio River water was spiked with chromate and then ferric sulfate was added to precipitate HFO. In the jar tests settling was permitted to occur for 1.5 hours, and then the supernatant was drawn off and centrifuged. The settling time in the 2 gpm (7.6 L/min) pilot plant was one hour and clarification was achieved by dual media filtration. The river water alkalinity was 50-60 mg/L as $CaCO_3$, the total concentration of chromate added was 0.15 mg/L (2.9×10^{-6} M), and the ferric sulfate doses examined were 30 mg/L in the jar tests and 24 mg/L in the pilot plant test.

Using a surface complexation model and parameters extracted from independent data sets, removal of chromate due to adsorption can be predicted for the conditions described above if certain assumptions are made. The assumptions required are (i) that the river water is low in dissolved organic carbon (DOC) so that these compounds do not compete with chromate for adsorption sites or adsorb in amounts sufficient to alter the surface characteristics, and (ii) that electrolyte ions in the river water are either inert (e.g. Na^+, Cl^-, K^+, NO_3^-), unable to compete with chromate because of weak binding (e.g. Ca^{2+}, HCO_3^-), or present at low enough concentrations so as to preclude competition. These assumptions are necessary because no chemical information other than alkalinity is provided for the Ohio River water in the experimental reports (8,9). However, river waters are typically low in DOC (1-10 mg/L, which corresponds to 10^{-6} - 10^{-5} M if MW = 1000), not all of which will adsorb (67), and the low alkalinity indicates that the concentration of specifically binding ions such as Ca^{2+} and Mg^{2+} are probably low.

With the above assumptions, the chemical system to be modelled is a relatively simple one: chromate (CrO_4^{2-}) and its hydrolysis species, sulfate (SO_4^{2-}), and surface species. The stability constants for the relevant solution species, available in handbooks (e.g., Ref. 107), are listed in Table 3a. No compilation of surface hydrolysis and complexation constants exists, however, and these must be extracted from original data.

To obtain surface hydrolysis constants for HFO, we chose to fit the data obtained by Davis (90), the most extensive (fast) titration data set available for HFO. As seen in Figure 16 Davis titrated HFO at three ionic strengths. For reproducibility and other reasons discussed by Davis (90) and Yates (35), it is best to titrate hydrous oxides rapidly and that is how the data in Figure 16 were obtained. Using the diffuse layer model, a surface area of 600 m^2/g as recommended by Davis (90), and a total site concentration equal to 20 percent of TOTFe (surface saturation for several anions and cations has been observed near this site density), surface hydrolysis constants were extracted from the 0.1 M ionic strength titration data with the nonlinear parameter optimization program FITEQL (108). The curves drawn in Figure 21 were computed for the three ionic strengths using the diffuse layer model (incorporated in MICROQL) and the extracted surface hydrolysis constants which are reported in Table 3b.

Stability constants for the formation of chromate and sulfate surface complexes with HFO were obtained from data of Leckie et al. (52,109). Because no sulfate adsorption data are available, we used the data for selenate (SeO_4^{2-}) whose adsorption on HFO was reported by Leckie et al.(52) to be identical to sulfate. Two constant pH isotherms for selenate adsorption are given in Figure 17 and pH edge plots for

TABLE 3.-Mass Law Constants used in the Example

a. Solution species[1]	log K
$H^+ + SeO_4^{2-} = HSeO_4^-$	1.70
$H^+ + SO_4^{2-} = HSO_4^-$	1.99
$H^+ + CrO_4^{2-} = HCrO_4^-$	6.51
$2H^+ + CrO_4^{2-} = H_2CrO_4^\circ$	6.31

b. Surface hydrolysis species[2]	
$\equiv FeOH^\circ + H_s^+ = \equiv FeOH_2^+$	7.1
$\equiv FeOH^\circ = \equiv FeO^- + H_s^+$	- 8.9

c. Sulfate surface complexes[2]	
$\equiv FeOH^\circ + SO_4^{2-} + 2H_s^+ = \equiv FeHSO_4^\circ + H_2O$	13.6
$\equiv FeOH^\circ + SO_4^{2-} + H_s^+ = \equiv FeSO_4^- + H_2O$	7.7

d. Chromate surface complex[2]	
$\equiv FeOH^\circ + CrO_4^{2-} + H_s^+ = \equiv FeCrO_4^- + H_2O$	9.8

1. The stability constants are for T = 25°C, I = 0, and were obtained from Ref. 107, V.4. The Davies equation (see Ref. 62) was used for ionic strength corrections. Ferric iron species were not considered because in this case they have no influence on the surface complexation calculations.

2. The stability constants listed are intrinsic surface complexation constants; the coulombic term for surface reactions includes activity corrections.

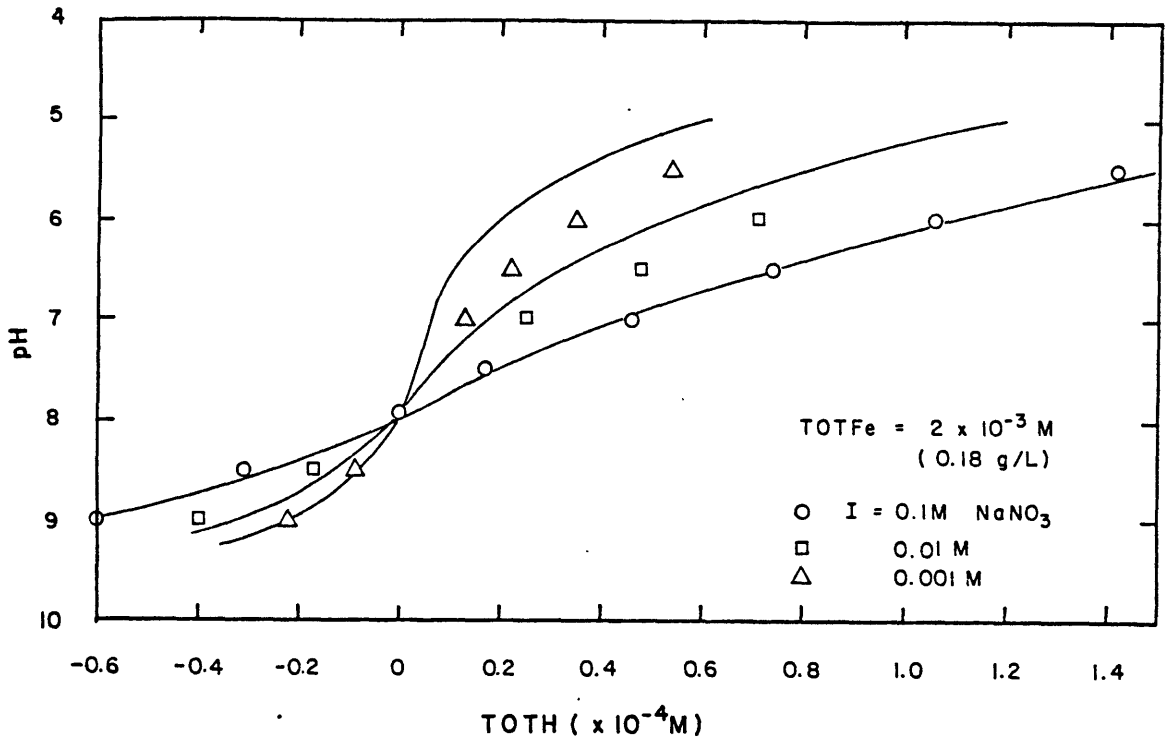

FIG. 16.-Acid-base titration data for hydrous ferric oxide in different concentrations of $NaNO_3$. The data for I = 0.1M were fit using the diffuse layer model and FITEQL(108); parameter values are given in Table 3b and in the text.

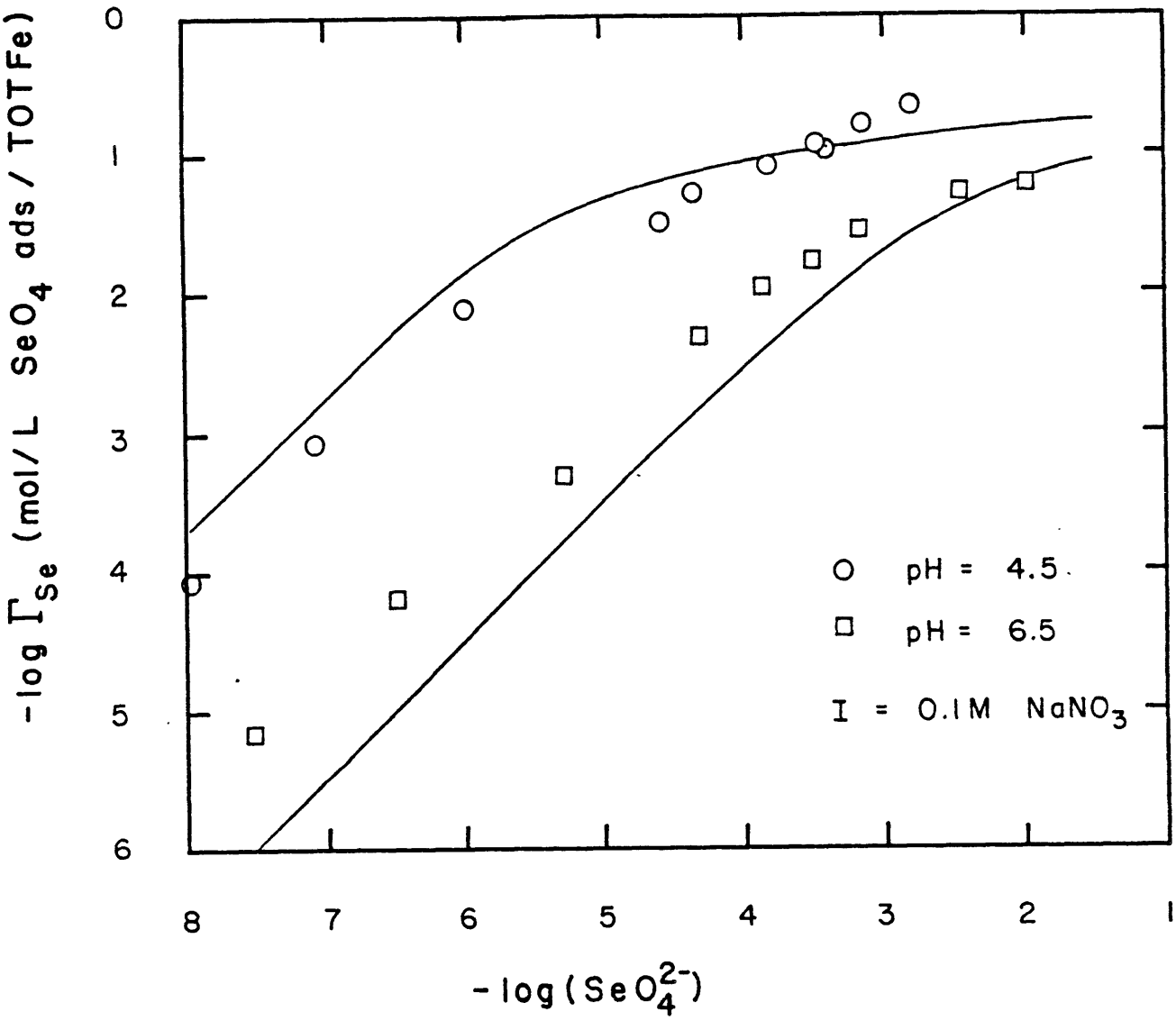

FIG. 17.-Constant pH isotherms for adsorption of selenate on hydrous ferric oxide. Data from Leckie et al. (52).

selenate and chromate adsorption are presented in Figures 18 and 19.

If constant pH isotherms are available, it is desirable for several reasons to fit these before attempting to fit a series of pH edges. First, satisfactory fits of isotherms corresponding to several pH values insures satisfactory fits of the pH edges. Second, the isotherm may indicate the total sites available for the particular adsorbate from the adsorption density at saturation. Finally, the appropriateness of postulated surface species at a given pH are readily discerned by fitting isotherms.

Two surface complexes are needed to fit the selenate isotherm data. The relevant reactions are

$$\equiv FeOH^{\circ} + SeO_4^{2-} + 2H^{+} = \equiv FeHSeO_4^{\circ} + H_2O \qquad [27]$$

$$\equiv FeOH^{\circ} + SeO_4^{2-} + H^{+} = \equiv FeSeO_4^{-} + H_2O \qquad [28]$$

and the constants used to obtain the fits shown in Figure 17 are given in Table 3c. The linear portions of the isotherms can be fit with reaction [28] alone, but reaction [27] is necessary in order to fit the high adsorption density data. It is evident in Figure 17 that the fits are not perfect, perhaps reflecting the need for noninteger stoichiometries in the surface complexation reactions. Nevertheless, the fits are adequate for engineering estimates. The curves drawn on Figure 18 are the pH edges predicted using the diffuse layer model, and the stability constants in Tables 3a, 3b, and 3c. Note that the slight overestimation of adsorption density for the pH=6.5 isotherm and the underestimation at pH=4.5 show up in the predicted pH edges.

Due to the lack of detailed chromate adsorption isotherms, it is necessary to fit the pH edge data directly in order to obtain chromate

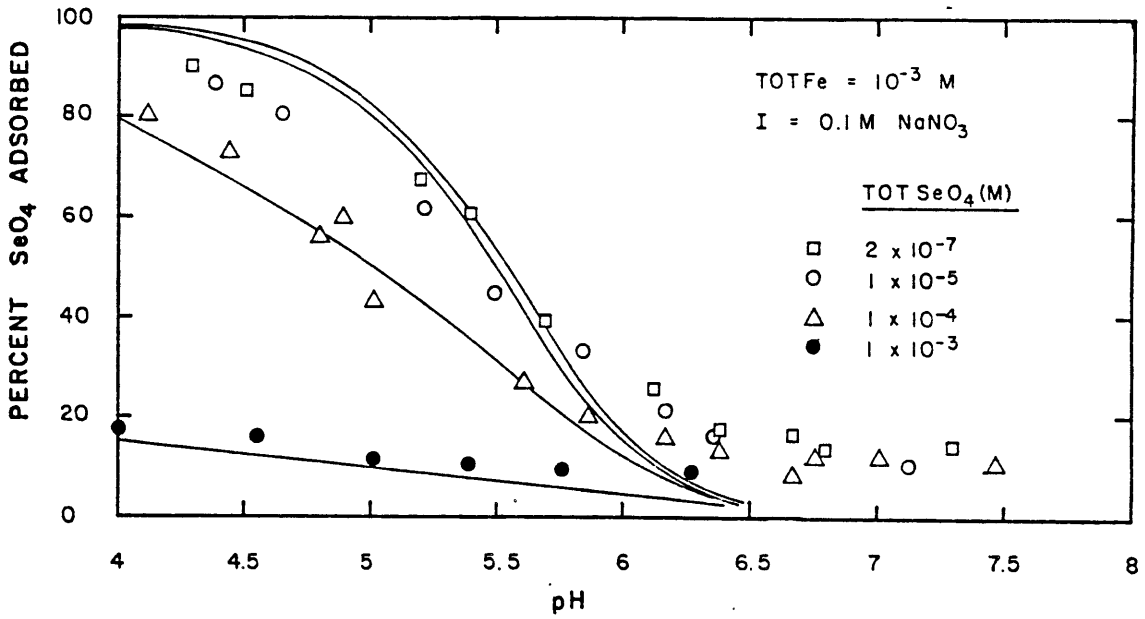

FIG. 18.-pH edges for selenate adsorption on hydrous ferric oxide. Data from Leckie et al. (52).

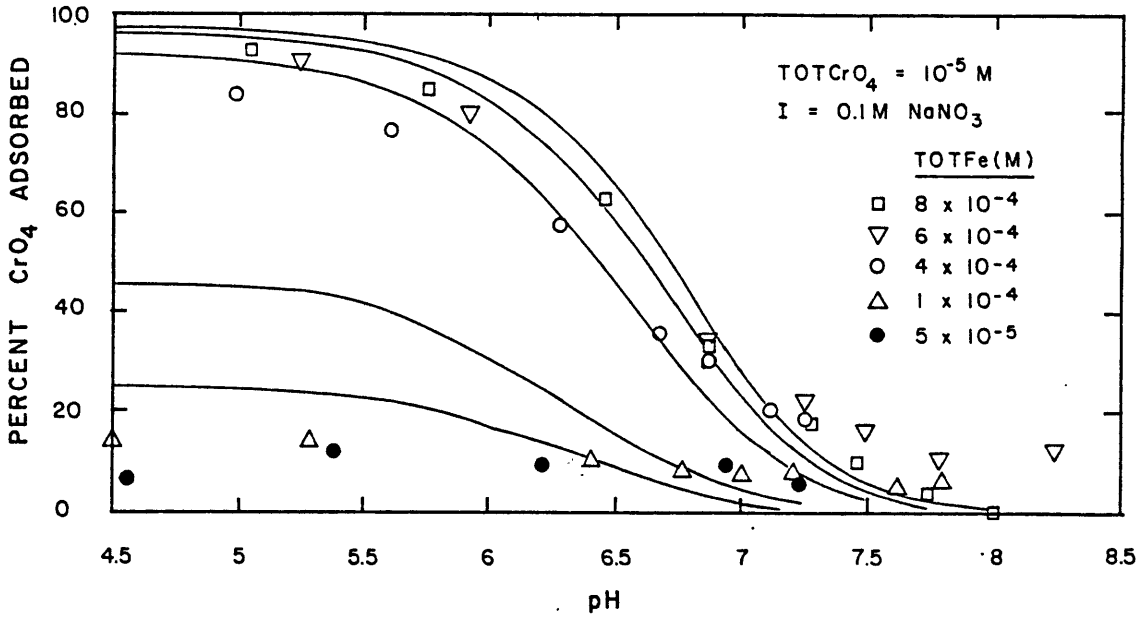

FIG. 19.-pH edges for chromate adsorption on hydrous ferric oxide. Data from Leckie et al. (109).

surface complexation constants. To model the chromate pH edges we considered two possible surface complexes:

$$\equiv FeOH^{\circ} + CrO_4^{2-} + 2H^{+} = \equiv FeHCrO_4^{\circ} + H_2O \quad [29]$$

$$\equiv FeOH^{\circ} + CrO_4^{2-} + H^{+} = \equiv FeCrO_4^{-} + H_2O \quad [30]$$

In testing some binding constants for each reaction, however, it quickly became apparent that reaction [30] was sufficient to fit the chromate adsorption data because of the relative steepness of the pH edge curves. The surface complexation constant that produced the fits shown in Figure 19 is listed in Table 3d.

Equilibrium adsorption of chromate to HFO (precipitated with ferric sulfate) can be calculated using the stability constants listed in Table 3 and the diffuse layer surface complexation model. We performed such calculations for a series of pH values and used TOTFe, $TOTSO_4$, and $TOTCrO_4$ values corresponding to the EPA experiments. The predicted pH edges are presented in Figure 20 along with the EPA chromate removal data. The calculated pH edge slightly overpredicts the adsorption observed in the jar tests and slightly underpredicts the removal achieved in the pilot plant test conducted under nearly the same conditions. The predicted decrease in chromate sorption at the lower pH values is due to competition for surface sites by sulfate. Considering the underprediction of the sulfate (selenate) pH edges for pH=6-7.5 (see Figure 18), unaccounted sulfate competition may be in part responsible for the overprediction of selenite sorption in this pH range. All uncertainties aside, however, the most important point is that with a surface complexation model and constants extracted from experimental data obtained in "clean" systems, we were able to estimate removals

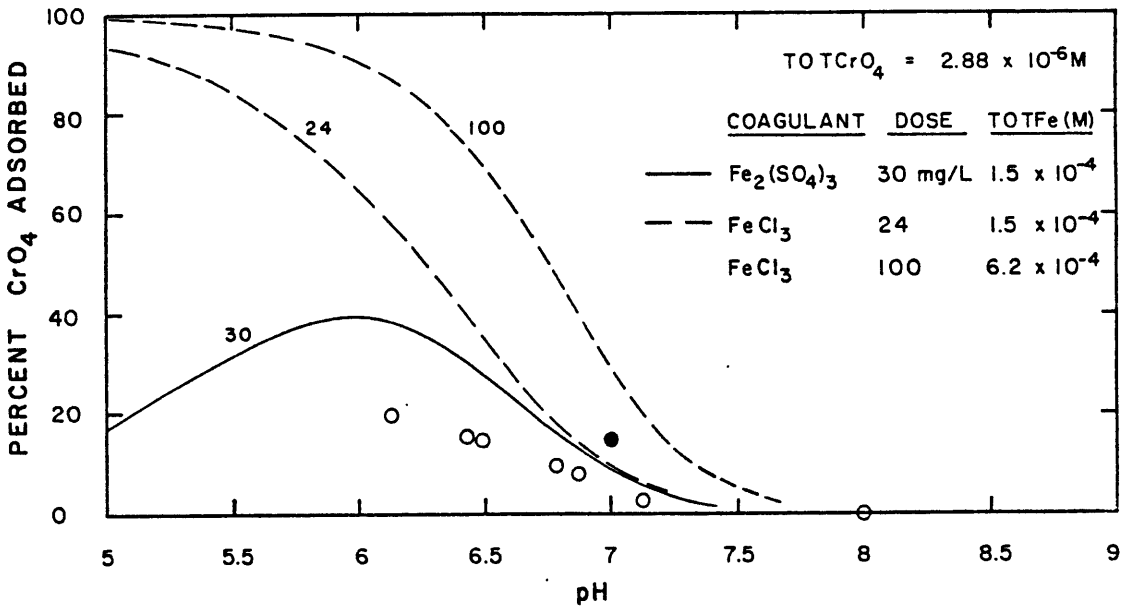

FIG. 20-pH edge data (from Sorg, (11)) for chromate adsorption on hydrous ferric oxide.
○ Jar tests, 0.15 mg/L Cr(VI), 30 mg/L ferric sulfate.
● Pilot plant test, 0.14 mg/L Cr(VI), 24 mg/L ferric sulfate.

fairly accurately. Moreover, with a surface complexation model it is possible, without conducting an experiment, to investigate effects of changing doses of ferric sulfate, of changing chromate loadings or ionic strength, and effects of competition with other ions such as sulfate or phosphate. As a result of modelling studies, for example, one might choose to precipitate HFO with ferric chloride instead of ferric sulfate in order to avoid sulfate competition, to adjust the coagulation tank inflow to a slightly lower pH, or to use a higher coagulant dose (see Figure 20). Also, modelling can be used to help design efficient bench scale or pilot experimental programs by identifying optimum conditions beforehand.

SUMMARY

This article reviews the surface complexation approach to modelling adsorption of ions on hydrous metal oxides which are dominant adsorbents in natural aquatic systems and in many water treatment processes as well. Hydrous oxides have reactive hydroxyl surface sites which can attain either positive or negative charge by binding or dissociating protons. Adsorption of protons and other ions on oxide surfaces can be viewed as analogous to the formation of soluble complexes, i.e. ions bind to functional groups at the surface and these reactions can be described with mass law equations. These concepts form the basis for surface complexation models which, through basic coordination chemistry, enable quantitative description of hydrolysis and specific adsorption at oxide/water interfaces.

For the adsorption of an ion on a charged oxide surface, the total energy of interaction includes an electrostatic contribution as well as a chemical contribution. The electrostatic contribution is variable since it is charge dependent and therefore a function of solution conditions. It is this variability of the electrostatic energy of interaction that distinguishes surface complexation reactions from reactions among solutes. Electrostatic effects are taken into account by applying a coulombic correction factor (in fact an explicit activity coefficient) to intrinsic surface complexation constants.

Several surface complexation models have been proposed that incorporate different assumptions concerning the location of adsorbed ions at the oxide/water interface. Because the models are based on different physical-chemical scenarios involving certain kinds of surface reactions taking place in certain locations, the number,

nature and values of parameters are model dependent. The primary experimental constraints on the various models are acid-base titration data and ion adsorption data. We do not consider zeta potential measurements to be constraining data because of the ambiguity involved in their interpretation.

The basic surface complexation models (diffuse layer and constant capacitance models) assume a single type of binding site and one surface layer. These models are successful in fitting acid-base titration data, anion adsorption, and cation adsorption at low adsorbate/adsorbent ratios. At higher adsorbate/adsorbent ratios the basic models are unable to predict the continuous increase in adsorption density evident in cation adsorption isotherms. Two surface complexation models of increased complexity -- the multiple site-type model and the surface precipitation model -- have been proposed to remedy this problem. We recommend the diffuse layer model for general use; if necessary, it can be expanded to include multiple site-types and surface precipitation. Surface complexation models can be employed as engineering tools to predict inorganic ion adsorption under conditions of changing pH, ionic strength, or solid concentration on the basis of fewer adsorption data than would be necessary with a purely empirical approach.

APPENDIX.-REFERENCES

1. Karickhoff, S.W., "Organic Pollutant Sorption in Aquatic Systems," Journal of Hydraulic Engineering, Vol. 110, No. 6, 1984, pp. 707-735.

2. Jenne, E.A., "Controls on Mn, Fe, Co, Ni, Cu, and Zn Concentrations in Soils and Water: the Significant Role of Hydrous Mn and Fe Oxides," Trace Inorganics in Water, Advances in Chemistry No. 73, American Chemical Society, Washington, D.C., 1968, pp. 337-387.

3. Jenne, E.A., "Trace Element Sorption by Sediments and Soils: Sites and Processes," Molybdenum in the Environment, W.R. Chappell and K.K. Peterson, eds., Vol. 2, Marcel Dekker, Inc., New York, NY, 1977, pp. 425-553.

4. Theis, T.L. and Wirth, J.L., "Sorptive Behavior of Trace Metals on Fly Ash in Aqueous Systems," Environmental Science and Technology, Vol. 11, No. 12, 1977, pp. 1096-1100.

5. Benjamin, M.M., Hayes, K.F., and Leckie, J.O., "Removal of Toxic Metals from Power-Generation Waste Streams by Adsorption and Coprecipitation," Journal of Water Pollution Control Federation, Vol. 54, No. 11, 1982, pp. 1472-1481.

6. Anderson, M.A. and Morel, F.M.M, "The Influence of Aqueous Iron Chemistry on the Uptake of Iron by the Coastal Diatom Thalassiosira Weisflogii," Limnology and Oceanography, Vol. 27, No. 5, 1982, pp. 789-813.

7. Krauskopf, K.B., "Factors Controlling the Concentrations of Thirteen Rare Metals in Seawater," Geochimica et Cosmoschimica Acta, Vol. 9, 1956, pp. 1-32b.

8. Logsdon, G.S. and Symons, J.M., "Removal of Heavy Metals by Conventional Treatment," Proceedings of the Symposium on Traces of Heavy Metals in Water: Removal Processes and Monitoring, U.S. Environmental Protection Agency, EPA-902/9-74-001, 1973, pp. 225-256.

9. Sorg, T.J. and Logsdon, G.S., "Treatment Technology to Meet the Interim Primary Drinking Water Regulations for Inorganics: Part 2," Journal of American Water Works Association, Vol. 70, No. 7, 1978, pp. 379-393.

10. Sorg, T.J., Csandy, M., and Logsdon, G.S., "Treatment Technology to Meet the Interim Primary Drinking Water Regulations for Inorganics: Part 3," Journal of American Water Works Association, Vol. 70, No. 12, 1978, pp. 680-691.

11. Sorg, T., "Treatment Technology to Meet the Interim Primary Drinking Water Regulations for Inorganics: Part 4," Journal of American Water Works Association, Vol. 71, No. 8, 1979, pp. 454-466.

12. Stumm, W. and Morgan, J.J., Aquatic Chemistry, 2nd ed., John Wiley and Sons, Inc., New York, NY, 1981.

13. James, R.O. and Parks, G.A., "Characterization of Aqueous Colloids by Their Electrical Double-Layer and Intrinsic Surface Chemical Properties," Surface and Colloid Science, E. Matijevic, ed., Vol. 12, Plenum Press, New York, NY, 1982, pp. 119-126.

14. Tanford, C., "Multiple Equilibria," Physical Chemistry of Macromolecules, John Wiley and Sons, Inc., New York, NY, 1961, pp. 526-586.

15. Kurbatov, M.H., Wood, G.B., and Kurbatov, J.D., "Isothermal Adsorption of Cobalt from Dilute Solutions," Journal of Physical Chemistry, Vol. 55, 1951, pp. 1170-1182.

16. Kinniburgh, D.G. and Jackson, M.L., "Concentration and pH Dependence of Calcium and Zinc Adsorption by Iron Hydrous Oxide Gel," Soil Science Society of America Journal, Vol. 46, 1982, pp. 56-61.

17. Boehm, P., "Acidic and Basic Properties of Hydroxylated Metal Oxide Surfaces," Discussions of the Faraday Society, No. 52, 1971, pp. 264-275.

18. Peri, J.B., "A Model for the Surface of γ-Alumina," Journal of Physical Chemistry, Vol. 69, No. 1, 1965, pp. 220-230.

19. Parfitt, R.L., Russell, J.D., and Farmer, V.C., "Confirmation of the Surface Structures of Goethite (α-FeOOH) and Phosphated Goethite by Infrared Spectroscopy," Journal of the Chemical Society, Faraday Transactions I, Vol. 72, 1976, pp. 1082-1087.

20. Dumont, F. and Watillon, A., "Stability of Ferric Oxide Hydrosols," Discussions of the Faraday Society, No. 52, 1971, pp. 352-360.

21. McCafferty, E. and Zettlemoyer, A.C., "Adsorption of Water Vapor on α-Fe_2O_3," Discussions of the Faraday Society, No. 52, 1971, pp. 239-254.

22. Harvey, D.T. and Linton, R.W., "Chemical Characterization of Hydrous Ferric Oxides by X-ray Photoelectron Spectroscopy," Analytical Chemistry, Vol. 53, No. 11, 1981, pp. 1684-1688.

23. Parks, G.A. and DeBruyn, P.L., "The Zero Point of Charge of Oxides," Journal of Physical Chemistry, Vol. 66, 1962, pp. 967-973.

24. Stumm, W., Huang, C.P., and Jenkins, S.R., "Specific Chemical Interactions Affecting the Stability of Dispersed Systems," Croatica Chemica Acta, Vol. 42, 1970, pp. 223-244.

25. Schindler, P.W. and Gamsjager, H., "Acid-Base Reactions of the TiO_2 (Anatase)-Water Interface and the Point of Zero Charge of TiO_2 Suspensions," Kolloid-Z.u.Z.-Polymere, Vol. 250, pp. 759-763.

26. Huang, C.P., "The Surface Acidity of Hydrous Solids," Adsorption of Inorganics at Solid-Liquid Interfaces, M.A. Anderson and A.J. Rubin, eds., Ann Arbor Science, Ann Arbor, MI, 1981, pp. 183-217.

27. Healy, T.W. and White, L.R., "Ionizable Surface Group Models of Aqueous Interfaces," Advances in Colloid and Interface Science, Vol. 9, 1978, pp. 303-345.

28. Lyklema, J., "The Electrical Double Layer on Oxides," Croatica Chemica Acta, Vol. 43, 1971, pp. 249-260.

29. Grahame, D.C., "The Electrical Double Layer and the Theory of Electrocapillarity," Chemical Reviews, Vol. 41, 1947, pp. 441-501.

30. Overbeek, J.Th.G., "Electrochemistry of the Double Layer," Colloid Science, Vol. I, H.R. Kruyt, ed., Elsevier Publishing Co., Amsterdam, Netherlands, 1952, pp. 115-193.

31. Lyklema, J. and Overbeek, J.Th.G., "On the Interpretation of Electrokinetic Potentials," Journal of Colloid Science, Vol. 16, 1961, pp. 501-512.

32. Smith, A.L., "Electrical Phenomena Associated with the Solid-Liquid Interface," Dispersion of Powders in Liquids, G.D. Parfitt, ed., 3rd ed., Applied Science Publishers, London, England, 1981, pp. 99-148.

33. Hiemenz, P.C., Principles of Colloid and Surface Chemistry, Marcel Dekker, Inc., New York, NY, 1977.

34. Overbeek, J.Th.G., "Electrokinetic Phenomena," Colloid Science, Vol. I, H.R. Kruyt, ed., Elsevier Publishing Co., Amsterdam, Netherlands, 1952, pp. 194-244.

35. Yates, D.E., "The Structure of the Oxide/Aqueous Electrolyte Interface," thesis presented to the University of Melbourne, at Melbourne, Australia, in 1975, in partial fulfillment of the requirements for the degree of Doctor of Philosophy.

36. Guggenheim, E.A., "The Conceptions of Electrical Potential Difference Between Two Phases and the Individual Activities of Ions," Journal of Physical Chemistry, Vol. 33, 1929, pp. 842-849.

37. Guggenheim, E.A., "On the Conception of Electrical Potential Difference Between Two Phases.II," Journal of Physical Chemistry, Vol. 34, 1930, pp. 1540-1543.

38. Chan, D., Perram, J.W., White, L.R., and Healy, T.W., "Regulation of Surface Potential at Amphoteric Surfaces during Particle-Particle Interaction," Journal of the Chemical Society, Faraday Transactions I, Vol. 71, 1975, pp. 1046-1057.

39. Westall, J.C., "Chemical Equilibrium Including Adsorption on Charged Surfaces," Particulates in Water, M.C. Kavanaugh and J.O. Leckie, eds., Advances in Chemistry No. 189, American Chemical Society, Washington, D.C., 1980, pp. 33-44.

40. Sposito, G., "On the Surface Complexation Model of the Oxide-Aqueous Solution Interface," Journal of Colloid and Interface Science, Vol. 91, No. 2, 1983, pp. 329-340.

41. James, R.O. and Healy, T.W., "Adsorption of Hydrolyzable Metal Ions at the Oxide-Water Interface.I," Journal of Colloid and Interface Science, Vol. 40, No. 1, 1972, pp. 42-52.

42. Stumm, W., Hohl, H., and Dalang, F., "Interaction of Metal Ions with Hydrous Oxide Surfaces," Croatica Chemica Acta, Vol. 48, No. 4, 1976, pp. 491-504.

43. Schindler, P.W., Furst, B., Dick, R., and Wolf, P.U., "Ligand Properties of Surface Silanol Groups.I," Journal of Colloid and Interface Science, Vol. 55, No. 2, 1976, pp. 469-475.

44. Morgan, J.J. and Stumm, W., "Colloid-Chemical Properties of Manganese Dioxide," Journal of Colloid Science, Vol. 19, 1964, pp. 347-359.

45. Kinniburgh, D.G., "The H^+/M^{2+} Exchange Stoichiometry of Calcium and Zinc Adsorption by Ferrihydrite," Journal of Soil Science, Vol. 34, 1983, pp. 759-768.

46. Benjamin, M.M. and Leckie, J.O., "Multiple-Site Adsorption of Cd, Cu, Zn, and Pb on Amorphous Iron Oxyhydroxide," Journal of Colloid and Interface Science, Vol. 79, No. 1, 1981, pp. 209-221.

47. Hohl, H. and Stumm, W., "Interactions of Pb^{2+} with Hydrous γ-Al_2O_3," Journal of Colloid and Interface Science, Vol. 55, No. 2, 1976, pp. 281-288.

48. Swallow, K.C., Hume, D.N., and Morel, F.M.M., "Sorption of Copper and Lead by Hydrous Ferric Oxide," Environmental Science and Technology, Vol. 14, No. 11, 1980, pp. 1326-1331.

49. Hohl, H., Sigg, L., and Stumm, W., "Characterization of Surface Chemical Properties of Oxides in Natural Waters," Particulates in Water, M.C. Kavanaugh and J.O. Leckie, eds., Advances in Chemistry No. 189, American Chemical Society, Washington, D.C., 1980, pp. 1-31.

50. Stumm, W., Kummert, R., and Sigg, L., "A Ligand Exchange Model for the Adsorption of Inorganic and Organic Ligands at Hydrous Oxide Interfaces," Croatica Chemica Acta, Vol. 53, No. 2, 1980, pp. 291-312.

51. Hingston, F.J., Posner, A.M., and Quirk, J.P., "Anion Adsorption by Goethite and Gibbsite.I," Journal of Soil Science, Vol. 23, No. 2, 1972, pp. 177-192.

52. Leckie, J.O., Benjamin, M.M., Hayes, K., Kaufman, G., and Altmann, S., "Adsorption/Coprecipitation of Trace Elements from Water with Iron Oxyhydroxide," EPRI RP-910-1, Electric Power Research Institute, Palo Alto, CA, 1980.

53. Hingston, F.J., Posner, A.M., and Quirk, J.P., "Adsorption of Selenite by Goethite," Adsorption from Aqueous Solution, W.J. Weber and E. Matijevic, eds., Advances in Chemistry No. 79, American Chemical Society, Washington, D.C., 1968, pp. 82-90.

54. Benjamin, M.M. and Leckie, J.O., "Competitive Adsorption of Cd, Cu, Zn, and Pb on Amorphous Iron Oxyhydroxide," Journal of Colloid and Interface Science, Vol. 83, No. 2, 1981, pp. 410-419.

55. Schindler, P.W., "Surface Complexes at Oxide-Water Interfaces," Adsorption of Inorganics at Solid-Liquid Interfaces, M.A. Anderson and A.J. Rubin, eds., Ann Arbor Science, Ann Arbor, MI, 1981, pp. 1-49.

56. Davis, J.A. and Leckie, J.O., "Effect of Adsorbed Complexing Ligands on Trace Metal Uptake by Hydrous Oxides," Environmental Science and Technology, Vol. 12, No. 12, 1978, pp. 1309-1315.

57. Benjamin, M.M. and Leckie, J.O., "Effects of Complexation by Cl, SO_4, and S_2O_3 on Adsorption Behavior of Cd on Oxide Surfaces," Environmental Science and Technology, Vol. 16, No. 3, 1982, pp. 162-170.

58. Theis, T.L. and Richter, R.O., "Adsorption Reactions of Nickel Species at Oxide Surfaces," Particulates in Water, M.C. Kavanaugh and J.O. Leckie, eds., Advances in Chemistry No. 189, American Chemical Society, Washington, D.C., 1980, pp. 73-76.

59. Benjamin, M.M. and Leckie, J.O., "Conceptual Model for Metal-Ligand-Surface Interactions during Adsorption," Environmental Science and Technology, Vol. 15, No. 9, 1981, pp. 1050-1057.

60. Reuter, J.H. and Perdue, E.M., "Importance of Heavy Metal-Organic Matter Interactions in Natural Waters," Geochimica et Cosmochimica Acta, Vol. 41, 1977, pp. 325-334.

61. Mantoura, R.F.C., Dickson, A., and Riley, J.P., "The Complexation of Metals with Humic Materials in Natural Waters," Estuarine and Coastal Marine Science, Vol. 6, 1978, pp. 387-408.

62. Morel, F.M.M., Principles of Aquatic Chemistry, John Wiley and Sons, Inc., New York, NY, 1983.

63. Hunter, K.A., "Microelectrophoretic Properties of Natural Surface-Active Organic Matter in Coastal Seawater," Limnology and Oceanography, Vol. 25, No. 5, 1980, pp. 807-822.

64. Tipping, E., "The Adsorption of Aquatic Humic Substances by Iron Oxides," Geochimica et Cosmochimica Acta, Vol. 45, 1981, pp. 191-199.

65. Davis, J.A., "Adsorption of Natural Dissolved Organic Matter at the Oxide/Water Interface," Geochimica et Cosmochimica Acta, Vol. 46, 1982, pp. 2381-2393.

66. Dalang, F., Buffle, J., and Haerdi, W., "Study of the Influence of Fulvic Substances on the Adsorption of Copper (II) Ions at the Kaolinite Surface," Environmental Science and Technology, Vol. 18, No. 3, 1984, pp. 135-141.

67. Davis, J.A., "Adsorption of Natural Organic Matter from Freshwater Environments by Aluminum Oxide," Contaminants and Sediments, Vol. 2, R.A. Baker, ed., Ann Arbor Science, Ann Arbor, MI, 1980, pp. 279-304.

68. Kummert, R. and Stumm, W., "The Surface Complexation of Organic Acids on Hydrous γ-Al_2O_3," Journal of Colloid and Interface Science, Vol. 75, No. 2, 1980, pp. 373-385.

69. Davis, J.A., "Complexation of Trace Metals by Adsorbed Natural Organic Matter," Geochimica et Cosmoschimica Acta, Vol. 48, 1984, pp. 679-691.

70. Hunter, K.A. and Liss, P.S., "The Surface Charge of Suspended Particles in Estuarine and Coastal Waters," Nature, Vol. 282, 1979, pp. 823-825.

71. Sigg, L., Stumm, W., and Zinder, B., "Chemical Processes at the Particle-Water Interface; Implications Concerning the Form of Occurrence of Solute and Adsorbed Species," Complexation of Trace Metals in Natural Waters, C.J.M. Kramer and J.C. Duinker, eds., Martinus Nijhoff/Dr W. Junk Publishers, The Hague, Netherlands, 1984, pp. 251-266.

72. Westall, J.C., Zachary, J.L., and Morel, F.M.M., "MINEQL: A Computer Program for the Calculation of Chemical Equilibrium Composition of Aqueous Systems," Ralph M. Parsons Laboratory Technical Note No. 18, Department of Civil Engineering, Massachusetts Institute of Technology, Cambridge, MA, 1976.

73. Morel, F.M.M., Yeasted, J.G., and Westall, J.C., "Adsorption Models: A Mathematical Analysis in the Framework of General Equilibrium Calculations," Adsorption of Inorganics at Solid-Liquid Interfaces, M.A. Anderson and A.J. Rubin, eds., Ann Arbor Science, Ann Arbor, MI, 1981, pp. 263-294.

74. Westall, J., "MICROQL, I. A Chemical Equilibrium Program in BASIC," Swiss Federal Institute of Technology EAWAG, Duebendorf, Switzerland, 1979.

75. Westall, J., "MICROQL, II. Computation of Adsorption Equilibria in BASIC," Swiss Federal Institute of Technology EAWAG, Duebendorf, Switzerland, 1979.

76. Huang, C.P. and Stumm, W., "Specific Adsorption of Cations on Hydrous γ-Al_2O_3," Journal of Colloid and Interface Science, Vol. 43, No. 2, 1973, pp. 409-420.

77. Westall, J. and Hohl, H., "A Comparison of Electrostatic Models for the Oxide/Solution Interface," Advances in Colloid and Interface Science, Vol. 12, 1980, pp. 265-294.

78. Barrow, N.J., Bowden, J.W., Posner, A.M., and Quirk, J.P., "An Objective Method for Fitting Models of Ion Adsorption on Variable Charge Surfaces," Australian Journal of Soil Research, Vol. 18, 1980, pp. 37-47.

79. Honeyman, B., "Cation and Anion Adsorption at the Oxide/Solution Interface in Systems Containing Binary Mixtures of Adsorbents: An Investigation of the Concept of Adsorptive Additivity," thesis presented to Stanford University, at Stanford, CA, in 1984, in partial fulfillment of the requirements for the degree of Doctor of Philosophy.

80. Dzombak, D.A. and Morel, F.M.M., "Adsorption of Inorganic Contaminants in Ponded Effluents from Coal-Fired Power Plants," MIT-EL 85-005, MIT Energy Laboratory, Cambridge, MA, 1985.

81. O'Connor, D.J. and Connolly, J.P., "The Effect of Concentration of Adsorbing Solids on the Partition Coefficient," Water Research, Vol. 14, 1980, pp. 1517-1523.

82. Gschwend, P.M. and Wu, S.C., "On the Constancy of Sediment-Water Partition Coefficients of Hydrophobic Organic Pollutants," Environmental Science and Technology, Vol. 19, No. 1, 1985, pp. 90-96.

83. Breeuwsma, A. and Lyklema, J., "Physical and Chemical Adsorption of Ions in the Electrical Double Layer on Hematite (α-Fe_2O_3)," Journal of Colloid and Interface Science, Vol. 43, No. 2, 1973, pp. 437-448.

84. Bowden, J.W., Posner, A.M., and Quirk, J.P., "Ionic Adsorption on Variable Charge Mineral Surfaces. Theoretical-Charge Development and Titration Curves," Australian Journal of Soil Research, Vol. 15, 1977, pp. 121-136.

85. Yates, D.E., Levine, S., and Healy, T.W., "Site-binding Model of the Electrical Double Layer at the Oxide/Water Interface," Journal of the Chemical Society, Faraday Transactions I, Vol. 70, 1974, pp. 1807-1818.

86. Davis, J.A., James, R.O., and Leckie, J.O., "Surface Ionization and Complexation at the Oxide/Water Interface.I," Journal of Colloid and Interface Science, Vol. 63, No. 3, 1978, pp. 480-499.

87. Farley, K.J., Dzombak, D.A., and Morel, F.M.M., "A Surface Precipitation Model for the Sorption of Cations on Metal Oxides," Journal of Colloid and Interface Science, in press, 1985.

88. Berube, Y.G. and DeBruyn, P.L., "Adsorption at the Rutile-Solution Interface.I," Journal of Colloid and Interface Science, Vol. 27, No. 2, 1968, pp. 305-318.

89. Blok, L. and DeBruyn, P.L., "The Ionic Double Layer at the ZnO/Solution Interface. I," Journal of Colloid and Interface Science, Vol. 32, No. 3, pp. 518-526.

90. Davis, J.A., "Adsorption of Trace Metals and Complexing Ligands at the Oxide/Water Interface," thesis presented to Stanford University, at Stanford, CA, in 1977, in partial fulfillment of the requirements for the degree of Doctor of Philosophy.

91. Motschi, H., "Correlation of EPR-Parameters with Theromodynamic Stability Constants for Copper(II) Complexes. Cu(II)-EPR as a Probe for the Surface Complexation at the Water/Oxide Interface," Colloids and Surfaces, Vol. 9, 1984, pp. 333-347.

92. Rudin, M. and Motschi, H., "A Molecular Model for the Structure of Copper Complexes on Hydrous Oxide Surfaces: An ENDOR Study of Ternary Cu(II) Complexes on δ-Alumina," Journal of Colloid and Interface Science, Vol. 98, No. 2, 1984, pp. 385-393.

93. Tewari, P.H. and Lee, W., "Adsorption of Co(II) at the Oxide-Water Interface," Journal of Colloid and Interface Science, Vol. 52, No. 1, 1975, pp. 77-88.

94. Schenck, C.V., Dillard, J.G., and Murray, J.W., "Surface Analysis and the Adsorption of Co(II) on Goethite," Journal of Colloid and Interface Science, Vol. 95, No. 2, 1983, pp. 398-409.

95. Harvey, D.T. and Linton, R.W., "X-ray Photoelectron Spectroscopy (XPS) of Adsorbed Zinc on Amorphous Hydrous Ferric Oxide," Colloids and Surfaces, Vol. 11, 1984, pp. 81-96.

96. Balistrieri, L.S. and Murray, J.W., "Metal-Solid Interactions in the Marine Environment: Estimating Apparent Equilibrium Binding Constants," Geochimica et Cosmochimica Acta, Vol. 47, 1983, pp. 1091-1098.

97. Luoma, S.N. and Davis, J.A., "Requirements for Modeling Trace Metal Partitioning in Oxidized Estuarine Sediments," Marine Chemistry, Vol. 12, 1983, pp. 159-181.

98. Tessier, A., Campbell, P.G.C., and Bisson, M., "Sequential Extraction Procedure for the Speciation of Particulate Trace Metals," Analytical Chemistry, Vol. 51, No. 7, 1979, pp. 844-851.

99. Tessier, A., Rapin, F., and Carignan, R., "Trace Metals in Oxic Lake Sediments: Possible Adsorption onto Iron Oxyhydroxides," Geochimica et Cosmochimica Acta, Vol. 49, 1985, pp. 183-194.

100. Lion, L.W., Altmann, R.S., and Leckie, J.O., "Trace-Metal Adsorption Characteristics of Estuarine Particulate Matter: Evaluation of Contributions of Fe/Mn Oxide and Organic Surface Coatings," Environmental Science and Technology, Vol. 16, No. 10, 1982, pp. 660-666.

101. Parks, G.A., "The Isoelectric Points of Solid Oxides, Solid Hydroxides, and Aqueous Hydroxo Complex Systems," Chemical Reviews, Vol. 65, 1965, pp. 177-198.

102. Schwarz, J.A., Driscoll, C.T., and Bhanot, A.K., "The Zero Point of Charge of Silica-Alumina Oxide Suspensions," Journal of Colloid and Interface Science, Vol. 97, No. 1, 1984, pp. 55-61.

103. Morel, F.M.M. and Yeasted, J.G., "On the Interfacing of Chemical, Physical, and Biological Water Quality Models," Fate of Pollutants in the Air and Water Environments, I.H. Suffet, ed., John Wiley and Sons, Inc., New York, NY, 1977, pp. 253-268.

104. Chapman, B.M., "Numerical Simulation of the Transport and Speciation of Nonconservative Chemical Reactants in Rivers," Water Resources Research, Vol. 18, No. 1, 1982, pp. 155-167.

105. Farley, K.J. and Morel, F.M.M., "The Role of Coagulation in the Kinetics of Sedimentation," Environmental Science and Technology, submitted, 1985.

106. Jennings, A.A., Kirkner, D.J., and Theis, T.L., "Multicomponent Equilibrium Chemistry in Groundwater Quality Models," Water Resources Research, Vol. 18, No. 4, 1982, pp. 1089-1096.

107. Smith, R.M. and Martell, A.E., Critical Stability Constants, Vols. 1-4, Plenum Press, New York, NY, 1976.

108. Westall, J.C., "FITEQL: A Program for the Determination of Chemical Equilibrium Constants from Experimental Data," Chemistry Department, Oregon State University, Corvallis, OR, 1982.

109. Leckie, J.O., Appleton, A.R., Ball, N.B., Hayes, K.F., and Honeyman, B.D., "Adsorptive Removal of Trace Elements from Fly-Ash Pond Effluents onto Iron Oxyhydroxide," EPRI RP-910-1, Electric Power Research Institute, Palo Alto, CA, 1984.

CHAPTER IV. SUMMARY AND CONCLUSIONS

The objectives of this study were [1] to conduct some experimental tests of the surface precipitation model (1,2), and [2] to work on the development of a simple yet widely applicable approach to modelling adsorption of inorganic ions on oxide surfaces. Several aspects of the surface precipitation model were tested in the experimental work which involved study of the rate and ultimate extent of cadmium adsorption of hydrous ferric oxide (HFO). The theoretical work represents the first portion of our continuing effort to develop a data base for adsorption of inorganic contaminants in oxide suspensions.

The kinetics experiments revealed that the rate of cadmium adsorption onto HFO is dependent on the ratio of adsorbate/adsorbent and that the rate slows considerably as this ratio is increased. The kinetics data obtained for systems with low adsorbate/adsorbent ratios could be fit with a rate expression derived with the assumption of surface complex formation; data obtained at higher ratios could not be fit with the same rate expression. These results confirm our hypothesis that adsorption kinetics should decrease as the adsorbate/adsorbent ratio is increased because of the shift from surface complexation to surface precipitation as the dominant adsorption mechanism. This hypothesis is further substantiated by recent XPS measurements (3) which provide direct evidence for the existence and slow formation of surface precipitates on oxide surfaces.

In addition to providing insight into an adsorption theory, the results of the kinetics experiments have several practical implications as well. First, it is clear that the short equilibration times (1-4 hours) employed in many "equilibrium" adsorption experiments are adequate

only for systems with low adsorbate/adsorbent ratios. In our experiments, 30 to 48 hours were required to achieve equilibrium for high TOTCd/TOTFe ratios. The results obtained in this study demonstrate that the adsorbate/adsorbent ratio must be taken into account in the design of equilibrium adsorption experiments and in the assessment of reported adsorption data for use in equilibrium models. Second, the results indicate that operation of an ash pond at a higher solids concentration will not only provide greater adsorption capacity but will also improve metal removal efficiency through faster adsorption rates. Pond operation at high solids concentration appears to be desirable in all respects because, as Farley et al. (1) have noted, this also leads to faster solid sedimentation rates.

Equilibrium adsorption experiments with cadmium and HFO were conducted for a wide range of adsorbate concentrations in order to develop a complete adsorption isotherm. A recently published, extensive isotherm for zinc adsorption on HFO was also examined for comparison. The surface precipitation model predicts a characteristic isotherm shape at high adsorbate concentrations, and past experimental studies have not been carried out at concentrations high enough to test this prediction.

The Cd-HFO and the Zn-HFO isotherms exhibit similar characteristics: linear with slope of 1.0 on a log-log plot for low free metal concentrations (Langmuir); linear with slope less than 1.0 for moderate to high free metal concentrations (Freundlich). At the highest adsorbate concentrations both isotherms show adsorptive saturation, but the plateau in adsorption density is more pronounced for cadmium which precipitates as $Cd(OH)_{2(s)}$ at higher concentrations than required for zinc precipitation as $Zn(OH)_{2(s)}$. For the Zn-HFO isotherm a rapid increase in adsorption density is observed above the plateau, indicating a smooth

transition between adsorption and precipitation. This is consistent with the surface precipitation model, but the transition occurs at higher metal concentrations than previously anticipated (1,2).

A two site-type surface complexation model is needed to fit both the Cd-HFO and Zn-HFO isotherms and, in addition, surface precipitation on Type II sites is needed to model the transition between adsorption and precipitation. Because this transition occurs at metal concentrations closer to bulk solution precipitation than we expected in our earlier work, two site-types are needed instead of one in order to model the extensive Freundlich character of the isotherm. A two site surface complexation model coupled with surface precipitation on Type II sites is capable of fitting all available metal adsorption data. In the range of metal concentrations of interest in most aquatic systems, a two site model will be sufficient for adsorption modelling. However, inclusion of surface precipitation will be necessary at high metal concentrations which may be encountered in some treatment processes.

As the first step in our effort to develop a data base for adsorption of inorganic ions in oxide suspensions, we have overviewed the available data and examined the various surface complexation models that have been proposed to describe these data. Before choosing a modelling approach for data base development, we wanted to identify the data that constrain the selection of a particular model. We concluded from our review that model selection is constrained chiefly by acid-base titration data and ion adsorption data. Zeta potential measurements were eliminated as model constraints because they are difficult to interpret, and too few proton release/uptake data exist to classify proton exchange stoichiometry as a major model constraint.

The basic surface complexation models assume a single type of binding site and binding in one surface layer. These models are successful in fitting acid-base titration data and cation and anion adsorption data. For cation adsorption, however, the basic models are unable to predict the continuous increase in adsorption density evident in cation adsorption isotherms. Two models of increased complexity -- the multiple site-type model and the surface precipitation model -- have been proposed to remedy this problem.

For a universal modelling approach we propose a two site surface complexation model with surface precipitation on Type II sites and the diffuse layer model to account for electrostatic effects. For acid-base and anion adsorption reactions, binding constants will be identical for both site-types; i.e., only one site-type is necessary for these reactions. From Chapter II.B, however, it is clear that two site-types are needed to model cation adsorption data. Moreover, inclusion of surface precipitation is necessary in order to model the transition between adsorption and precipitation at high adsorbate concentrations for cations as well as for some anions. The combined model has a minimum of four and possibly five adjustable parameters, depending on whether or not the solubility product for the adsorbing ion is used as an adjustable parameter in the surface precipitation formulation. The diffuse layer electrostatic model is fixed by Gouy-Chapman theory and has no adjustable parameters.

As a result of this study the stage is set for a major data base development effort. In future work we plan to interpret existing acid-base titration data and ion adsorption data for the major oxides in aquatic systems in terms of the combined model described above. The resulting consistent set of constants will serve as a data base for

modellers who want to account for adsorptive equilibria in aquatic systems containing oxide particles. To make the forthcoming adsorption data base usable to practicing engineers, however, a more convenient and interactive computer code than presently exists for chemical equilibrium models is needed. The equilibrium adsorption models discussed in this report can be run on microcomputers such as the IBM PC, and an effort to utilize the flexible input/output features (including graphics) of these machines would do much to make adsorption models for inorganic adsorption more useful to the engineering community.

REFERENCES

1. Farley, K.J., Harleman, D.R.F., and Morel, F.M.M., "Ponding of Effluents from Fossil Fuel Steam Electric Power Plants," MIT-EL 84-007, MIT Energy Laboratory, Cambridge, MA, 1984.

2. Farley, K.J., Dzombak, D.A., and Morel, F.M.M., "A Surface Precipitation Model for the Sorption of Cations on Metal Oxides," Journal of Colloid and Interface Science, in press, 1985.

3. Harvey, D.T. and Linton, R.W., "X-ray Photoelectron Spectroscopy (XPS) of Adsorbed Zinc on Amorphous Hydrous Ferric Oxide," Colloids and Surfaces, Vol. 11, 1984, pp. 81-96.

4. Kinniburgh, D.G. and Jackson, M.L., "Concentration and pH Dependence of Calcium and Zinc Adsorption by Iron Hydrous Oxide Gel," Soil Science Society of America Journal, Vol. 46, 1982, pp. 56-61.

APPENDIX A

EXPERIMENTAL DATA: KINETICS OF CADMIUM ADSORPTION ON HYDROUS FERRIC OXIDE

TOTCd = 6.5×10^{-7} M; TOTFe = 1.0×10^{-3} M

I = 0.1 M $NaNO_3$; T = 25.0 ± 0.1°C

t(hrs)	percent Cd ads (expt)	percent Cd ads (corr)
2.3	42.9	35.8
4.0	54.2	48.5
4.5	55.9	50.4
6.0	60.1	55.1
8.0	62.2	57.5
8.0	66.1	61.9
11.0	69.6	65.8
19.5	72.3	68.8
21.0	78.4	75.7
22.0	75.1	72.0
25.0	81.2	78.9
26.5	77.9	75.1
29.0	77.8	75.0
30.0	84.0	82.0
33.0	78.3	75.6
45.0	81.5	79.2
46.3	78.3	75.6

$TOTCd = 5.0 \times 10^{-6}$ M; $TOTFe = 1.0 \times 10^{-3}$ M

I = 0.1 M $NaNO_3$; T = 25.0 ± 0.1°C

t(hrs)	percent Cd ads (expt)	percent Cd ads (corr)
2.0	33.1	24.7
4.0	45.9	39.1
4.3	41.2	33.9
6.0	49.7	43.4
6.0	49.2	42.9
7.0	55.9	50.4
9.0	56.1	50.6
19.0	65.9	61.6
20.0	64.0	59.5
20.5	62.5	57.8
23.0	63.6	59.1
23.5	62.5	57.8
25.0	62.5	57.8
28.0	65.1	60.7
28.0	59.7	54.7
30.0	63.3	58.7
31.3	65.4	61.1
33.8	60.0	55.0

TOTCd = 5.0×10^{-5} M; TOTFe = 1.0×10^{-3} M

I = 0.1 M $NaNO_3$; T = 25.0 ± 0.1°C

t(hrs)	percent Cd ads (expt)	percent Cd ads (corr)
4.0	16.8	6.4
4.0	19.8	9.8
6.0	21.7	11.9
8.0	25.7	16.4
18.5	33.5	25.2
20.3	34.0	25.8
23.0	38.2	30.5
25.0	41.5	34.2
27.5	45.5	38.7
30.0	46.3	39.6
43.3	44.5	37.6
43.5	44.4	37.5

TOTCd = 1.0×10^{-4} M; TOTFe = 1.0×10^{-3} M

I = 0.1 M $NaNO_3$; T = 25.0 ± 0.1°C

t(hrs)	percent Cd ads (expt)	percent Cd ads (corr)
3.0	18.8	8.7
3.8	17.9	7.6
4.0	21.0	11.1
5.0	15.9	5.4
6.3	22.7	13.0
13.5	27.5	18.4
13.5	25.6	16.3
15.8	28.0	19.0
16.0	28.9	20.0
17.0	23.6	14.1
17.8	33.4	25.1
19.0	24.9	15.5
19.3	26.9	17.8
20.3	34.7	26.5
21.0	27.3	18.2
24.0	30.9	22.3
24.5	36.7	28.8
27.6	34.1	25.9
40.0	34.1	25.9
43.0	34.0	25.8
43.0	40.9	33.5
43.0	37.9	30.1
45.8	38.9	31.3

TOTCd = 6.5×10^{-7} M; TOTFe = 5.0×10^{-3} M

I = 0.1 M $NaNO_3$; T = 25.0 ± 0.1°C

t(hrs)	percent Cd ads (expt)	percent Cd ads (corr)
1.0	91.8	90.8
2.0	88.9	87.5
3.3	86.8	85.2
4.0	91.8	90.8
6.3	86.3	84.6
9.0	91.7	90.7
19.3	92.8	91.9
20.5	91.3	90.2
22.0	95.1	94.5
24.5	91.8	90.8
25.0	92.2	91.2
27.0	91.8	90.8
30.0	95.1	94.5
44.0	87.9	86.4

TOTCd = 6.5×10^{-7} M; TOTFe = 1.0×10^{-4} M

I = 0.1 M $NaNO_3$; T = 25.0 ± 0.1°C

t(hrs)	percent Cd ads (expt)	percent Cd ads (corr)
1.3	32.1	23.6
2.2	34.4	26.2
2.3	34.4	26.2
3.8	37.7	29.9
4.0	44.4	37.5
4.8	40.2	32.7
6.0	39.8	32.3
8.0	44.7	37.8
18.0	46.3	39.6
18.8	47.5	40.9
20.0	50.5	44.3
20.0	51.4	45.3
22.3	48.4	42.0
24.0	47.5	40.9
24.8	51.9	45.9
26.0	48.3	41.8
27.0	52.7	46.8
31.5	53.2	47.4
42.0	54.1	48.4

APPENDIX B

EXPERIMENTAL DATA: EQUILIBRIUM

ADSORPTION OF CADMIUM ON HYDROUS FERRIC OXIDE

TOTFe (M)	TOTCd (M)	percent Cd ads[a] at equil (expt)	p(Cd)[b]	$p\Gamma_{Cd}$[c]
1.0×10^{-3}	1.9×10^{-7}	91.3	7.72	3.76
		(96.0)	(8.06)	(3.73)
		(86.4)	(7.53)	(3.79)
1.0×10^{-3}	6.5×10^{-7}	78.0	6.79	3.31
		(81.0)	(6.86)	(3.29)
		(75.0)	(6.74)	(3.33)
1.0×10^{-3}	1.0×10^{-6}	76.3	6.57	3.13
		(83.6)	(6.73)	(3.09)
		(67.0)	(6.43)	(3.20)
1.0×10^{-3}	5.0×10^{-6}	63.0	5.68	2.53
		(67.0)	(5.73)	(2.50)
		(58.0)	(5.63)	(2.58)
1.0×10^{-3}	1.0×10^{-5}	60.6	5.35	2.25
		(63.1)	(5.38)	(2.23)
		(58.2)	(5.33)	(2.28)
1.0×10^{-3}	5.0×10^{-5}	45.0	4.51	1.72
		(49.0)	(4.54)	(1.67)
		(41.0)	(4.48)	(1.77)
1.0×10^{-3}	1.0×10^{-4}	38.0	4.16	1.52
		(42.0)	(4.19)	(1.46)
		(33.0)	(4.12)	(1.61)
1.0×10^{-3}	2.0×10^{-3}	10.0	2.74	0.70
		(13.6)	(2.76)	(0.57)
		(6.3)	(2.73)	(0.90)
1.0×10^{-3}	1.0×10^{-2}	5.3	2.02	0.28
		(7.7)	(2.03)	(0.11)
		(2.8)	(2.01)	(0.55)
1.0×10^{-4}	1.9×10^{-7}	52.5	6.99	3.05
		(55.5)	(7.00)	(3.03)
		(46.8)	(6.94)	(3.11)
1.0×10^{-4}	6.5×10^{-7}	50.0	6.44	2.55
		(54.0)	(6.47)	(2.50)
		(46.0)	(6.40)	(2.59)
2.0×10^{-4}	6.5×10^{-7}	61.0	6.54	2.74
		(63.0)	(6.57)	(2.72)
		(59.2)	(6.53)	(2.75)
2.0×10^{-4}	5.0×10^{-6}	30.9	5.41	2.26
		(33.7)	(5.43)	(2.20)
		(27.0)	(5.39)	(2.35)

TOTFe (M)	TOTCd (M)	percent Cd ads[a] at equil (expt)	p(Cd)[b]	$p\Gamma_{Cd}$[c]
5.0×10^{-3}	6.5×10^{-7}	92.5	7.29	3.94
		(95.0)	(7.44)	(3.91)
		(90.0)	(7.14)	(3.94)
1.0×10^{-2}	1.0×10^{-3}	57.2	3.32	1.29
		(59.0)	(3.34)	(1.27)
		(53.3)	(3.28)	(1.32)
5.0×10^{-2}	1.0×10^{-2}	69.6	2.52	0.86
		(73.7)	(2.58)	(0.83)
		(65.2)	(2.46)	(0.88)
5.0×10^{-2}	6.0×10^{-2}	19.4	1.32	0.63
		(24.7)	(1.35)	(0.53)
		(14.1)	(1.29)	(0.77)
1.0×10^{-1}	1.0×10^{-1}	33.8	1.18	0.47
(I = 0.5 M)		(36.2)	(1.20)	(0.44)
		(31.4)	(1.16)	(0.50)
1.0×10^{-1}	6.0×10^{-2}	42.7	1.46	0.59
(I = 0.4 M)		(44.2)	(1.48)	(0.58)
		(41.3)	(1.45)	(0.61)
1.0×10^{-1}	6.8×10^{-2}	41.7	1.40	0.55
(I = 0.4 M)		(43.5)	(1.42)	(0.53)
		(40.0)	(1.39)	(0.57)

[a] upper and lower error estimates (from replicate samples; includes counting error) are indicated in parantheses

[b] $p(Cd) = - \log(Cd^{2+})$; correction for adsorption on the filter apparatus is included where applicable (i.e. for TOTCd < 1 mM)

[c] $p\Gamma_{Cd} = - \log [\text{Cd ads (M)}/ \text{TOTFe (M)}]$

APPENDIX C

COMMENTS ON THE QUALITY OF EQUILIBRIUM ADSORPTION DATA REPORTED IN THE LITERATURE

It is an unfortunate fact that much poor quality data has been published for adsorption of metal ions on oxide surfaces. Before using adsorption data reported in the literature, one should assess the quality of the data by close examination of experimental details. Below we list some of the more important details that should be included in such an assessment.

In order to verify the identity of the adsorbent oxide, the method of synthesis and the physical-chemical properties of the oxide should be checked. Differences in methods of synthesis can lead to significant variations in physical-chemical properties of metal oxides, and for this reason more or less standard preparation methods have been adopted by informal consensus for the most common metal oxides. If properties of the oxide adsrobent such as ZPC and surface area are not available for comparison with other reported values, it is important to insure that a standard method was used to synthesize the oxide. Methods of synthesis and physical-chemical properties of the major hydrous oxides can only be obtained by search of the literature as no compendium of this information is available. James and Parks (1) give an extensive bibliography of recent studies conducted with oxides of iron, aluminum, and silicon.

The reaction vessel material is an important experimental detail because artifacts caused by adsorption of suspension components to and leaching of contaminants from vessel walls depend on the type of material. Losses of adsorbate and adsorbent to vessel walls, although seldom mentioned in reports of adsorption data, can be significant, especially at low concentrations. With adsorption of solids to vessel walls, suspended solids concentration is reduced (an important consideration for solid phase adsorption measurements) and available surface area may be reduced (important for solution phase adsorption

measurements). It may be possible to correct for these effects in some circumstances, but when adsorbate tends to adsorb to reaction vessel walls the effects are much more difficult, if not impossible, to isolate. When vessel walls are not inert with respect to an adsorbate, the affinity of the suspended solid may appear to be greater (solution phase adsorption measurement) or less (solid phase adsorption measurement - walls outcompete solids) than the true affinity. Struempler (2) has shown that glass and polypropylene reaction vessels adsorb metal cations and that the extent of adsorption increases with pH and equilibration time.

Leaching of contaminants from reaction vessels is seldom discussed but potentially important in some circumstances. In particular, leaching of silicon from glass reaction vessels is likely to have affected a number of adsorption experiments. Although silicon contamination is probably small for oxides synthesized and experiments conducted at 20°C, Anderson and Benjamin (3) recently demonstrated that in synthesizing goethite (an iron oxide) at high temperature (50°C) and high pH, significant amounts of silicon were leached from glass reaction vessels and incorporated in the solid formed. The resulting solid had surface properties different from either the pure iron oxide or pure silica. Since preparation methods for crystalline oxides often involve high temperature, high pH conditions and glass reaction vessels are frequently employed, many reported adsorption data may correspond to experiments for mixed oxides. One must be aware of this possibility when selecting data from the literature.

Exclusion of CO_2 is important for adsorption experiments conducted with higher concentrations of metal cations because the formation of carbonate precipitates and/or nonlabile metal-carbonate solution

complexes can affect results significantly. Although CO_2 exclusion from reaction vessels is claimed in many published reports of metal adsorption experiments, actual measurements of CO_2 contamination levels are virtually nonexistent. Moreover, close examination of experimental techniques often reveals abundant opportunities for CO_2 invasion (e.g., transfers of aliquots to centrifuge tubes for batch experiments, opening of centrifuge tubes for pH measurements). Any assessment of metal adsorption data should therefore include consideration of precautions taken to avoid CO_2 contamination.

The use of appropriate reaction times in adsorption experiments is critical to insuring the achievement of equilibrium. Specific adsorption of metal cations and anions to oxide surfaces is generally characterized by two-step kinetics (see Chapter II), with the first step being completed in a few minutes and the second, slower step requiring days, weeks, or even months for completion. In many adsorption experiments (sometimes by design) reaction times are only long enough to permit completion of the rapid adsorption step. It is important to recognize that such data are not <u>equilibrium</u> adsorption data. The amount of time required for equilibration varies from system to system but in general is dependent on pH and on the adsorbate/adsorbent ratio: at low adsorbate/adsorbent ratios equilibrium is achieved quickly, while in systems with high ratios adsorption kinetics slow considerably (Chapter II; Ref. 4).

pH control, or lack thereof, can also affect results of adsorption experiments. Common buffer systems cannot be employed in metal ion adsorption experiments with oxides because the major ions in these systems (e.g., $B(OH)_4^-$, PO_4^{3-}) can either form solution complexes with the adsorbing ion or compete for adsorption sites. Hence, pH is usually

controlled by small additions of strong acid or base. This can be done automatically with a pH-stat system (e.g., Chapter II; Refs. 5,6) or manually (e.g., Ref. 7). Some experiments are conducted without pH control, however. In the case of cation adsorption the pH is allowed to drop and for anion adsorption the pH is allowed to increase. In such experiments the equilibrium pH value is taken as the pH value measured at the time of sampling. This approach assumes rapidly reversible adsorption since adsorption is strongly dependent on pH and the initial pH is either higher or lower than the final pH value. For short equilibration times the validity of this assumption is questionable because desorption kinetics are usually slower than adsorption kinetics (8).

The method of solid-liquid separation is an especially important experimental detail. Aqueous suspensions of metallic oxides often contain a significant fraction of very small particles, or colloids, particularly when the suspension is created by precipitation in situ. For example, freshly precipitated suspensions of amorphous iron hydroxide consist largely of spherical particles 1.5-3.5 nm in diameter (9). To insure complete or nearly complete separation of solid and liquid at the end of an adsorption experiment, it is thus necessary to employ methods that will remove colloids with the rest of the solid phase. This means that the use of a small pore size filter (Chapter II) or of a large centrifugal acceleration. Relatively large pore size filters (e.g. 450 nm) and weak gravitational fields are used in many adsorption experiments. Moreover, when centrifugation is used for solid-liquid separation many authors do not report the centrifugal acceleration but rather the speed of rotation in RPM. Because the conversion factor

depends on the geometry of the particular centrifuge, it is usually not possible to discern the strength of the gravitational field.

Finally, contamination problems may influence adsorption data obtained in systems with trace (less than 10^{-6} M) metal concentrations. These experiments are frequently performed with radioactive tracers and hence no direct measurements of metal concentrations are made. At very low metal concentrations, however, contributions of metal ions from electrolyte salts and oxide particles can exceed the the concentration of added metal so that the tracer is immersed in a larger total metal concentration than expected. For example, Kinniburgh and Jackson (7) estimated that, due to contamination from ferric nitrate, the lower limit for total zinc concentration was 10^{-7} M in their experiments with amorphous iron hydroxide precipitated in situ. In our lab, micromolar concentrations of arsenic have been detected in 0.1 M NaCl and other electrolyte solutions prepared with reagent grade chemicals (A. Carey, unpublished data). Acceptance of adsorption data corresponding to trace concentrations of metal ions should be conditioned on confirmation of total adsorbate metal concentration by direct measurement.

REFERENCES

1. James, R.O. and Parks, G.A., "Characterization of Aqueous Colloids by Their Electrical Double-Layer and Intrinsic Surface Chemical Properties," Surface and Colloid Science, E. Matijevic, ed., Vol. 12, Plenum Press, New York, NY, 1982, pp. 119-216.

2. Struempler, A., "Adsorption Characteristics of Silver, Lead, Cadmium, Zinc, and Nickel on Borosilicate Glass, Polyethylene, and Polypropylene Container Surfaces," Analytical Chemistry, Vol. 45, No. 13, 1973, pp. 2251-2254.

3. Anderson, P.R. and Benjamin, M.M., "Effects of Si on the Crystallization and Adsorption Properties of Ferric Oxides," Environmental Science and Technology, submitted, 1984.

4. Van Riemsdijk, W.H. and Lyklema, J., "Reaction of Phosphate with Gibbsite ($Al(OH)_3$) beyond the Adsorption Maximum," Journal of Colloid and Interface Science, Vol. 76, No. 1, 1980, pp. 55-66.

5. James, R.O., "The Adsorption of Hydrolysable Metal Ions at the Oxide-Water Interface," Ph.D. Thesis, University of Melbourne, Australia, 1971.

6. Kinniburgh, D.G., "The H^+/M^{2+} Exchange Stoichiometry of Calcium and Zinc Adsorption by Ferrihydrite," Journal of Soil Science, Vol. 34, 1983, pp. 759-768.

7. Kinniburgh, D.G. and Jackson, M.L., "Concentration and pH Dependence of Calcium and Zinc Adsorption by Iron Hydrous Oxide Gel," Soil Science Society of America Journal, Vol. 46, 1982, pp. 56-61.

8. Leckie, J.O., Appleton, A.R., Ball, N.R., Hayes, K.F., and Honeyman, B.D., "Adsorptive Removal of Trace Elements from Fly-Ash Pond Effluents onto Iron Oxyhydroxide," EPRI RP-910-1, Electric Power Research Institute, Palo Alto, CA, 1984.

9. Murphy, P.J., Posner, A.M., and Quirk, J.P., "Characterization of Partially Neutralized Ferric Nitrate Solutions," Journal of Colloid and Interface Science, Vol. 56, No. 2, 1976, pp. 270-283.